

https://dspace.org/

The uranium and radon gas concentrations and impact on human health: a case from abandoned gold mine tailings in the West Rand area, Krugersdorp, South Africa.

Moshupya, Paballo Marry

2019
https://hdl.handle.net/10539/29647

Downloaded from a DSpace repository. https://dspace.org/

The uranium and radon gas concentrations and impact on human health: a case from abandoned gold mine tailings in the West Rand area, Krugersdorp, South Africa.

Paballo Marry Moshupya

(Email: 729843@students.wits.ac.za)

'A Research Report submitted to the Faculty of Science, University of the Witwatersrand Johannesburg, in partial fulfilment of the requirements for the degree of Master Science'



Supervisors:

Prof. Tamiru Abiye

School of Geosciences, University of the Witwatersrand

Prof. Hassina Mouri

Department of Geology, University of Johannesburg

Dr. Mannie Levin

Private consultant, P O Box 1731, Pretoria 0043, South Africa

2019

DECLARATION

I, Paballo Marry Moshupya, hereby declare that the work embodied in this research report entitled "The uranium and radon gas concentrations and impact on human heath: a case from abandoned gold mine tailings in the West Rand area, Krugersdorp, South Africa" is the original record of my own findings. Concepts from other relevant sources have been acknowledged by complete references. This work is submitted in partial fulfillment of the Master of Science degree in Hydrogeology at the University of the Witwatersrand, Johannesburg, South Africa and has never been submitted before in any institute for any examination or award of any degree.

Name: Paballo Moshupya



(Signature)

Date: July 2019

Place: Johannesburg (Wits University)

ABSTRACT

The occurrence of uranium and radon gas has long been recognized as a cause of adverse health impacts on the exposed population. The current study was conducted in the Krugersdorp area, West Rand. The area is dominated by abandoned tailings dams from gold and uranium mines, which could be the potential source for toxic metals and gases. In this study, the sampling of rocks, tailings, construction materials and water was carried out for geochemical analyses. For the characterisation of radon, 60 radon monitors were installed in indoor and outdoor environments. The results showed that mine tailings in the area contained high uranium levels, with a maximum of 149.76 ppm and a mean value of 48.87 ppm, which exceptionally exceeds the levels found in underlying rocks. Surface water samples were found to contain uranium levels ranging between 1.93 mg/l and 4.7 mg/l, which are above the safe level of 0.015 mg/l recommended by the World Health Organization. The high uranium concentrations were found to be derived from the residue of adjacent tailings dams.

Results show that the radon levels in the area range from 31.7 Bq/m^3 to 1068.8 Bq/m^3 and thus immensely exceed the typical expected outdoor radon level of about 10 Bq/m^3 estimated by the United Nations Scientific Committee on the Effects of Atomic Radiation. Significantly high average values of 187.4 Bq/m^3 were obtained from gold tailings dams. The radon levels released from tailings were found to contribute to elevated levels in the natural background. In general, a decrease in radon levels with increasing distance from tailings was noted. In indoor environments, radon concentration ranged up to a maximum of 173.5 Bq/m^3, which is above the 100 Bq/m^3 recommended by the World Health Organization.

The effective doses received by the public showed a maximum of 10.11 mSv/y, which is above the recommended value of 1 mSv/y, and thus have a greater potential to pose a high health risk to the residents. Corroborating the aforementioned statement, a high frequency of deaths that are related to lung cancer were documented in the area and were related to elevated radon levels.

DEDICATION

The work is dedicated to my parents (Mr L.R. Moshupya and Mrs D.C. Moshupya)

ACKNOWLEDGEMENTS

Foremost, I would like to send sincere thanks to my main supervisor Prof. Tamiru Abiye for his efforts, financial contributions and support with fieldwork throughout the entire course of the research project. His immense knowledge and insightful comments are valued. I would also like to express my sincere gratitude to my co-supervisor Prof. Hassina Mouri for allowing me to be part of the Medical Geology UJ initiative in Africa and providing me with a bursary through the National Research Foundation. Her support and guidance are highly appreciated. Profound thanks go to Dr Mannie Levin my second co-supervisor for his enthusiasm and assistance throughout the research. All their collaboration and contributions made this work a success. I would also like to express my gratitude to Mr Khuliso Masindi for his valuable recommendations.

My sincere appreciation also goes to Dr Rian Strydom and Dr Marius Strauss for their passionate participation and for providing useful guidelines on radon monitoring. This study would not be possible without the supply of radon monitors and assistance in analysis from the Parc Radon Gas Monitoring (Parc RGM); their excellent services and cooperation are highly treasured. I would also like to thank the South African Weather Service (SAWS), National Cancer Registry (NRC) and Statistics South Africa (StatsSA) for providing useful data employed in this study.

Lastly, I gratefully forward many thanks to my parents (Mr L.R. Moshupya and Mrs D.C. Moshupya) and the whole family at large for their continuous support and encouragement throughout the entire research process. Profound thanks are also directed to Mr M. M. Marakalla for his support and inspiration. The support from all friends is highly appreciated.

TABLE OF CONTENTS

1 **INTRODUCTION** 1

1.1 Background 1

1.2 Research problem 2

1.3 Aims and objectives 2

2 **DESCRIPTION OF THE STUDY AREA** 3

2.1 Location of the study site 3

2.2 Climate 3

2.2.1 Temperature 3

2.2.2 Rainfall 4

2.2.3 Wind speed 5

2.2.4 Wind direction 6

2.3 Physiography 9

2.4 Land use 9

2.4.1 Mining 9

2.4.2 Residential framework 10

3 **GEOLOGICAL SETTING** 12

3.1 Regional geology 12

3.2 Deformation and structural framework 12

3.3 Local geology 14

3.4 Hydrogeological framework 16

4 **LITERATURE REVIEW** 17

4.1 Overview of uranium 17

4.2 Radon in the environment 18

4.2.1 Radon geological association 19

4.2.2 Human influenced associations 20

4.2.3 Radon in the soil 20

4.2.4 Climate and radon 21

4.2.5 Hydrogeological attributes explaining radon in water 22

4.2.6 Radon in indoor environments 22

4.3 Radon exposure and associated health problems 24

5 **METHODOLOGY** 26
5.1 Field reconnaissance survey 26
5.2 Field work 26
5.2.1 Sampling of rocks, tailings, water and construction material 26
5.3 Analytic procedures 29
5.3.1 Chemical analysis for rocks, tailings and bricks using XRF 29
5.3.2 Chemical analysis for water samples by the use of XRF 30
5.3.3 Stable isotope analysis 30
5.4 Geochemical and hydrogeochemical standards and background values 30
5.5 Radon monitoring 31
5.5.1 Radon monitoring 31
5.5.2 Solid-state nuclear track device 32
5.5.3 Sampling site selection and measurement 32
5.5.4 Laboratory analysis 35
5.6 Effective dose 36
5.7 Data analysis and evaluation 37
5.8 Existing data collection 38
6 **RESULTS AND DISCUSSION** 40
6.1 Rock and tailings geochemistry 40
6.1.1 Overall trace element concentration 40
6.1.2 Uranium and thorium concentration in rocks and tailings 41
6.2 Hydrochemistry 42
6.2.1 Physiochemical parameters 42
6.2.2 Uranium observations 43
6.2.3 Uranium toxicity and health impact 46
6.3 Radon concentration 46
6.3.1 Outdoor radon concentration 46
6.3.2 Characterisation of prominent radon sources and distribution in outdoor environment 48
6.3.3 Uranium and radon correlation 51
6.3.4 The radon spatial distribution 52
6.3.5 Indoor radon concentration 53

6.4 Effective dose 55
6.5 Health effects related to radon exposure 58
7 **CONCLUSIONS** 62
8 **RECOMMENDATIONS** 63
9 **REFERENCES** 64
10 **APPENDICES** 73

LIST OF FIGURES

Figure 1: Location map of the study area 3
Figure 2: Mean daily maximum and minimum temperatures in the study area 4
Figure 3: Annual total rainfall (a) and mean monthly rainfall (b) in the study area 5
Figure 4: Monthly averages of wind speed and monthly variabilities at different times of the day 6
Figure 5: The monthly average representation of frequency of counts by wind direction (%) 8
Figure 6: Topography map of the study area 9
Figure 7: Location of the study area showing the distribution of mine tailings and residential areas 10
Figure 8: Population density (number of people per km^2) of the Mogale City Local Municipality 11
Figure 9: Regional geology map of the study area 14
Figure 10: Local geology map of the study area 16
Figure 11: Uranium-238 radioactive decay chain 18
Figure 12: Processes resulting in radon release to the atmosphere 21
Figure 13: Potential sources and entry pathways of radon for a typical house 23
Figure 14: Satellite map of sampling sites where rocks and tailings samples were collected 26
Figure 15: Various water sources where water sampling was conducted 28
Figure 16: Satellite map of sampling locations for water collected in the study area 28
Figure 17: Radon monitors 32
Figure 18:Radon monitoring points for first period 34
Figure 19:Localities for second radon monitoring period 35
Figure 20: Laboratory apparatus used for etching and washing 36
Figure 21: Light microscopy and automated computer-based technique for counting nuclear tracks 36
Figure 22: Distribution of mining in South Africa 38
Figure 23: Comparative plot of trace element concentrations in tailings and rocks 40
Figure 24: Uranium concentration in tailings samples in the study area 42
Figure 25: Dissolved organic matter in water in ponds found in the study area 43
Figure 26: Uranium concentration in water samples collected in the study area 44
Figure 27: Observed impact of abandoned gold mine tailings on surface water samples 45
Figure 28: Isotopic signature of water samples collected in the area 45
Figure 29: A histogram plot presenting outdoor radon concentration 47
Figure 30: Average radon concentration as a function of distance from the closest tailings residues 48
Figure 31: Radon distribution in relation to the underlying geology 49
Figure 32: Radon distribution in relation to tailings 49
Figure 33: Large slime dam in the study area which could results in higher radon releases 50
Figure 34: Distribution of radon in different directions from the tailings dominated region 51
Figure 35: Regression analysis results showing a correlation between uranium and radon 52
Figure 36: Radon spatial distribution in the study area 53
Figure 37: Extensive unprotected tailings which cover a large area nearby residential areas 54
Figure 38: Comparison between trace element concentration found in tailings and bricks 55
Figure 39: Calculated effective dose estimated from the outdoor radon levels obtained 56

Figure 40: Spatial distribution map of effective doses received by the population 57
Figure 41: Frequency of histologically diagnosed lung cancer in South Africa with age 58
Figure 42: Lung cancer deaths in various municipalities of the West Rand 59
Figure 43: Plot showing lung cancer deaths in radon exposed and non-exposed areas 59

LIST OF TABLES

Table 1: Total population group according to age in the Mogale City Local Municipality 11
Table 2: Regional lithostratigraphy of the study area indicating major rock types and subdivisions 13
Table 3: Average Pb, Th and U in the shales of the Witwatersrand Supergroup 15
Table 4: Threshold concentration to generate radon levels 19
Table 5: Sampling locations for tailings and rock samples collected in the study area 27
Table 6: Sample location for water collected in the study area 29
Table 7: Statistical summary of metal concentration in South African soils 31
Table 8: Guideline values for physical parameters and uranium in potable water 31
Table 9: Classification of radon monitoring sites 33
Table 10: Detailed classification for both the target and reference population 39
Table 11: Statistical summary of uranium and thorium found in tailings and rock 41
Table 12: Field measured physio-chemical parameters 43
Table 13: Statistical results for outdoor radon levels measured in Krugersdorp 47
Table 14: Indoor radon levels obtained in dwellings at various locations 54
Table 15: Uranium, thorium and lead composition of the bricks used for construction in the area 55
Table 16: Statistical summary of trace elements found in tailings and rock samples collected 60

LIST OF ABBREVIATIONS

Units

Bq/m^3	Becquerels per cubic metre
mg/kg	milligrams per kilogram
mg/l	milligrams per litre
mSv/y	milli Sieverts per year
ppm	parts per million
µg/l	micrograms per litre
µS/cm	micro Siemens per centimetre

Universal

DWAF	Department of Water and Forestry
EC	Electrical Conductivity
GMWL	Global Meteoric Water Line
IARC	International Agency for Research on Cancer
ICRP	International Commission on Radiological Protection
LMWL	Local Meteoric Water Line
MCLM	Mogale City Local Municipality
NNR	National Nuclear Regulator
NRC	National Cancer Registry
ORP	Oxidation-Reduction Potential
Parc RGM	Parc Radon Gas Monitoring
SAWS	South African Weather Service
StatsSA	Statistics South Africa
TDS	Total Dissolved Solids
UNSCEAR	United Nations Scientific Committee on the Effects of Atomic Radiation
USEPA	United States Environmental Protection Agency
WHO	World Health Organization

1 INTRODUCTION

1.1 Background

Mining has long been recognized as a major economic activity for many developing countries. Despite the positive impacts brought by mining, these operations often result in significant environmental and health hazards. In South Africa, the historic extraction of gold from the rocks of the Witwatersrand Supergroup led to the deposition of vast quantities of tailings, which cover large areas. These tailings are often enriched with significant quantities of toxic metals and radioactive uranium (Winde and de Villiers, 2002; Winde and Sandham, 2004). Studies associated with contamination from uranium mine residues across the world demonstrated increased health risks with prolonged exposure to uranium and its decay products, of which radon is one (Au et al., 1995).

Radon (^{222}Rn) occurs ubiquitously in the natural environment, and its occurrence is mainly related to uranium and thorium bearing geological formations. On the other hand, anthropogenic activities such as mining and milling of ores, residuals from nuclear facilities and industrialization could result in substantial quantities of radon in the environment (National Research Council, 1999a). It forms as an immediate decay product of radium (^{226}Ra), which is derived primarily from radioactive decay of uranium (^{238}U) (Nero et al., 1990; Ball et al., 1991; Otton et al., 1992; Siegel and Bryan, 2004; Scheib et al., 2009). Radon disintegrates into a series of short-lived alpha emitting daughter radionuclides ^{214}Po and ^{218}Po, which are considered a health hazard when inhaled or ingested (NRC, 1999b). It is reported to be the second largest contributor to lung cancer after smoking (WHO, 2009) and first in lifelong non-smokers.

The Witwatersrand area host uranium-bearing deposits and residues, which could serve as a significant source of radon. However, very little attention has been given to this issue. In the context of gold and uranium mining in the Witwatersrand area, the subject of most studies was environmental uranium toxicity and pollution, acid mine drainage (AMD) and water quality (Rösner and van Schalkwyk, 2000; Naicker et al., 2003; Winde and Sandham, 2004; Winde and Van der Walt, 2004; Winde and Wade, 2006; Tutu et al., 2008; Coetzee et al., 2009; Durand, 2012, Abiye, 2014). Although there might be radon monitoring done by most mines in the area as part of regulatory public safety assessments outlined in the Nuclear Energy Act of 1999, not much has been published in the open literature. In general, there are only a few studies available which give insights on the magnitude of radon exposure in South Africa (Leuschner et al., 1988; Leuschner et al., 1992; Lindsay et al., 2008). In the Witwatersrand area specifically, research on radon was limited to radon exhalation rate (Lindsay et al., 2004a; Lindsay et al., 2004b; Speelman, 2004; Ongori et al., 2015). Not much effort has been dedicated towards the assessment of radon concentration and the magnitude of its risk on human health in areas where most populations reside proximal to tailings.

The likely possibility that cannot be ignored is that abandoned gold and uranium mine tailings distributed across the Witwatersrand area could substantially contribute to elevated radiation exposure and act as a constant source of radiation. Therefore, this study deals with the levels of radionuclides, specifically uranium and radon in one of the former historically known mining regions in and around the Krugersdorp area. This will assist in determining the significant radiation sources, and the potential health risks posed to humans in the area. Moreover, from the

regulatory point of view, the findings will be of importance in the management of radioactive waste materials in the West Rand area.

1.2 Research problem

Uranium in the form of uraninite (UO_2) was initially extracted as a by-product of gold in the West Rand area. Therefore, the gold refining process disposes of more uranium than any other minerals in the tailing dams. The area of about 400 km^2 was found to constitute more than 270 tailing dams (AngloGold Ashanti, 2004). Most of these mine tailings are now abandoned and disposed of in an open space, therefore, leading to the readily dispersal of radioactive and toxic metals through wind and water erosion. The main concern is that the tailings are situated nearby or directly within densely populated residential areas in the West Rand region. Under such circumstances, the exposure to uranium and its progeny may be substantial thus hazardous to health. The other issue that motivated this study are concerns that are commonly raised in the West Rand area where most communities nearby the mine wastes suffer from respiratory related diseases (Matooane et al., 2014; Bench Marks Foundation, 2017). However, there is no detailed study to prove this assertion. It is, therefore, essential to understand the nature and extent of radiation in regions highly contaminated with radioactive waste materials in order to prevent increased health risks to the public**.**

1.3 Aims and objectives

The main aim of this project was to understand the occurrence and distribution of radon gas in the West Rand with a particular emphasis to the Krugersdorp area. Also to investigate whether the radon gas released from uranium-bearing geological formations and anthropogenic sources result in significant health effects such as lung cancer in the area. To fulfill the aim of this study, the objectives were to:

- Measure the concentration of radioactive materials most importantly uranium and radon,
- Determine the major sources of the radioactive materials within the extent of the study area,
- Delineate areas of high radon concentration,
- Establish radon effective doses and,
- Examine the impact of radon levels on human health.

2 DESCRIPTION OF THE STUDY AREA

2.1 Location of the study site

The study area forms part of the Mogale City Local Municipality (MCLM) in the West Rand district of Gauteng Province (Figure 1). The area is situated within the latitudes **(**26°05'S and 26°10'S) and longitudes (27°43'E and 27°49'E), approximately 30 km West of Johannesburg. It encompasses the greater parts of Krugersdorp town and Kagiso Township. The area covers a total of about 130 km^2 and straddles close to Roodepoort and Randfontein.

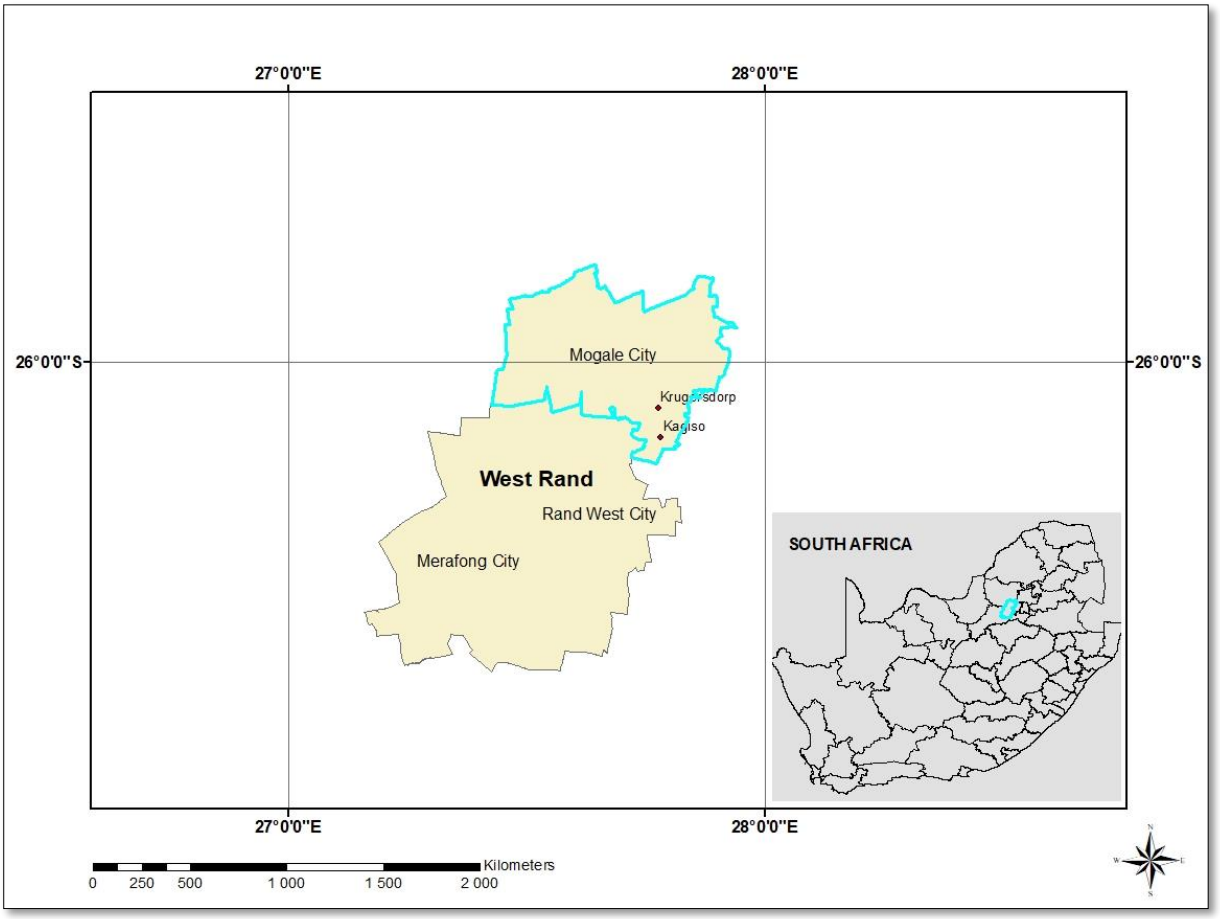


Figure 1: Location map of the study area.

2.2 Climate

2.2.1 Temperature

The research area is characterized by a typical highveld climate. It experiences warm to hot summers with mean monthly daily temperatures ranging between 18^{0}C and 25^{0}C. Maximum temperatures were recorded between October and March. Winter season is characterized by moderate cool days with mean monthly temperatures of about 9 ^{0} C estimated from meteorological data of 1990 to 2017 (27 years of data), Figure 2.

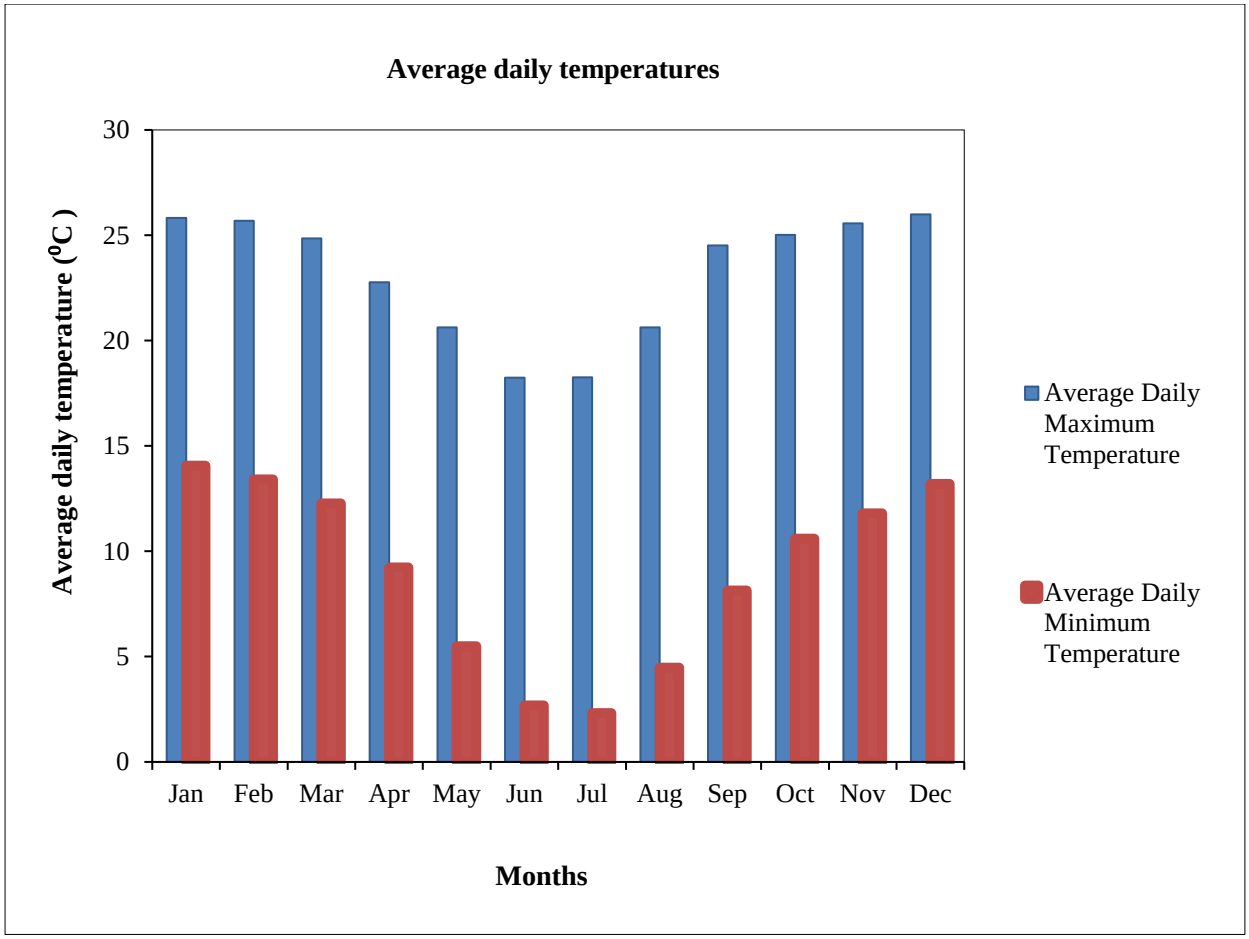


Figure 2: Mean daily maximum and minimum temperatures in the study area. (Data source: South African Meteorological Service; data station 0475668 5 and 0475637 1-Roodepoort).

2.2.2 Rainfall

The area generally receives the mean annual rainfall of 701 mm, which is estimated from meteorological data of 1990 to 2017 (27 years of data) for the Roodepoort station (Figure 3a). High rainfall patterns are recorded in summer and little or no rain in winter months. The highest rainfall commonly occurs in January with average of 132 mm and the driest month is July (Figure 3b).

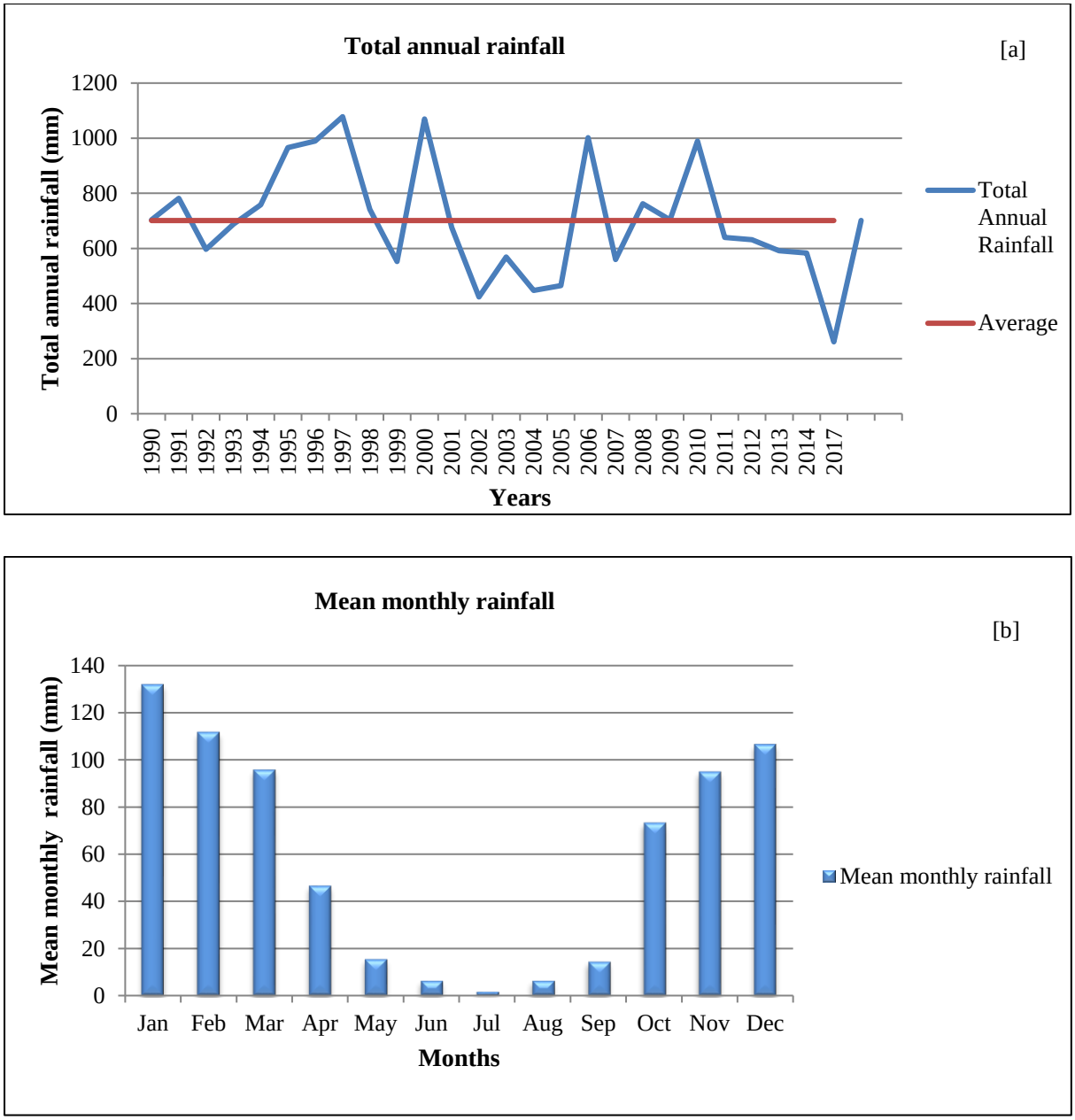


Figure 3: Annual total rainfall (a) with horizontal line representing mean annual rainfall and mean monthly rainfall (b) in the study area. (Data source: South African Meteorological Service; data station 0475668 5 and 0475637 1-Roodepoort).

2.2.3 Wind speed

The average wind speed ranges between 0.9 to 1.6 m/s and reaches to maximum of about 3.5 m/s during the day. This was estimated using 25 years of data from 1992 to 2017. The windiest conditions were experienced between the months of August and December whereas the calmest conditions were between March and June. The wind speed changes instantaneously throughout the course of the day, with peak records during daytime. Calm conditions occur at night hours (Figure 4).

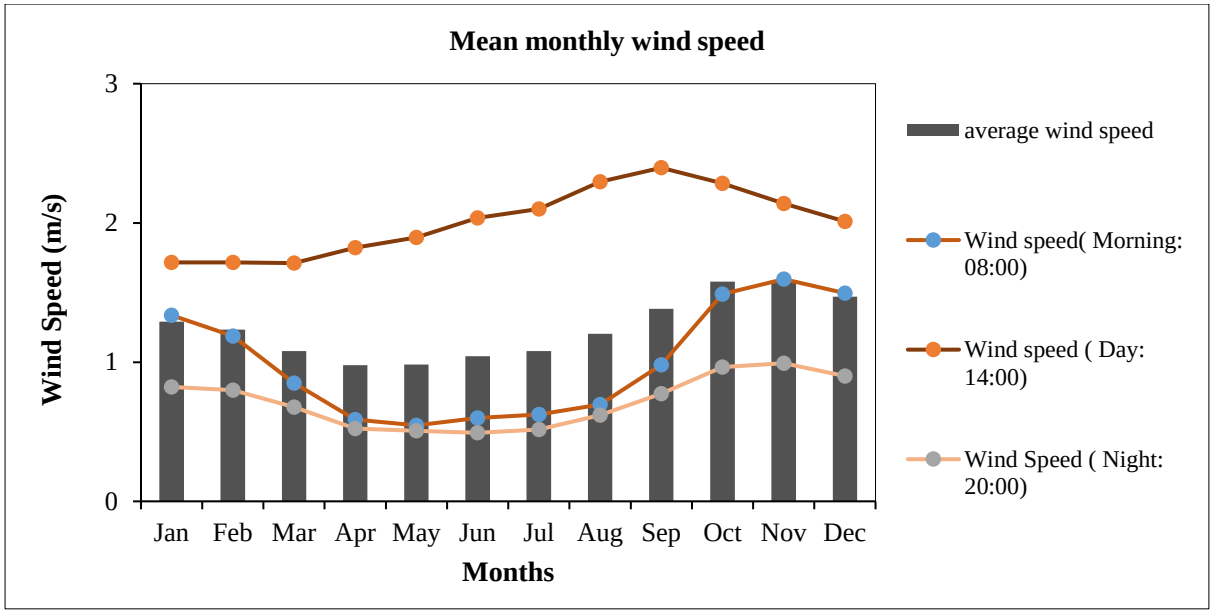


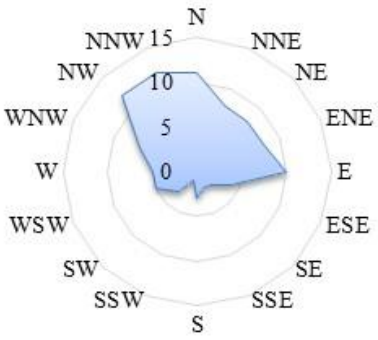
Figure 4: Monthly averages of wind speed and monthly variabilities at different times of the day. (Data source: South African Meteorological service (SAWS), station- [0475879 0] JHB BOT TUINE).

2.2.4 Wind direction

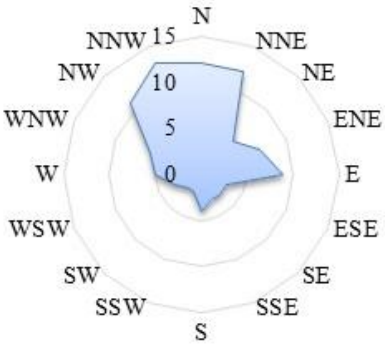
In general, the wind direction varies extensively throughout the year and occurs in all directions, although, some are dominant. In general, the wind direction predominately alternates in a clockwise direction between North-North-West (NNW) and East (E) (Figure 5). The predominant wind direction is the North-North Westerly direction (NNW), most especially in the months between June and January followed by North-West (NW), North (N) and North-North-East (NNE). In May, there is a significant change to the Southerly direction (S), however, the Northerly (N) winds prevail (Figure 5). Moreover, there are diurnal and hourly variations in wind direction whereby morning and night hours are calm, and daytimes show intense changes thus chosen to be a representative of the dominant wind direction as they further exhibit greater wind speeds than morning and night times which may only portray negligible wind effects. The observed sudden changes in wind direction is due to thunderstorms.

Monthly wind direction

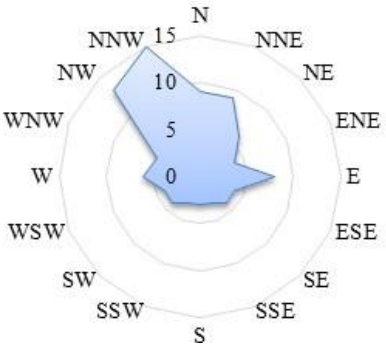
January



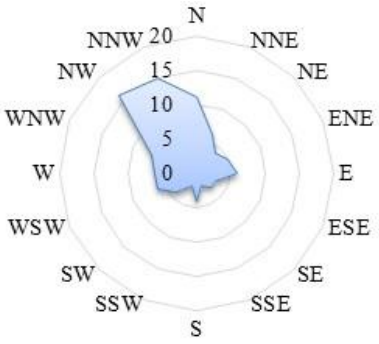
February



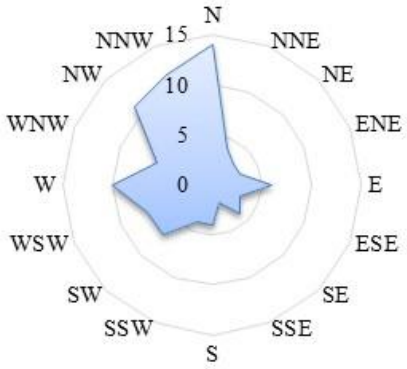
March



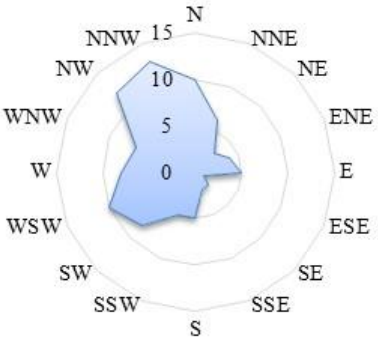
April



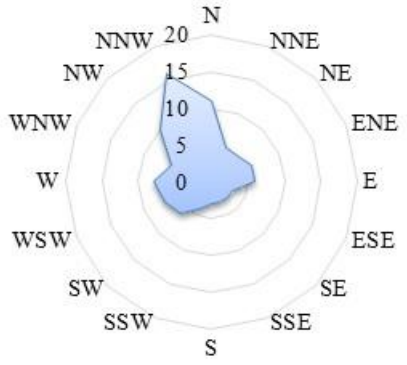
May



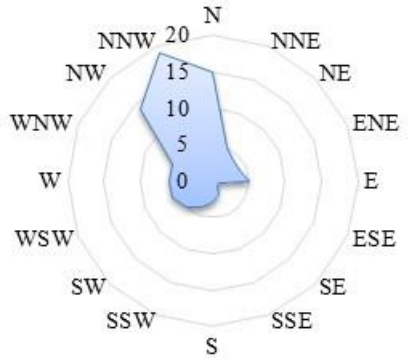
June



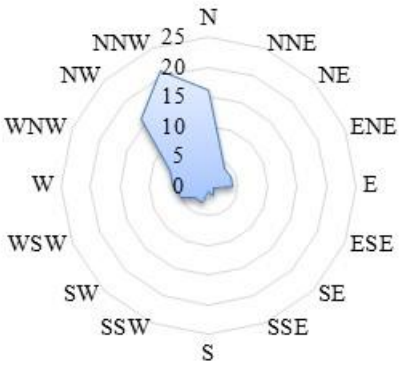
July



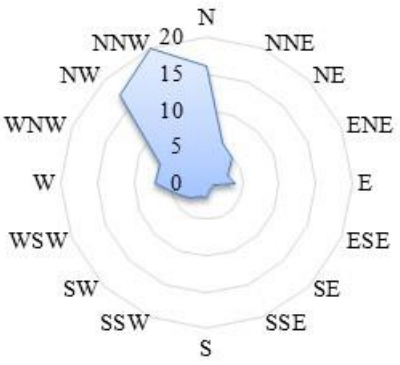
August



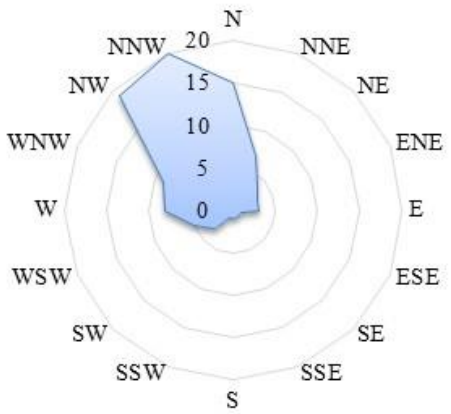
September



October



November



December

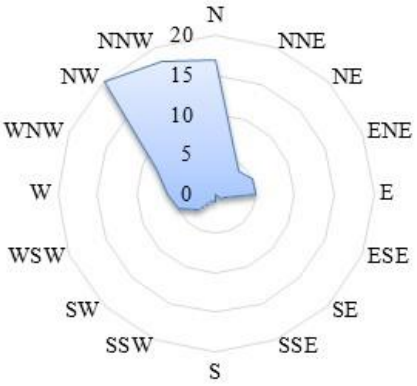


Figure 5: The monthly average representation of frequency of counts by wind direction (%) from 1992 to 2018 indicating the predominant wind direction (Data source: SAWS, station- [0475879 0] JHB BOT TUINE).

2.3 Physiography

The topography around the Krugersdorp and Kagiso area where the study area is located varies from 1650 m to 1750 m above sea level. In general, the area has high elevations as compared to surrounding areas in the north and northwestern parts of the Mogale City Local Municipality as depicted in Figure 6. It is straddled by two major perennial rivers, Rietspruit River in the west and Crocodile River in the east (Figure 6). The landscape of the area has a significant influence on the micro-climatic conditions and local air quality. In addition, could impact on the local dispersion of air pollutants.

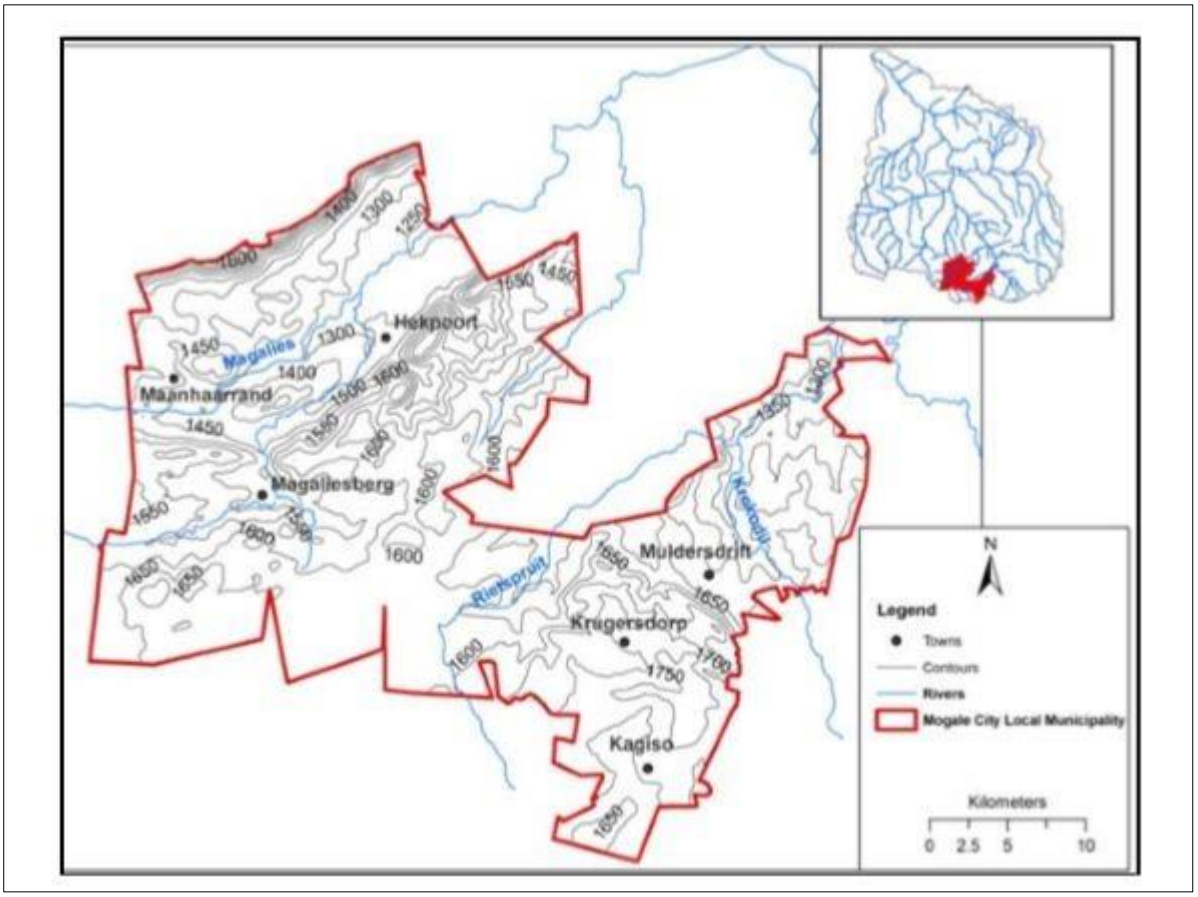


Figure 6: Topography map of the study area (From: MCLM, 2013).

2.4 Land use

The land is predominately used for mining purposes, most specifically gold and uranium mining. However, some parts within the extent of study are dominantly used for residential development.

2.4.1 Mining

Historically, the study area is known as the centre for mining in the West Rand due to the production of uranium as a by-product of gold for over a century. Currently, the area is dominated by abandoned gold and uranium tailings, which are mainly scattered in the central and southern parts of the study area (Figure 7). The tailings were found to contain mostly quartz, approximately 70% to 90%, variable sulphide minerals of which pyrite is

dominant, muscovite, pyrophyllite, gypsum, jarosite and clinochlor. In general, about 10% to 30% phyllosilicates are found. About 1% to 2% of minerals in tailings include uraninite, monazite, rutile and chromite (Rosner 1999; Nengovhela et al., 2006; Abegunde 2015) that generate toxic chemicals through leaching into the environment (Abiye et al., 2018).

2.4.2 Residential framework

Some parts of the study area are dominantly used for residential development. These residential areas lie proximal to tailings dams (Figure 7). Most of the houses found in the study area are made from stock bricks and some of them had already been built in the 1960s. There are also small residential settlements dominated by shacks.

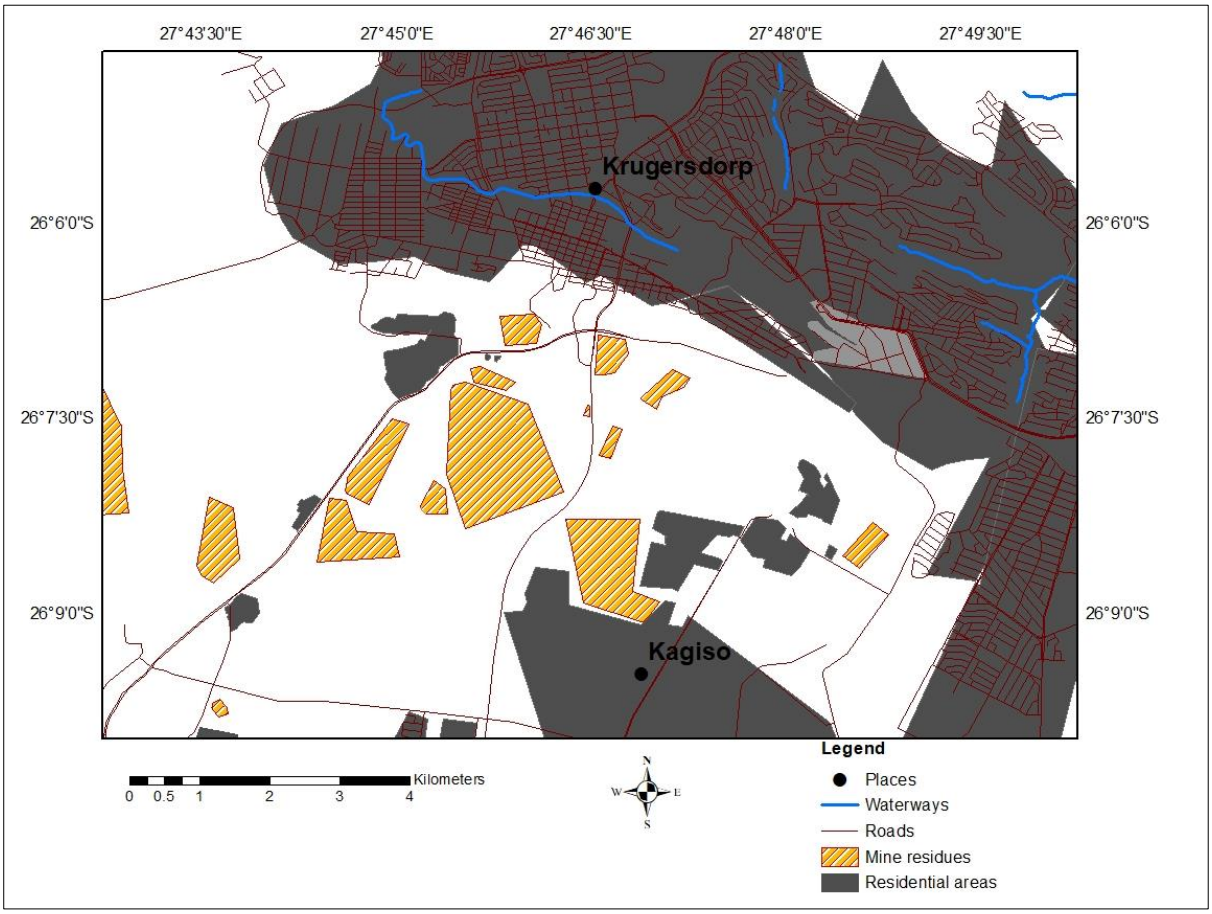


Figure 7: Location of the study area showing the distribution of mine tailings and residential areas.

The study area forms part of the Mogale City Local Municipality (MCLM), which is divided into different clusters of wards (MCLM, 2016). Of these, the Kagiso Township contains largely populated residential areas (Figure 8) with the total area of 14.17 km^2 and a population of approximately 115, 802 (with a population density of 8172/km^2). There are 35098 households, of which there are 2477.10 per km^2. Based on the statistics from the Kagiso water provision, 99 % of the residents have access to piped water and only 1% of the population does not have access (MCLM, 2016). In addition, the Munsieville area is densely populated (Figure 8). In general, the total

population from different clusters within the Mogale City Local Municipality is approximately 362421 of which 51% is male and 49% is female. The total population in terms of the age group is presented in Table 1.

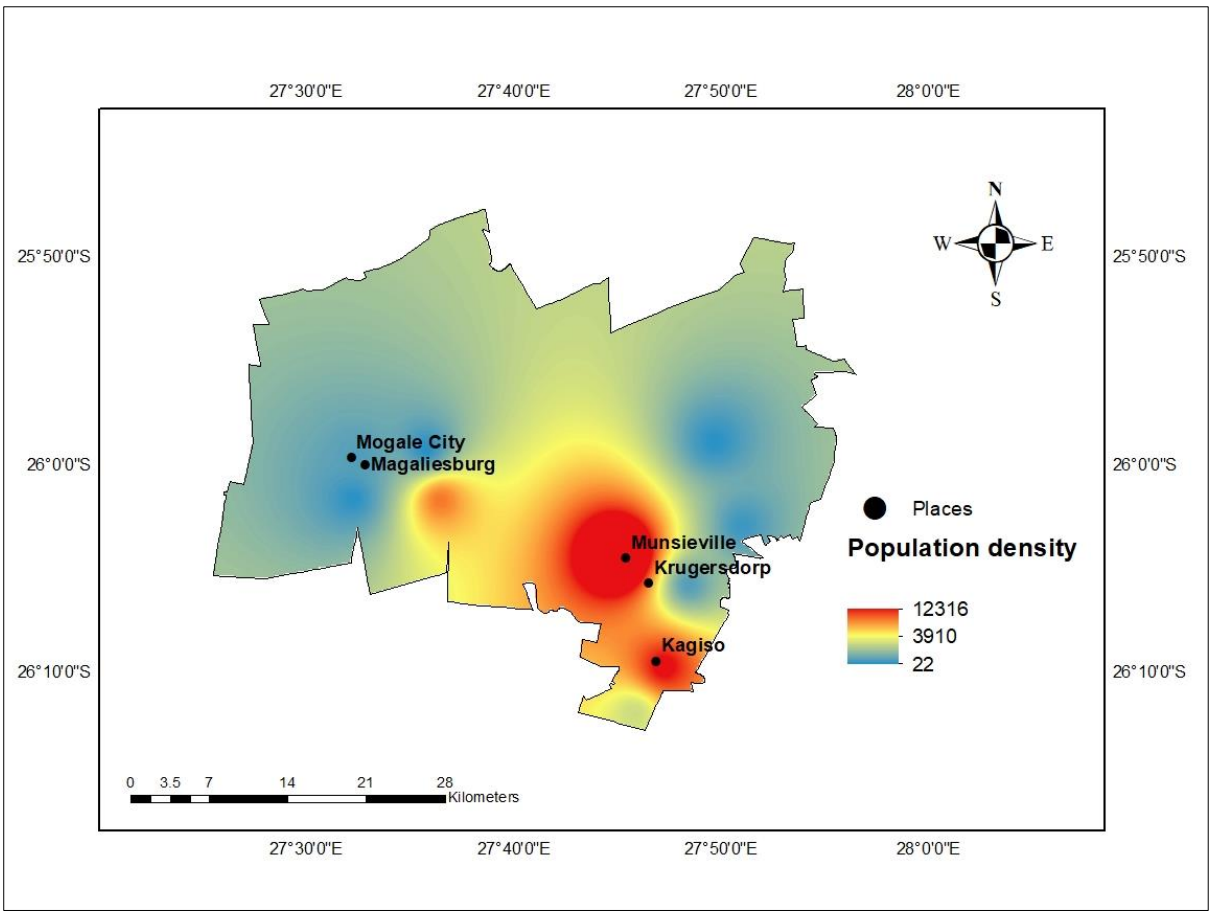


Figure 8: Population density (number of people per km^2) of Mogale City Local Municipality (Data source: StatsSA).

Table 1: Total population group according to age in the Mogale City Local Municipality (From: MCLM, 2016)

Age group	% of total population	Number
0-14 (Children)	24%	86 013
15-34 (Youth)	39%	142 164
35-64 (Adults)	32%	117 753
65-84+ (Elders)	5%	16 491

3 GEOLOGICAL SETTING

3.1 Regional geology

The study area forms a dominant part of the Witwatersrand Basin of where its formation occurred between 3074 and 2714 Ma and deposited within the Kaapvaal Craton in dimensions of 350 km long and 200 km wide (Pretorius, 1976; Robb and Meyer, 1995; Robb et al., 1997). It is notable for being the largest gold deposit in the world. The basin contains the Witwatersrand Supergroup rocks, which are largely comprised of meta-sedimentary rocks that conformably overlie the sediments and volcanic rocks of the Dominion Group as well as the granitic basement rocks. Stratigraphically, the Witwatersrand Basin has a thickness of approximately 7000 m, dominantly characterized by a succession of areneceous and argillaceous rocks (Robb and Meyer, 1995). The succession as a whole is separated into two major Groups: the lower West Rand and the upper Central Rand Group (Table 2).

The West Rand Group was formed between 2970 to 2914 Ma in shallow marine environments with fluvial deposition (Tankard et al., 1982). It comprises mainly of alternating layers of shales and sandstones and conglomerates that have been metamorphosed at low grade to form quartzites and slate. The West Rand Group has been subdivided into three subgroups; Hospital Hill, Government and Jeppestown. On the other hand, the Central Rand Group deposition occurred in a braided stream system (Pretorius, 1976) between 2894 and 2714 Ma. It is subdivided into the Johannesburg and Turffontein Subgroups, which comprise conglomerate, quartzite and minor shale. To a great extent, the rocks of the Witwatersrand Supergroup are covered by younger sequences of Proterozoic and Phanerozoic formations of Ventersdorp and the Transvaal Supergroup (Pretorius, 1976; Robb and Meyer, 1995) (Figure 9).

Following the deposition of the Witwatersrand Supergroup sequence was the 1600 m thick Ventersdorp Supergroup, which accumulated between 2714 and 2665 Ma and overlain by rocks of the Transvaal Supergroup (Table 2). The Transvaal Supergroup includes non-metamorphosed and undeformed volcanic, chemical and clastic sedimentary rocks, which were deposited during the early Proterozoic (Eriksson and Clendenin, 1990; Eriksson, 2006). Of the early Proterozoic Transvaal Supergroup, there is a basal unit forming the Black Reef Formation known to be the youngest in the South African lithostratigraphic succession with a remarkable content of placer gold (Els et al., 1995). It is characterized by quartzitic sandstone and conglomerate (Coward et al., 1995). This basal unit of the Transvaal Supergroup is overlain by thick succession of the Chuniespoort Group, which are; dolomites, shales and ironstone. Following this sequence is the overlying sequence of the Pretoria Group represented by shales, sandstones and volcanics (Eriksson and Clendenin, 1990; Coward et al., 1995; Errikson et al., 2006).

3.2 Deformation and structural framework

The Witwatersrand Basin experienced several metamorphic events. At about 2500 and 2300 Ma, the rocks were affected from continuous loading of sedimentation of the Ventersdorp and Transvaal Supergroups. The following event was due to thermal perturbations from the Bushveld Complex intrusion and the Vredefort Catatrophism (Robb and Meyer, 1995). Besides metamorphism, the rocks in the Witwatersrand Basin experienced deformational events synchronous to or post development of the West Rand and Central Rand Group rocks. The fold-thrust belt during the Umzawami event 2.90 to 2.72 Ga and Ukubambana event 2.2 to 2.0 Ga resulted in

rocks of the Witwatersrand Basin to be deformed and allowed for the occurrence of local faults (Dankert and Hein, 2010) which may serve as potential channels for radon distribution (Figure 9). In the Witwatersrand Basin, mainly the West Rand, the structural features include the WNW trending Rietfontein Fault zone, the curved Witpoortje and Roodeport Faults as well as the North trending West Rand Fault (Dankert and Hein, 2010).

Table 2: Regional lithostratigraphy of the study area indicating major rock types and subdivisions (From: South African Council for Stratigraphy, 1980)

Lithology	Stratigraphic subdivisions	
	Group	Supergroup
shale and sandstone	Ecca	KAROO
alternating quartzite and shale, chert, lava	Pretoria	TRANSVAAL
dolomite, banded iron formation, shale, chert	Chuniespoort	
quartzite, shale	(Black Reef Formation)	
quartzite, conglomerate, shale/siltstone, lava	Pniel	VENTERSDORP
	Platberg	
lava	Kliprivierberg	
quartzite, minor shales and conglomerates	Central	WITWATERSRAND
quartzite, reddish and ferruginous magnetic shale	West Rand	
quartzite and interbedded lava	Dominion	
granite, gneiss		BASEMENT COMPLEX

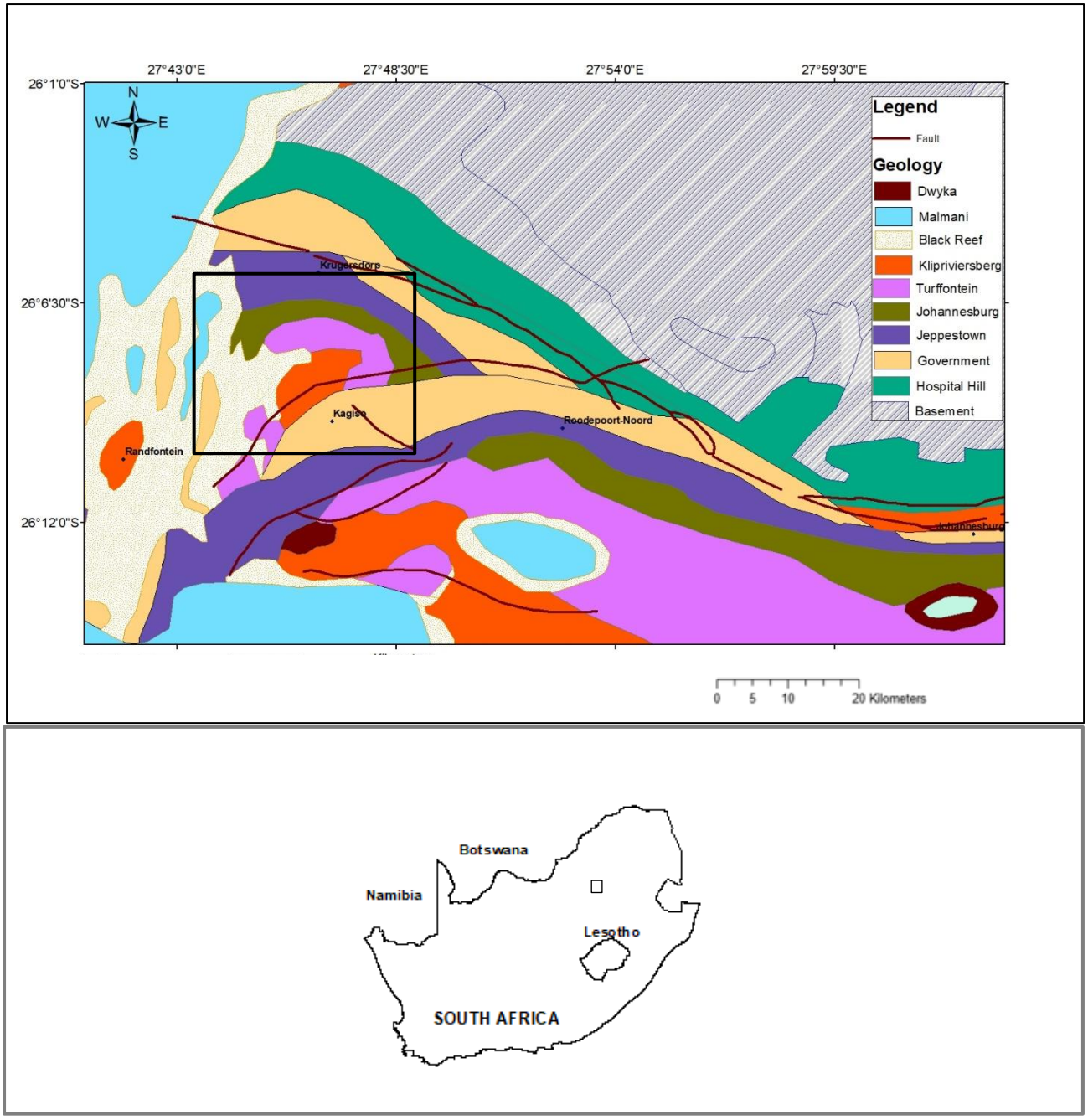


Figure 9: Regional geology for the area (with the study area marked in square).

3.3 Local geology

On a local scale, the main rock types dominating the area include quartzite of the Government, Johannesburg and Turffontein Subgroup, conglomerate of the Witwatersrand Supergroup, the quartzite of the Transvaal Supergroup (Black Reef Formation) and shales of the Jeppestown Subgroup. There are also outliers of Malmani Subgroup dolomites. (Figure 10). The quartzites found in the study reflects an average grain size of approximately 1 mm forming interlocking grain network and a granular texture. Its colour ranges from white fresh surfaces to grey-yellow weathered surfaces, which could be a result of iron stains and associated impurities. Some quartzite outcrops are characterized by quartz veins, which are 0.5-8 cm in thickness. The quartzites are poorly mineralized.

From the geochemistry point of view quartzites of the Black Reef Formation comprises uranium concentration that range between 0.41 ppm to 0.63 ppm, thorium levels between 1.0 ppm and 1.3 ppm and lead concentrations of 11 ppm to 176 ppm (Wronkiewicz and Condie, 1990).

The shales show a pronounced variability of Pb, Th and U concentration. It is notable that the shales of the Orange Grove and K8 Formation indicate a relative enrichment of Th and U as shown in Table 3. However, the study area is dominated by shales of the Jeppestown Subgroup (Roodeport Formation) which are depleted relative to the Orange Grove and K8 Formation shales. According to Camden-Smith (1980), 95% of shales in the West Rand Group comprise modal elemental abundance of quartz and clay minerals and trace elements occur as traces within the clay fraction.

Table 3: Average Pb, Th and U in the shales of the Witwatersrand Supergroup (Wronkiewicz and Condie (1987))

GROUP		WEST RAND				CENTRAL RAND	
Subgroup		Hospital	Hospital	Government	Jeppestown	Johannesburg	Turffontein
(Formation)		(Orange Grove)	(Parktown-Brixton)	(Promise)	(Roodepoort)	(Boyssens)	(K8)
Concentration (ppm)	Pb	12	5.8	5.2	14	14	20
	Th	14	3.9	3.5	5.5	4.7	9.8
	U	3.7	1.7	0.07	1.7	1.6	4.3

The conglomerates are made of pebbles of quartz (70-90%), supported by a fine grained matrix of quartz, phyllosilicates and accessory minerals such as U-bearing minerals and metal sulphides, but most abundant being pyrite. These rock types host economically viable Au, U and sulphides orebodies (Minter, 1977; Robb and Meyer, 1995; Frimmel, 1997; Robb et al., 1997). In the conglomerates of the Witwatersrand Supergroup, uranium exists mainly as uraninite (UO_2), which, as a result of oxidation occurs as U_3O_8 (Turker et al., 2016).

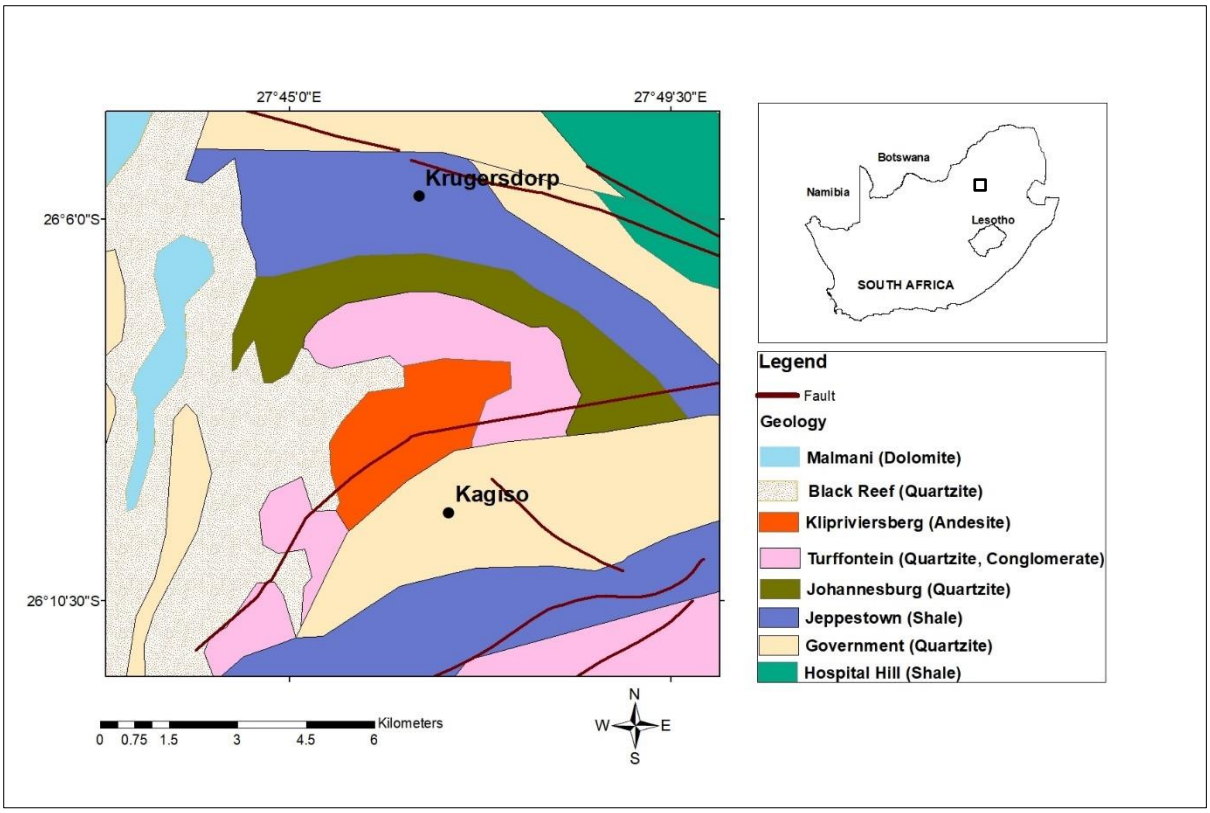


Figure 10: Local geology map of the study area.

3.4 Hydrogeological framework

The landscape of the area, characterized by elongated ridges and plain gentle areas, play an important role in controlling groundwater recharge. The fractures, joints, faults and weathered zones in the Witwatersrand Supergroup rocks (Figure 10) are the most suitable hydro-structures to enhance recharge and water circulation in the area (Abiye, 2011; Abiye et al., 2011; Abiye et al., 2018). From the hydrogeological point of view, water–bearing units in the area are characterized by fractured hardrocks with groundwater productivity of approximately 2 L/s and dolomites with high productivity of greater than 5 L/s (Barnard, 2000; Abiye et al., 2011). The high productivity in dolomites is due to the presence of secondary structure, particularly dissolution cavities. These are compartmentalized by strike slip faults found in the area. The shale units in the area are found to comprise tight fractures with extremely low productivity. Barnard (2000), identified four main water bearing units; intergranular, fractured, karst and intergranular and fractured. However, within the extent of the study area, groundwater is commonly stored within fractures, within dissolution cavities and within the weathered profiles near surface (Abiye, 2011; Abiye et al., 2011). The quartz veins found in the area form local aquifers (Abiye, 2011). Springs are also common in the area and are more exposed to leaching from gold mines dumps. Following a heavy rain season, temporary springs can be found in the area.

4 LITERATURE REVIEW

4.1 Overview of uranium

Uranium occurs naturally as ^{238}U, ^{235}U and ^{234}U with a natural isotopic abundance of 99.2746 %, 0.720 % and 0.0054 %, respectively. However, the most diffused isotope is ^{238}U (Sheppard, 1980). Uranium, being a primordial radionuclide, is naturally contained in different geological units and varies extensively with rock types. Its average concentration in the earth crust is in a range of less than 2 to 4 mg/kg (NRC, 1999a; Rosner, 1999). However, anthropogenic sources such as uranium mining and milling, coal mining, nuclear effluents and fertilizers can add to high uranium levels in the environment (Banning et al., 2013). Almost all times tailings dams, contain higher uranium levels than concentrations found in the earth's crust (Othmane et al., 2013). It is the physiochemical nature of uranium and characteristics of tailings that control the concentrations and behavior of uranium in tailings (Abdelous, 2006; Liu et al., 2017).

Owing to its chemical and geochemical character, uranium occurs in various oxidation states and forms stable compounds (Wendle, 1998). In natural waters, uranium occurs as U^{6+}, U^{5+}, U^{4+} and U^{3+} although in nature U^{6+} and U^{4+} are the most prevalent. The hexavalent U in most instances exists with oxygen to form a divalent uranyl ion (UO_2^{2+}) in oxidizing conditions, while in reducing environments the tetravalent U prevails, and has greater affinity with organic-rich materials (Sheppard, 1980). The mobility and solubility of uranium is highly influenced by numerous interactions such as complex formation, dissolution, desorption-sorption processes, redox potential and pH conditions (Tricca et al., 2000; Abdelous, 2006; Liu et al., 2009; Fox et al., 2012; Lui et al., 2017). Generally, under acidic and reducing environments, U solubility is less as compared to oxidizing and alkaline waters. Again, it is highly soluble in very acidic and oxidizing waters associated with acid mine drainage (Bjorkuland et al., 2017).

The public is always exposed to a specific amount of uranium since it is widely spread in the natural environment. The main route of uranium exposure is through inhalation of uranium-rich dust particles in the air or consumption of contaminated water and food by uranium. The effects following exposure are due to its chemical toxicity and radiological nature. However, the most prominent effects arise from chemical toxicity than from susceptibility to radiation (WHO, 1998**).** The significant consequences linked with exposure to high levels of uranium are kidney related diseases (Kurttio et al., 2002; Orloff et al., 2004; Selden et al., 2009**;** Brojkuland et al., 2017). Although kidneys are the main target organs to uranium chemo-toxic effects, the brain is also sensitive to high levels of uranium (Lestaevel et al., 2005). Uranium is a concern relatively at all exposures. At low exposures, it alters the morphologic character and functionality of the kidney whereas at elevated levels it results in renal failure. Thus, to prevent renal toxicity, the concentration limit of uranium in drinking water is set to a guideline value of 0.015 mg/l by WHO (2008).

As presented in Figure 11**,** when uranium-238 decays, it forms a series of radionuclides until it reaches the stable element, lead-206. Certain radionuclides that are formed through the process pose serious health risks, especially radon and its progeny. Therefore, this study focused on radon gas, which is the primary source of ionizing radiation.

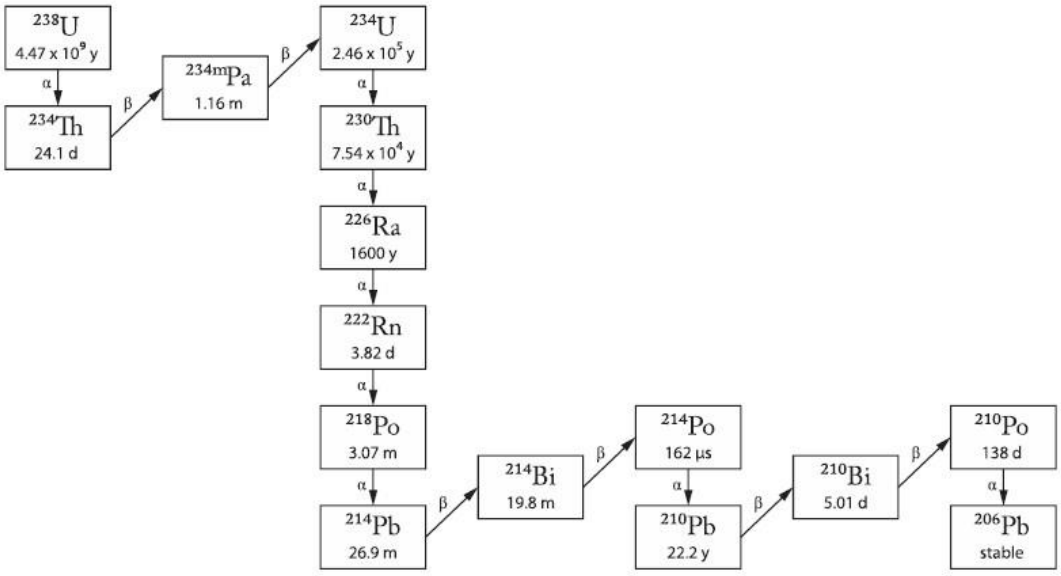


Figure 11: Uranium-238 radioactive decay chain (From: Nero et al., 1990).

4.2 Radon in the environment

Radon is a chemical element with 86 protons and an atomic nucleus with different numbers of neutrons. For example, radon-220 has 134 neutrons and radon-222 has 136 neutrons. It is primarily derived from variable parent decay chains; the uranium decay series; ^{238}U and ^{234}U and thorium series ^{232} Th. The decay series form specific isotopes of radon denoted as radon (Rn-222), actinon (Rn-219) and thoron (Rn-220). These three naturally occurring isotopes of radon; Rn-222, Rn-220 and Rn-219 are produced by the alpha decay of radium isotopes Ra-226, Ra-224 and Ra-223 respectively (Ishmori et al., 2013). However, amongst these three isotopes, Rn-219 has the shortest half-life of 3.98 seconds, and Rn-220 has a half-life of 55.6 seconds. They both exist in exceptionally low concentrations (Samet, 1989). It is, therefore, unusual for preferred conditions to develop for these radon radioisotopes to accumulate to significant levels (Mudd, 2008). As such, their contribution to human exposure is negligible, and thus this study considers only Rn-222 which is the most dominant and has the most significant radiological effects on humans.

Radon-222 is naturally radioactive and decays through alpha emissions. As stated, it is a progeny of radium-226 which results from the radioactive decay of uranium-238 (Nero et al., 1990; Ball et al., 1991; Otton et al., 1992; Siegel and Bryan, 2004; Scheib et al., 2009), Figure 11. It is the longest-lived radon isotope with a half-life of 3.82 days and disintegrates into a series of short-lived daughter radionuclides which are chemically active and considered to be carcinogens,^{218}Po and ^{214}Po (Berkowitz et al., 2007). Furthermore, radon in its natural form is inert, colorless, and odorless and found in different proportions in all media; rocks, soils, air water and building materials (Otton et al., 1992**;** Cecil and Green, 2000).

4.2.1 Radon geological association

In natural environments, the geological formations and deposits with uranium and thorium are the prime sources of radon as they continue to generate the ^{238}U radionuclide series, which is accountable for a constant flux of radon isotopes. In most cases, radionuclides such as uranium and thorium are found naturally in very low quantities in rocks whereby the uranium content in common rock types is in a range of 0.5 and 4.7 ppm (NCR, 1999a).

Nevertheless, there are particular exceptions in some rocks such as felsic volcanic rocks, granites, organic-rich clays and dark shales, hydrothermal ore deposits in structural disconformities, carbonatites and phosphates (NRC, 1999a; Cecil and Green, 2000, Appleton, 2007), which are notable for high radon fluxes. Under some circumstances; limestone, permeable sandstone and ironstones result in a relatively high proportion of radon releases (Scheib et al., 2006; Appleton, 2013). The diagenetic processes involved in the deposition of black shales are commonly associated with the enrichment of uranium (Appleton, 2007), which in turn leads to relatively high radon emissions. Locally, this is supported by the study conducted by Lueschner et al. (1988) where it was found that areas dominated by shales of the Pretoria Group gave rise to high indoor radon levels of about 300 Bq/m^3 and outdoor levels of 94 Bq/m^3. On the other hand, there are rocks with less potential of resulting in high radon levels. These are marine quartz sands, non-carbonaceous shales and siltstones, fluvial sediments, igneous and metamorphic rocks, which are mafic in composition (Gundersen et al., 1992).

Ordinarily, the rocks with uranium content greater than 2 ppm are very likely to result in high radon occurrences (Gundersen et al., 1992). Based on Drolet et al. (2013), there is less variability in radon concentration released from sediments with uranium concentration below 20 ppm, all resulting in fluxes equivalent to an average of 84 Bq/m^3 (Table 4). Equivalent uranium concentration of 2 ppm is set as the threshold concentration for potential high radon concentrations (Drolet et al., 2013). Again, in radioactive materials with concentrations of about 3 ppm of uranium and 10 ppm of thorium are more likely to result in typical outdoor radon activity of about 5 to 10 Bq/ m^3, respectively (Mudd, 2008). In Ielsch et al. (2001) study, geological formations with uranium content above 8 ppm likely results in radon levels of about 100 Bq/m^3 in ambient air. There is no definite amount of uranium required to result in specific radon concentrations. However, uranium concentration as low as 2 ppm and greater, in most bedrocks, could be the threshold concentration to elevated radon concentration based on the findings of Gundersen et al. (1992) and Drolet et al. (2013).

Table 4: Threshold concentration to generate radon levels (Modified after Drolet et al., 2013)

U concentration	**Geometric mean (Bq/m^3)**
0 < x < 20	84
x ≥ 20	215
eU concentration (ppm)	**Geometric mean (Bq/m^3)**
0 < x < 0.75	64
0.75 < x < 1.25	89
x ≥ 1.25	116

Not only the presence and distribution of uranium in host rocks hold a significant effect on radon emanation but also the nature of the geological substrata as a whole; their permeability, and attributes of the transporting medium (Ball et al., 1991; Gundersen et al., 1992; Mudd, 2008; Scheib et al., 2009). For example, surficial sediments that are coarse-grained in nature such as gravel and sand due to their relatively high permeability provide immediate pathways for radon movement whereas fine-grained sediments occur as impermeable barriers to upward radon migration (Miles and Ball, 1996).

4.2.2 Human-influenced associations

Even though the ultimate source of radon is the underlying rocks and soils with high uranium content, the mining of uranium-bearing geological formations critically contributes to the significant accumulation of radon in the natural environment. This is attributable to the circumstance that mining involves different stages which bring to the surface radioactive materials that were buried deep underground. Amongst all the stages, the long-term source of radon is the significant mining residues left after extraction and chemical processing of uranium and gold as they contain indefinite quantities of radioactive materials, most commonly uranium, thorium, radium and the stable element lead.

Although uranium mining is a principal source of loads of radon in the environment, there are several other mining industries with ores extracted for non-radioactive materials, which results in residues with considerable amounts of radionuclides. These include phosphorous ore which may contain up to 120 ppm uranium concentration (NRC, 1999a). Residues produced from other commodities such as oil and gas, coal mining, mineral sands mining as well as gold mining are likely to result in acute radioactive exposures as they comprise uranium and thorium in the radioactive chain series (Ishimori et al., 2013). Since the composition of tailings is dependent on the mineralogy and chemistry of ore, host rock and the leaching processes (Abdelouas, 2006), this ultimately indicates that the predominant source of radon in the environment is primarily the lithological units present and their uranium concentration.

4.2.3 Radon in the soil

Soils rich in uranium and radium form significant potential radon sources (Appleton, 2007). Moreover, materials with high affinity to adsorb radium-226 such as clay minerals, manganese and ferric oxyhydroxides have a greater potential to result in high radon levels (Hobbs et al., 2010). For radon to be released from the soil medium and to be concentrated in the environment, three significant processes need to take place; emanation, transportation and exhalation as depicted in Figure 12 (Ishmori et al., 2013).

The emanation process is the initial stage of accumulation whereby radon atoms formed from radium decay escape from grains and deposited into interstitial space between grains. Not all radon atoms formed get to be distributed into pore spaces; there are several pathways encountered. The atoms may be retained in the original grain, become attached to adjacent grains or may be released into interstitial spaces depending on how radium atoms are distributed in soil grains, the size and texture of grains, porosity and permeability, temperature and pressure (Tanner, 1980; Gunderson and Schuman, 1996). The moisture content, in general, has the most significant impact on emanation power. It controls the recoil distance a radon atom may travel. When pore spaces are filled with water, radon migrates within a short distance than in air-filled pores as the film of water present between grains

lessens the recoil distance. Excessive moisture content in the interstitial spaces may block soil pores, therefore, inhibit radon transport through the soil profile, therefore, resulting in less radon in a gas phase (Strong and Levins, 1982; Gundersen et al., 1992; Porstendorfers, 1994).

Once radon forms in the part of the pore volume of the soil, it migrates through advective and diffusive mechanisms (Nero et al., 1990). Of the two, the primary process is diffusion (Nazaroff and Nero, 1988). Its distribution to the surface is then determined by the transmissivity attributes present in the medium (Ball et al., 1991). The major faults, fractures and micro-fractures provide pathways for radon to reach the surface (Zielinski, 1981; Hall et al., 1987; Churchill, 1991). Exhalation process is the final stage whereby radon atoms that have been transported to the ground surface get to be released into the atmosphere. Once concentrated in the atmosphere, it decays into charged daughter products which are chemically reactive to rapidly attach to aerosol particles in ambient air or form unattached radionuclides (Turekian et al., 1977; Porstendorfer, 1994).

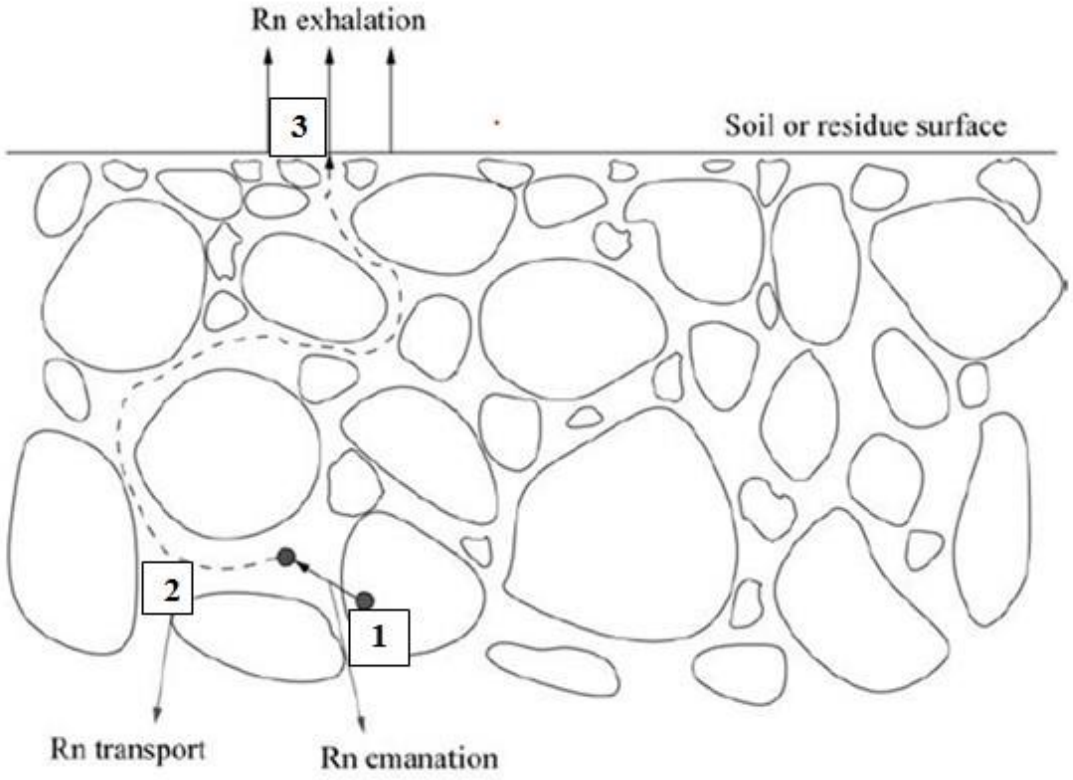


Figure 12: Processes resulting in radon release to the atmosphere (From: Ishmori et al., 2013).

4.2.4 Climate and radon

Climatic conditions have a significant role in controlling radon concentration and its distribution. In soil, variations of radon concentration may be a result of changes in climatic conditions on seasonal, diurnal and hourly time frames (Gundersen et al., 1992). Meteorological parameters such as rainfall, snowfall and high atmospheric pressure may cause a decline in the rate of exhalation whereas high temperatures and wind speed may result in increasing the rate of release and dissemination from source (Porstendorfer, 1994).

Once radon is released into the atmosphere, it becomes widely dispersed without any chemical interference (Ball et al., 1991; Otton et al., 1992; Levin and Verhagen, 2013) and attach to particulates in the atmosphere (Mudd, 2008). Its transport is then mainly controlled by meteorological processes (Porstendorfer, 1994). The driving forces of dispersion of these radionuclides are dependent upon the stability of the atmosphere and wind speed (Ikebe, 1970).

4.2.5 Hydrogeological attributes explaining radon in water

Radon as a naturally occurring element is also found in all natural waters in a wide variety of concentrations. It is soluble in water and thus able to diffuse from small pores and fractures and travels for long distances (LeGrand, 1987; Ball et al., 1991). In groundwater, the aquifer matrix enriched in uranium (^{238}U) and radium (^{226}Ra) results in considerable radon-222 content in groundwater. As documented by Hobbs et al. (2010), the Black Reef Formation and the quartzite strata of the Government Subgroup of the Witwatersrand Supergroup which are uraniferous in composition produce groundwater with radon-222 activity levels of approximately 65 Bq/l, which is above the maximum concentration level set of 11 Bq/l (NRC, 1999c).

On the other hand, negligible radon concentration with activities below 4 Bq/l was found in surface waters (Hopke et al., 2000). This is mainly attributable to a lower interaction between surface waters and the radium-bearing lithologic unit, which is the primary radon source (Schubert et al., 2006; Schmidt et al., 2009). Also, radon-222 in water directly exposed to air degasses rapidly (Hobbs et al., 2010). However, groundwater discharge may result in high concentrations of radon in open surface waters during surface water and groundwater interaction processes.

Radon-222 that is derived from the aquifer matrix dissolves in groundwater and can virtually be transported with groundwater throughout the flow. However, among the prominent transport mechanisms identified, dispersion and advection play a fundamental role in radon movement in groundwater. The diffusion mechanism has less effect on radon transport as it can only diffuse to a length of about 2 cm in water (Schubert et al., 2006). However, in the vadose zone diffusion could be the primary process. Physical mechanisms mostly influence the mobility of radon in natural waters as compared to chemical processes as radon itself does not ionize in solution or precipitate, however, in the presence of organic materials it can be strongly adsorbed (Hobbs et al., 2010).

4.2.6 Radon in indoor environments

In indoor environments, there are five most significant potential sources of radon as outlined by Sextro (1987); Figure 13.

1: The radium-bearing subsoil,

2: Rocks beneath households,

3: Building materials used for construction,

4: Potable water, and

5: Natural gas and outdoor air.

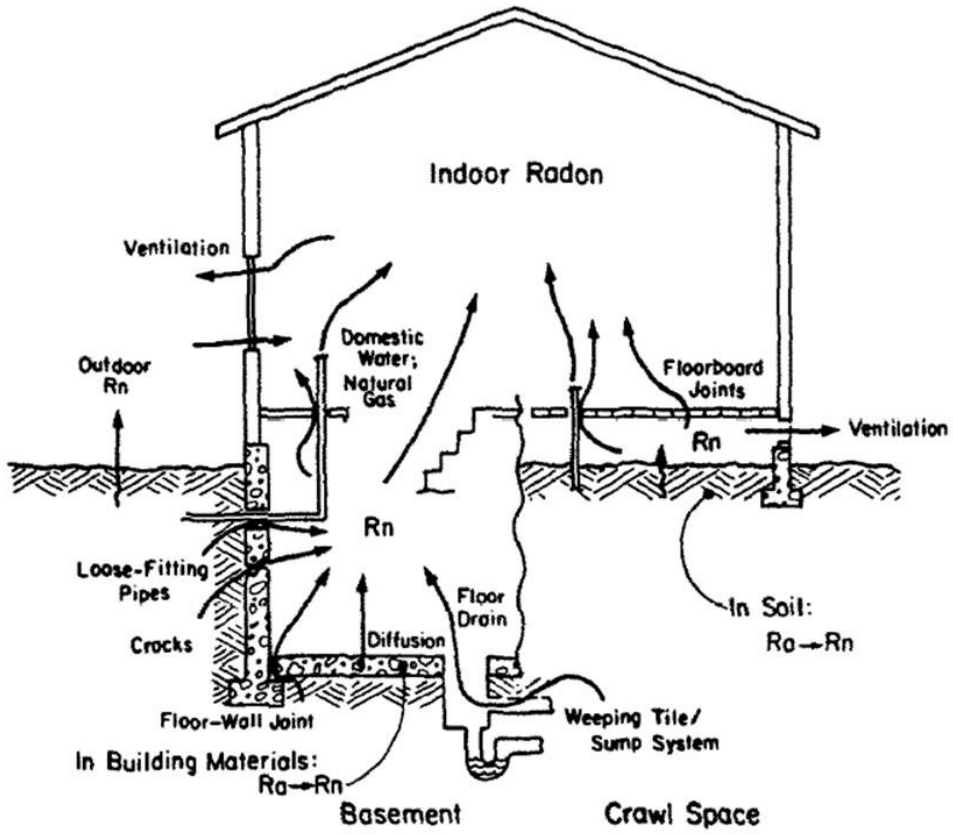


Figure 13: Potential sources and entry pathways of radon for a typical house (From: Sextro, 1987).

For a specific set of observation, it is well demonstrated that direct entry from subsoil ordinarily contributes high indoor radon levels in comparison to other potential sources with generally negligible contributions (Lueschner et al., 1988; Nero et al., 1990; Nazaroff, 1992; Porstendofer, 1994; WHO, 2009). In other circumstances, structural features such as faults and shear zones can be traced to be associated with high indoor radon levels when confined with uranium (Gundersen et al., 1992). After soil, building materials are considered the second major source of indoor radon levels (Kumar et al., 2014). An evident example is in the study of Man and Yeung (1998) whereby building blocks and wall fillings made from granite aggregates resulted in greater contribution to indoor radon. Nonetheless, in most circumstances, the materials used for building construction only account for a small part (Samet, 1989). This occurs only when the material comprises exceptionally negligible radionuclides content (Sahoo et al., 2011).

Ordinarily, radon concentrations in surface and groundwater used for public water supplies are generally low and found at an average of 1×10^3 and 1×10^4 Bq/m^3, respectively (Sextro, 1987) and thus has little strength to accumulate high radon levels. Exceptions occur in specific situations whereby water used in homes adds substantial amounts of radon in the indoor environments (Nero et al., 1990). However, such enhancements highly depend on local geological conditions (Sextro, 1987) and subsequently on the total amount of water used and the size of the dwelling (Cosma et al., 2008). In general, the levels of radon and its progeny in indoor air are governed

by the production rate from the primary source and the ventilation rate in the building shell (Sextro, 1987; Nero et al., 1990; Cosma et al., 2008).

The indoor levels yield appreciable exposures to the public as compared to outdoor air (Leuschner et al., 1988). According to UNSCEAR (2000), typical outdoor radon levels are equivalent to 10 Bq/m^3. In homes, radon is commonly found at levels of about 40 Bq/m^3 (Lubin et al., 1995; UNSCEAR, 2000). The maximum acceptable limit in indoor environments for radon is 100 Bq/m^3 as recommended by WHO (2009). It has been noted that in certain circumstances, the levels may exceed the reference level set and result in substantial exposures.

4.3 Radon exposure and associated health problems

Radon is present both in outdoor and indoor environments. It has long been classified as a human carcinogen by the International Agency for Research on Cancer (IARC, 1988). Its main route of exposure to the public is through inhalation and ingestion. However, the substantial hazard occurs when radon is inhaled than when ingested (Folger et al., 1994; Khan et al., 2009). It was discovered that it is not directly radon that contributes much to the radiation dose received by lung cells as it is most likely inhaled and respired immediately due to its lifetime being greater than breathing times (Darby et al., 2005). The major concern is its short-lived decay products ^{214}Po and ^{218}Po, which exist as electrically charged solid particles that are respirable and easily attach to respiratory organs during inhalation (Harley, 1980; Cross, 1987; NRC, 1999b). These radioactive daughters decay by alpha particle emission on surfaces of bronchial airways and give off substantial radiation doses to result in the mutilation of the DNA in vulnerable lung tissues thereby leading to lung cancer (NRC, 1991; Siegel and Bryan, 2004; Mittal et al., 2016; Bekteshi et al., 2017).

There are multiple modification factors in association with the way individuals respond to the dose received from radon exposure. This includes the rate of exposure and duration, age, smoking history and exposure to other carcinogens as outlined by NRC (1991). Moreover, the properties and the amount of inhaled air, breathing patterns and characteristics of the lung also play a significant role in determining the amount received from radon exposure (Samet, 1989).

The chances to develop radon-related lung cancer are greatest for individuals exposed to higher levels than those exposed to low levels (Darby et al., 2001). However, not only high levels of exposure pose a concern but also long-term exposures to low levels have a potential to cause lung cancer (Lubin et al., 1995; Kruezer et al., 2015). Radon was considered a carcinogen at all exposures as demonstrated by findings from Darby et al. (2001) whereby most deaths attributable to radon exposures are found to occur at levels below 25 Bq/m^3. This may be because even a single alpha particle can damage the DNA thus it is improbable that there is a threshold concentration wherein radon cannot cause mutation and genetic damage to cells (WHO, 2009). Conversely, radon exposures of about 100 Bq/m^3 results in increased lung cancer incidences (Sethi et al., 2012).

The expected period for lung cancer development as a result of radon exposure is estimated to be between 5 to 25 years (NRC, 1999b). However, the risk of developing lung cancer substantially declines with increasing time since the last exposures; with the greatest declines at 30 to 35 years since the last exposure (Lubin et al., 1995). Cessation to radon exposure significantly lessens the risk to develop lung cancer. Radon attributable deaths are most likely found in individuals between the age range of 55 and 75 and extremely few under the age of 35 (Darby

et al., 2001). For children exposed at a young age, findings from Lubin et al. (1995) show that they tend to be at a slight risk to develop lung cancer in adulthood provided the exposure to radon progeny discontinues as they grow.

Exposure to the combination of radon and other lung cancer-causing agents have a more significant effect than radon alone. In general, lung cancer is known to be caused by numerous risk factors including active and passive smoking, radon, family history, occupational carcinogens and ambient air pollution (NRC, 1999b). Among all risk factors, individuals who smoke cigarettes are at the ultimate risk (Thomas, 2016). In those who have never smoked, exposure to radon progeny is the primary cause of lung cancer (NRC, 1999b). Studies showed that radon-induced lung cancers are statistically higher for smokers than individuals with a long life non-smoking record (Lubin et al., 1995; Hopke et al., 2000; Darby et al., 2001; Darby et al., 2005). Even under circumstances whereby the exposure is below the reference level set of a few hundred Becquerels per cubic meter, smokers happen to be at high risk. This is a resultant factor of the synergism relationship found between radon exposure and smoking.

The synergy between the two lung cancer causes is explained by the fact that smoking becomes responsible in modifying the risk linked with radon offspring by merely altering the bronchial morphologic and physiologic parameters in individuals who smoke (NRC, 1999b). It impairs the regular functioning of the lung by increasing mucus generation and slowing down the mucus clearance out of the lungs thus modify the makeup of bronchial tissues (Bias et al., 2009). In addition, the particulates from smoke allow more radon progeny to be deposited, therefore amplifying the radiation dose received by the lung cells (Samet, 1989). The exposure to other occupational carcinogens such as arsenic, asbestos, nickel, mine dust and chromates result in an absolute risk that alters the effects of radon decay products (NRC, 1999b; Lubin et al., 1995). The compounds of these elements; nickel, chromium (IV), arsenic have long been classified as carcinogens by the International Agency for Research on Cancer (IARC, 1990; 1991).

Extensive studies on underground miners across various countries including Czech Republic, USA, Canada, Australia, China, France and Sweden, demonstrated a strong correlation between radon and lung cancer (NRC, 1988; Samet, 1989; Lubin et al., 1995). At present, the evidence for lung cancer occurrence as a result of radon exposure is quantitatively available from different published works (Darby et al., 2005; 2006; Krewski et al., 2006). Even though there is adequate evidence on the cause of lung cancer by radon, other effects were documented. A positive relationship was found between radon and leukemia even though it showed a weak correlation (IARC, 2012). Gastrointestinal cancers are also suggested to be a potential consequence induced by drinking water with high levels of radon (Hopke et al., 2000; Zhuo et al., 2001; Kendall and Smith, 2002). Also, the cancer of the gallbladder and liver were also found to be the possible radiological effects associated with radon exposure (Tomasek et al., 1993). Most studies attempted to identify the risk beyond lung cancer but failed to obtain sufficient evidence on other possible radiological effects associated with inhaled radon (Tomasek et al., 1993; Darby et al., 1995; Auvinen et al., 2005; Sethi et al., 2012; Kruezer et al., 2015). To date, no scientifically proven cancer is linked to the intake of radon other than the cancer of the lung.

5 METHODOLOGY

Prior to the undertaking of the study, a literature review on the topic was conducted in order to identify the major problems, gaps and to select the appropriate study site.

5.1 Field reconnaissance survey

This part of the study played an important role in selecting a defined area of study and identifying specific areas to be sampled. The survey was done with the purpose of obtaining ample information with reference to the area and further identifies the location, accessibility and distribution of gold mine tailings. The survey also involved preliminary sample collection of rocks, tailings and water.

5.2 Field work

5.2.1 Sampling of rocks, tailings, water and construction material

Samples from outcropping rocks, tailings, bricks and water (acid mine drainage, drinking water and ponds) found within the study area were collected from various locations (Figure 14 and Table 5). Twelve (12) tailings samples, and ten (10) rocks samples were collected whereby four (4) were collected in the same locations where tailings were sampled. Bricks were also collected in order to determine their chemical concentration and assess their potential impact on radon accumulation based on their uranium concentration. The collected samples were kept in plastic bags to avoid contamination.

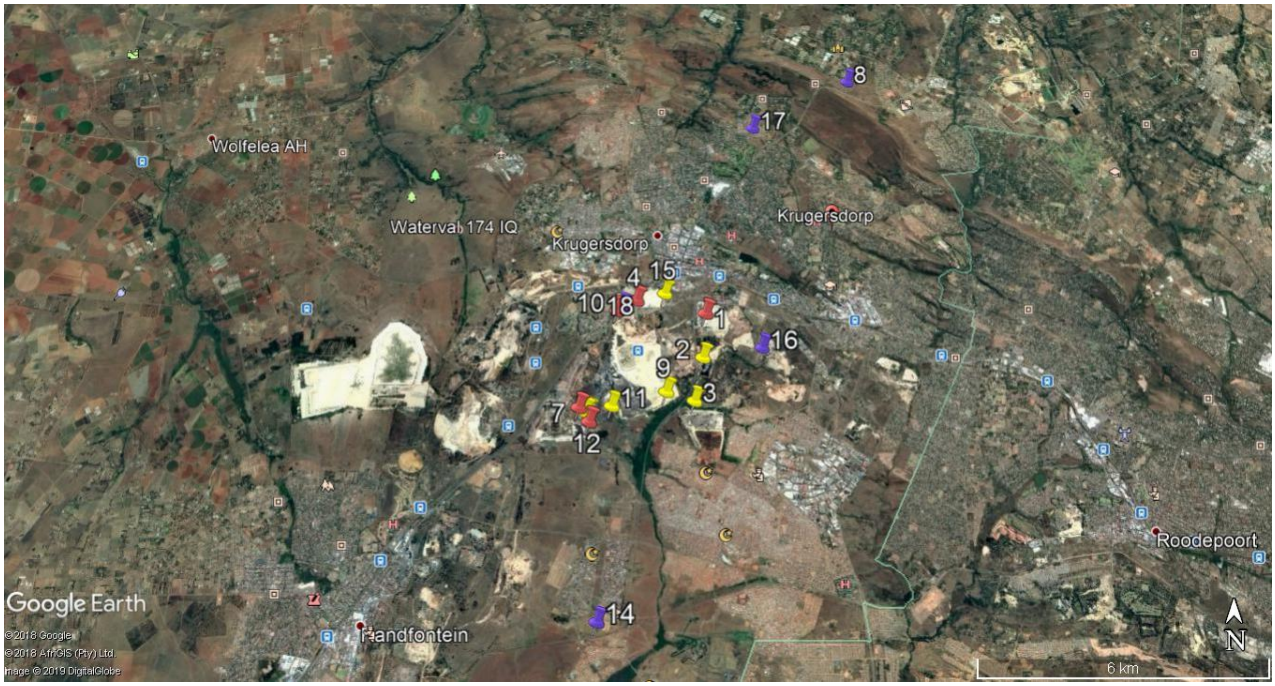


Figure 14: Satellite map of sampling sites dominated by tailings whereby red shows the locations where both rocks and tailings samples were collected at same location, yellow indicate tailings only and purple indicate rocks. The sample numbers correlate with the data given in Table 5 below.

Table 5: Sampling locations for tailings and rock samples collected in the study area.

Site number	Sample name	Sample location (Latitude, Longitude)	Sample category
1	TA/PB01R TA/PB01T	-26.119892, 27.776561	Rock Tailings
2	TA/PB02T	--26.129200, 27.775761	Tailings
3	TA/PB03T	-26.116977, 27.773686	Tailings
4	TA/PB04T TA/PB04R	-26.116977, 27.760878	Tailings Rock
7	TA/PB07T TA/PB07R	-26.139619, 27.748022	Tailings Rock
8	TA/PB08R	-26.064590, 27.812880	Rock
9	TA/PB09T	-26.136370, 27.767440	Tailings
10	TA/PB10T TA/PB10R	-26.119260, 27.756470	Tailings Rock
11	TA/PB11T	-26.139290, 27.756470	Tailings
12	TA/PB10T TA/PB10R	-26.142530, 27.750320	Tailings Rock
13	TA/PB13T/Top TA/PB13T/Bottom	-26.140590, 27.749440 -26.140526, 27.749988	Tailings Tailings
14	TA/PB14R	-26.181110, 27.752360	Rock
15	TA/PB15T	-26.115520, 27.767340	Tailings
16	TA/PB16R	-26.127230, 27.789090	Rock
17	TA/PB17R	-26.076560, 27.789080	Rock
18	TA/PB18R	-26.118437, 27.757625	Rock

Water samples were collected during the rainy season from five locations (AMD, runoff from tailings, municipal water (tap) and two ponds) (Figure 15). The sampling was based on the availability of water points found in the area. Figure 16 and Table 6 present the sampling localities of water samples. Physio-chemical parameters for each water sample were directly measured in the field using AQUARead instrument. The instrument measures Temperature, pH, Total Dissolved Solids (TDS), Electrical Conductivity (EC), Oxidation-Reduction Potential (ORP) and Dissolved Oxygen (DO). This was done with the purpose of determining the water quality based on the standards set by WHO (2008) and DWAF (1996), and to understand the geochemical behavior. For quality control purposes, the samples were kept in bottles in a cool place and prior to sampling, the bottles were rinsed 5 times with sample water. Before collecting tap water, the tap was left running for 5 minutes.



Figure 15: Various water sources where water sampling was conducted, (a) tailings dam (pbw2) (b) Runoff from tailings (pbw3) (c) pbw5 and (d) pbw6 ponds.



Figure 16: Satellite map of sampling locations for water collected in the study area. The sample numbers correlate with the data given in Table 6 below.

Table 6: Sample location for water collected in the study area.

Sample name	Sample location	Sample category
Pbw2	-26.129990, 27.776035	Tailings pond
Pbw3	-26.137560, 27.773678	Runoff from tailings
Pbw4	-26.117100, 27.761483	Municipal tap water
Pbw5	-26.145500, 27.757087	Pond in the vicinity of mine tailings
Pbw6	-26.141715, 27.752211	Pond in the vicinity of mine tailings
Pbw7	-26.124337, 27.774225	Runoff from tailings

The collected rock, tailings, water and brick samples were analyzed for a variety of chemical constituents in order to determine their absolute concentration using ICPMS and XRF (X-ray Fluorescence Spectrometry) techniques, most importantly to measure the uranium content of the collected samples. The study only employed these techniques as other more sophisticated methods for analyzing individual radioactive species proved to be more costly. Metal determination for these samples will help in identification of major sources for toxic metals and gases.

5.3 Analytic procedures

5.3.1 Chemical analysis for rocks, tailings and bricks using XRF

5.3.1.1 Overview on XRF technique

X–Ray Fluorescence (XRF) is one of the analytical techniques well-known to measure concentrations of elements in materials such as rocks, sediments and fluids. It operates on the principle that when atoms get excited by incident X-ray radiation, they release excess energy in the form of fluorescent X-ray radiation. Therefore, the resultant fluorescent x-rays emitted, due to their relative specific characteristic are used to estimate and quantify the elements present in a sample.

5.3.1.2 Sample preparation and analysis

The rock, tailings and brick samples were prepared into a fine powder in the Crushing and Milling Laboratory at the University of the Witwatersrand. The tailings samples were dried before milling procedure was undertaken. For quality control, the crushing and milling machines were cleaned with water, acetone and quartz crystals for preparation before every sample. The milled samples were packaged, labeled and submitted to the EARTH LAB at University of Witwatersrand for qualitative and quantitative analysis of elemental composition by XRF.

The samples were then pressed into pellets whereby the fine powder was ground to a grain sizes of less than 75µm and mixed with a binding aid of cellulose wax mixture. It was then compressed at a pressure of between 20T and

30T to form a homogenous sample pellet and taken for chemical analysis. This preparation technique was chosen because it yields homogenous samples with no void spaces, which give more accurate analytical results than loose powders. It is considered an appropriate approach for analysis of traces. The results obtained are presented in Appendix A.

5.3.2 Chemical analysis for water samples by the use of XRF

Water samples were collected with 100 ml bottle and submitted to the EARTH lab for determination of trace elements in order to obtain an insight in the concentration and understand the chemical characteristics of water. The Handheld XRF instrument was used for this analysis whereby water was poured into cups and then covered with a Mylar film that provides transmission capabilities for the X-ray analyzer to detect the trace elements present. The instrument was put into contact with the Mylar film for 180 seconds. The uranium soils method with high sensitivity in detecting uranium was selected during analysis.

5.3.3 Stable isotope analysis

Stable isotopes of oxygen ($\delta^{18}O$) and hydrogen ($\delta^{2}H$**)** display different isotopic signatures in waters of different types, and are therefore used in various applications in hydrology. Most importantly they can be used to characterize water in terms of the origin, trace the movement of water through the hydrologic cycle and provide significant insights on aquifer evolution (Fitts, 2002; Hiscock, 2005). They also help in identifying possible interactions between pollutants (e.g. acid mine drainage) and various water sources, and in addition, trace the geochemical history.

To conduct the analysis, 10 ml of sample was collected and analysed in the Hydrogeology Laboratory, University of the Witwatersrand with the Liquid Water Isotope Analyzer-model 45-EP machine. The machine is made of various components including a laser analysis system and an internal computer, a membrane vacuum pump, a liquid auto-sampler and a room air intake line that enables air transport via a drierite column for moisture removal. The sample was pipetted into a 2 ml vial and closed with polytetrafluoroethylene septum caps. The sample (0.75µl) was then injected into a polytetrafluoroethylene septum in the auto sampler using a Hamilton microlitre syringe. To vaporize the sample injected, the injection port contained in the auto-sampler was heated to 46˚C. For each sample standards with known values of $\delta^{18}O$ and $\delta^{2}H$ were used for analysis. The machine automatically standardizes itself and records values of measured stable isotopes, with the precision of about 0.2‰ for $\delta^{18}O$ and 1‰ for $\delta^{2}H$. The values are reported as δ notation which is expressed in parts per 1000 relative to the standard. The results are reported by the use of plots whereby the observed trends help in delineating the origin and possible interactions between different water samples. The analytical results are reported in Appendix B.

5.4 Geochemical and hydrogeochemical standards and background values

To evaluate the degree of contamination caused by trace elements and radionuclides contained in gold tailings, the measured levels were compared with the background and standards values. This was important in identifying if the concentrations obtained were within or above the standards, thereby helping to assess chemical and radiation toxicity along with possible health impacts. Table 7 summarizes the range of background values found in South

African soils and the soil quality standards. With regards to water samples, the guidelines values for potable water are presented in Table 8.

Table 7: (1) Statistical summary of metal concentration in A-horizon of South African soils (From: Herselman et al., 2005) and (2) the target standard value from Dutch list (From: Netherlands Ministry of housing, physical planning and Environment, 1997)

Trace element	**Cr**	**Ni**	**Pb**	**Zn**	**Cu**	**Co**
1.Range (mg/kg) (Background)	5.82-353	3.43-159	2.99-65.8	12.0-115	2.98-117	1.51-68.5
Average (mg/kg)	71.9	38.7	21.7	45.2	29.5	18.0
2.Target value (mg/kg)	100	35	85	140	36	20
Intervention value (mg/kg)	380	210	530	720	380	240

Table 8: Guideline values for physical parameters and uranium in potable water recommended by WHO (2008) and DWAF (1996).

Physiochemical parameters	**Guideline values for potable water (WHO, 2008)**	**Guideline values for potable water (DWAF, 1996)**
pH	6.5-9.2	6-9
TDS (mg/l)	100-500	0-450
EC (µS/cm)	300	-
Chemical element	**Guideline value (mg/l)**	**Guideline value (mg/l)**
Uranium	0.015	-

5.5 Radon monitoring

5.5.1 Radon monitoring

Measuring radon concentration is a prerequisite for understanding the occurrence and distribution of radon in the natural environment and also plays a significant role in risk assessment and development of effective management plans (Nero et al., 1990). There are different well-established methods used to measure radon concentration in the environment; identified as active and passive techniques. The active method encompasses alpha spectrometry, filters and pumps and is effective for short-term radon measurements. On the other hand, the passive method operates on the principle of alpha track detection and useful for long term measurements (Tommasino, 1990). This study employed the passive method using the solid-state nuclear track device.

5.5.2 Solid-state nuclear track device (RGM_S)

The solid-state nuclear track device (RGM_S) was used specifically for this study (Figure 17). The device is comprised of a white membrane at the base of the monitor which is used as the filter material to allow only gases to enter the monitor. It has a 1 mm CR-39 plastic material**,** which is a polyallyl diglycol carbonate (PADC) known to be highly sensitive to alpha particles. The black O-ring is used to hold the CR-39 material in place. Each monitor has its own bar code specification (Figure 17). The device operates in such a way that when alpha particles are produced by radon nearby the measuring device, they strike the device thus leaving microscopic areas of damage on the film. It is simple to utilize at relatively low cost. The fact that it is insensitive to temperature and humidity makes it more advantageous. Furthermore, it is well suited to provide desirable measurements for longer periods with high precision thus very effective and useful for remediation purposes (Baskaran, 2016).

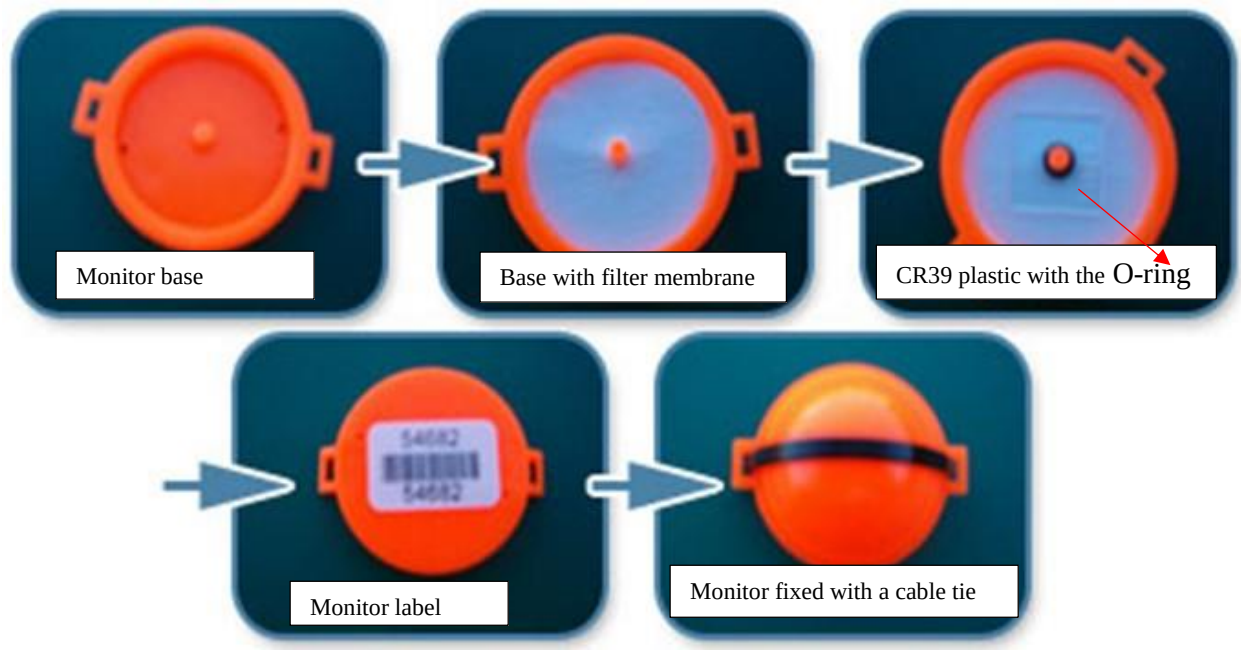


Figure 17: Radon Gas Monitors (RGM_S) (From : Parc RGM).

5.5.3 Sampling site selection and measurement

Radon concentration is significantly determined by the type of soils and rocks present in the local environment and man-made facilities such as uranium tailings. In nature, it is expected that areas with high levels of uranium have greater chances of experiencing high radon concentrations. Since the release of radon from tailings dams could be a major health problem for people residing nearby, the survey is aimed to determine the general levels of radon in the area in order to obtain estimates on the amount of radon released and radiological doses received by the population residing nearby the abandoned mining areas. It is impossible to differentiate between the natural and man-made radon contributions from average radon levels only. The only reliable way to analyse the potential sources of radon was by measuring the levels released from tailings as well as from the natural background. As such, the measurement localities for outdoor monitoring were classified into four different categories as outlined in Table 9 in order to understand the occurrence and distribution of radon in the area.

Table 9: Classification of radon monitoring sites.

Category	**Definition**
Directly on tailings	Measurement points located directly on tailings
Nearby tailings	Measurement points within a range of less than 1 km from tailings
Background	Measurement points within the selected study area representing natural contributions from soil and rocks. These points are situated far away from mining disturbances in geologically similar areas.
Controls	Measurement points outside the selected study area in regions with similar rock types and meteorological characteristics but far away from tailings.

In general, the main focus was on outdoor measurement rather than indoor measurement in order to assess if the tailings distributed throughout the area hold a greater potential to generate elevated radon levels, which could impact on the health of people residing in the area and neighboring regions. For the reason that the study is also aimed at presenting health hazards related to radon exposure, some radon monitors were placed in houses nearby the tailings in the Krugersdorp area. However, accessibility to place monitors indoor was a challenge, thus only two (2) monitors were placed in occupied dwellings and three (3) in abandoned houses in the study area. Since radon levels can differ significantly owing to various parameters including the distance from mine tailings, seven (7) radon detectors were also placed in houses away from uranium mining disposal sites in the same geological units for quality control and assurance.

The total of 60 RGM_S were installed across the Krugersdorp and surrounding areas (Figure 18 and 19), however, 5 monitors were damaged by bush fire. The measurement points were chosen with respect to the convenience of installing the monitors. Each monitor had a specific label attached at the base and was placed above the ground in an upright position, mostly tied to the tree stem or branches, fence and electric poles in order to continuously measure the radon concentration. The first 30 monitors were left in the field for 3 months from late August to late November 2017 during the first round of radon monitoring (Figure 18). A second round field installation was conducted on the 10th of March 2018 and monitors were collected on the 10th of June 2018 for analysis. The measurements were performed during two different periods in order to obtain representative overview of exposure. In addition, the second radon monitoring was done with the objective to establish a detailed dataset and enhance the statistical power of the results. Hence, monitors were concentrated in and around similar locations where elevated radon levels were identified during the first radon survey. Also, the background measuring points were expanded with 4 new monitoring points and 2 in similar locations where first radon survey was done in order to make out for deficiencies. All monitoring points for the second period are presented in Figure 19. Appendix C shows localities for all measurements.

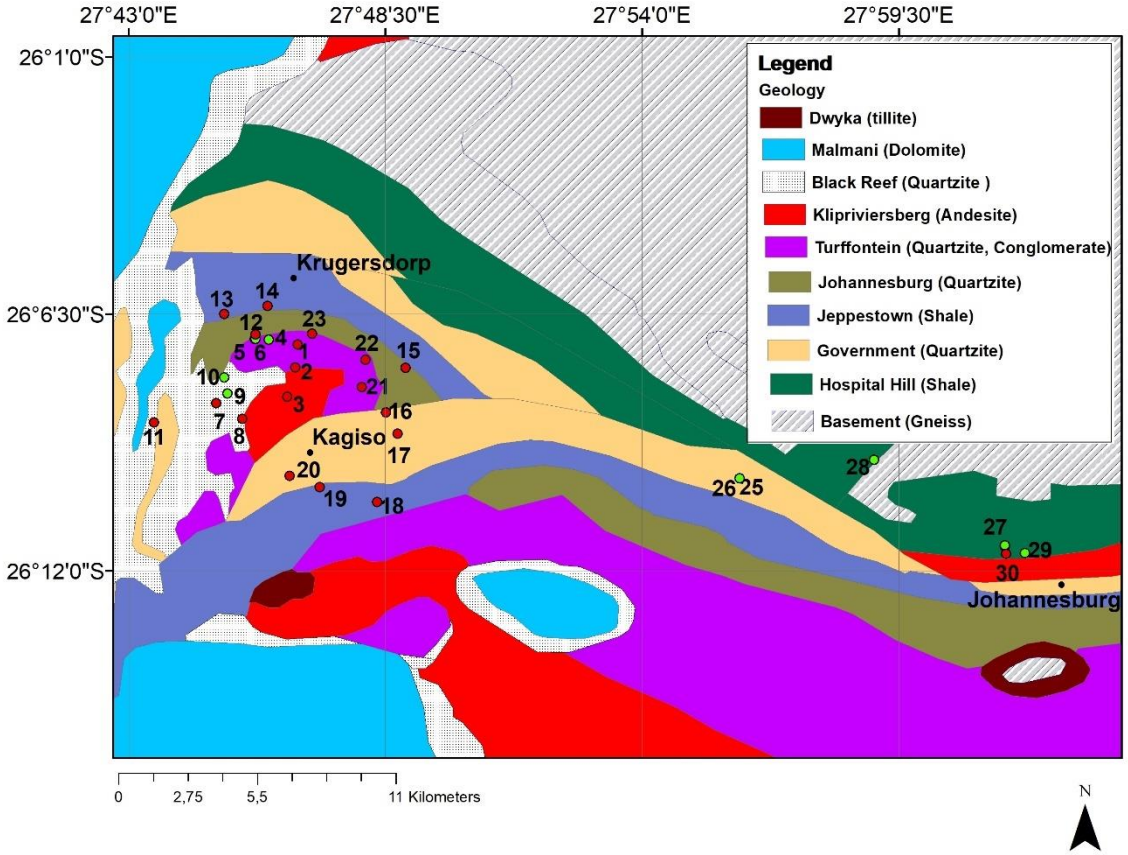


Figure 18:Radon monitoring points for first period. Red dots indicate outdoor points and green dots represent indoor points.

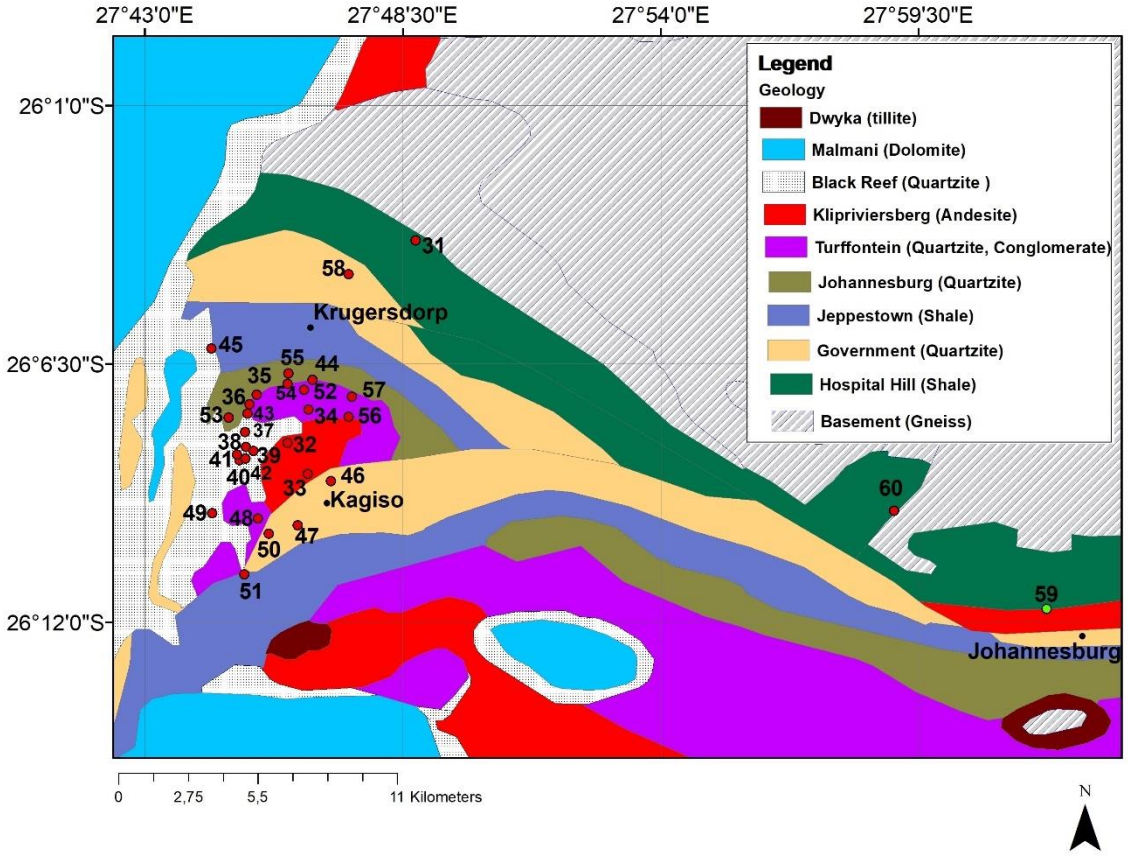


Figure 19:Localities for second radon monitoring period. Red dots indicate outdoor points and green dots represent indoor points.

5.5.4 Laboratory analysis

Following three months of exposure, the RGM$_s$ were retrieved and submitted to the Parc RGM laboratory, Pretoria for chemical etching analysis. The sheets are etched by the use of NaOH solution at 90 ˚C (Figure 20). The etching process enhances the visibility of alpha tracks on the film and thus makes them observable by the use of light microscopy. The tracks are then individually counted through the use of visual detection and a computer automated system (Figure 21). Measurement of radioactivity is done in Becquerels (Bq) whereby one Becquerel is equivalent to one atomic disintegration per second. For radon, the level of radioactivity measured represents the quantity of radioactivity in air volume for a definite time period. As such, the number of tracks per unit area is equivalent to radon exposure in Bq.h/ m^3, which gives the amount of Becquerels (Bq) in a cubic meter of air (m^3) for a specified time period (h), in this case hours (see Appendix D). To change to the standard unit of Bq/m^3 which gives radon concentration (Equation 1), the values were divided by the total number of hours placed in the field which is equivalent to 3 months (2208 hours) as indicated in Appendix E.

Radon concentration = Exposure/ exposed time = (Bq/m^3) ……. (1)



Figure 20: Laboratory apparatus used for etching and washing (From: Parc RGM).

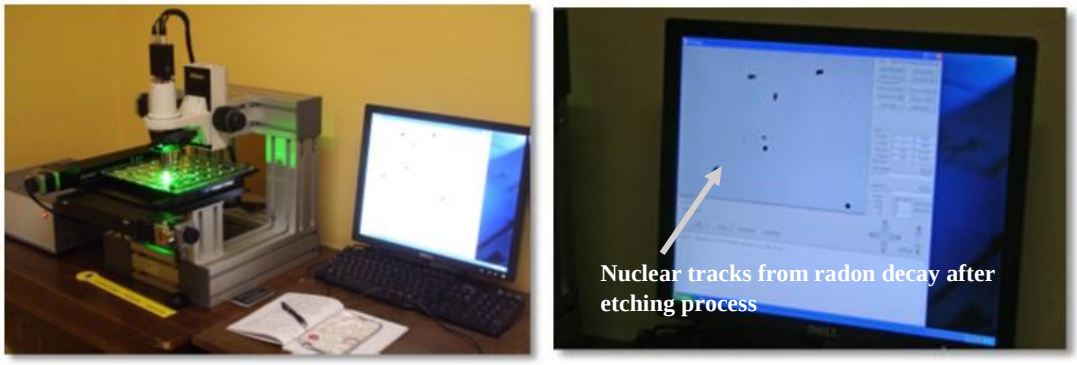


Figure 21: Light microscopy and automated computer-based technique used for counting nuclear tracks (From: Parc RGM).

5.6 Effective dose

Effective dose is defined as the sum of the tissue-weighted equivalent doses adsorbed by particular body organs and tissues (ICRP, 2013). It is mainly used for radiological protection purposes, to assess compliance with reference levels set and optimize protection for the public (ICRP, 2007). The unit for representing effective dose is sievert (Sv).

There are various methods available to compute annual effective dose employing different radon equilibrium factors and dose conversions (Ravikumar and Somashekar, 2013). In this study, the estimation of the annual effective dose to the population due to radon and its decay products is assessed by the use of UNSCEAR model (2000) as it uses the radon dose conversion factor that aligns with dosimetric and epidemiological dose conversions thus results into more reliable results (Chen, 2005). According to the UNSCEAR model (2000) the annual mean effective dose is estimated by the following equation 2:

$$E = C \times F \times H \times T \times D \ldots\ldots\ldots (2)$$

Where:

E: Effective dose

C: Radon concentration

F: Occupancy factor whereby for outdoor is (0.2) and indoor is (0.8)

H: Equilibrium equivalent concentration factor outdoor (0.6) and indoor (0.4)

T: Hours in a year (8760 h/y)

D: Dose conversion factor (9×10^{-6}(mSv $(Bqhm^3)^{-1}$)

The UNSCEAR (2000) model further represent global average of indoor annual effective dose equivalent to 1.0 mSv and outdoor annual effective dose equivalent to 0.095 mSv based on typical worldwide concentration as stated in equation 3 and 4.

Indoors: 40 Bq m^3 × 0.4 × 7,000 h × 9 nSv (Bq h m^3) $^{-1}$ = 1.0 mSv …… (3)

Outdoors: 10 Bq m^3 × 0.6 × 1,760 h × 9 nSv (Bq h m^3) $^{-1}$ = 0.095 mSv…… (4)

The ICRP (2013) recommended dose limit of 1 mSv/y from all radiological sources for public exposures. NNR (1999) also recommended the annual effective dose limit of 1 mSv for the public. For waste disposals dose limit of 0.3 mSv/y is recommended (ICRP, 2013). The global average effective dose is estimated to be 1.15 mSv/y by UNSCEAR (2000) whereas ICRP (1993) recommended a dose of 3-10 mSv/y as the action level in indoor.

5.7 Data analysis and evaluation

To evaluate geochemical, hydrogeochemical and radon data acquired, statistical and spatial analysis were employed. Descriptive statistical analysis, which includes computation of minimum, median, arithmetic mean, geometric mean, range and standard deviations was used to get an overview on the general concentration levels and relative elemental abundance. This was also useful in determining outliers and spatial distribution. The calculated figures obtained were then compared with recommended limits (guideline values). Correlation coefficients were calculated using the Spearman approach with the purpose of identifying relationships among the variables. Spearman approach was calculated by the following equation (5).

$$r_s = 1 - \frac{6\sum d_i^2}{n(n^2-1)}. \qquad \text{…….. (5)}$$

d_i = denotes the difference between the two ranks of each observation

n = number of observations

Spatial analysis was used to establish the distribution of radon, also, to find correlation between radon and other parameters. ArcGIS (version 10.5) was used for this analysis. The Inverse Distance Weighted (IDW) interpolation

method was employed to show the spatial distribution of radon in the study area. This method was selected as the most appropriate as it assumes that the influence of the mapped variable decreases with distance from its point of measurement. Thus, give more weight to the sampled points.

5.8 Existing data collection

Existing data on lung cancer has been collected from the National Cancer Registry in order to obtain statistics on lung cancer incidences, and also from StatsSA with the aim of obtaining statistics on deaths related to lung cancer. Thereafter, correlated the statistics with the obtained data from radon monitoring. To further compare lung cancer rates and maintain the quality of the findings, two municipalities in the Eastern Cape were selected as control. The selection criteria was based on the fact that the areas are located in a region with less mining activities (Figure 22) that could be linked to radon exposure and in a province with comparable smoking prevalence as the Gauteng Province where the study site is located as indicated in Reddy et al. (2015). The municipalities selected include the Joe Gqabi municipality with comparable population statistics to the Mogale City Local Municipality and OR Tambo district municipality with the highest population numbers. Table 10 present detailed classification for both the target and reference population.

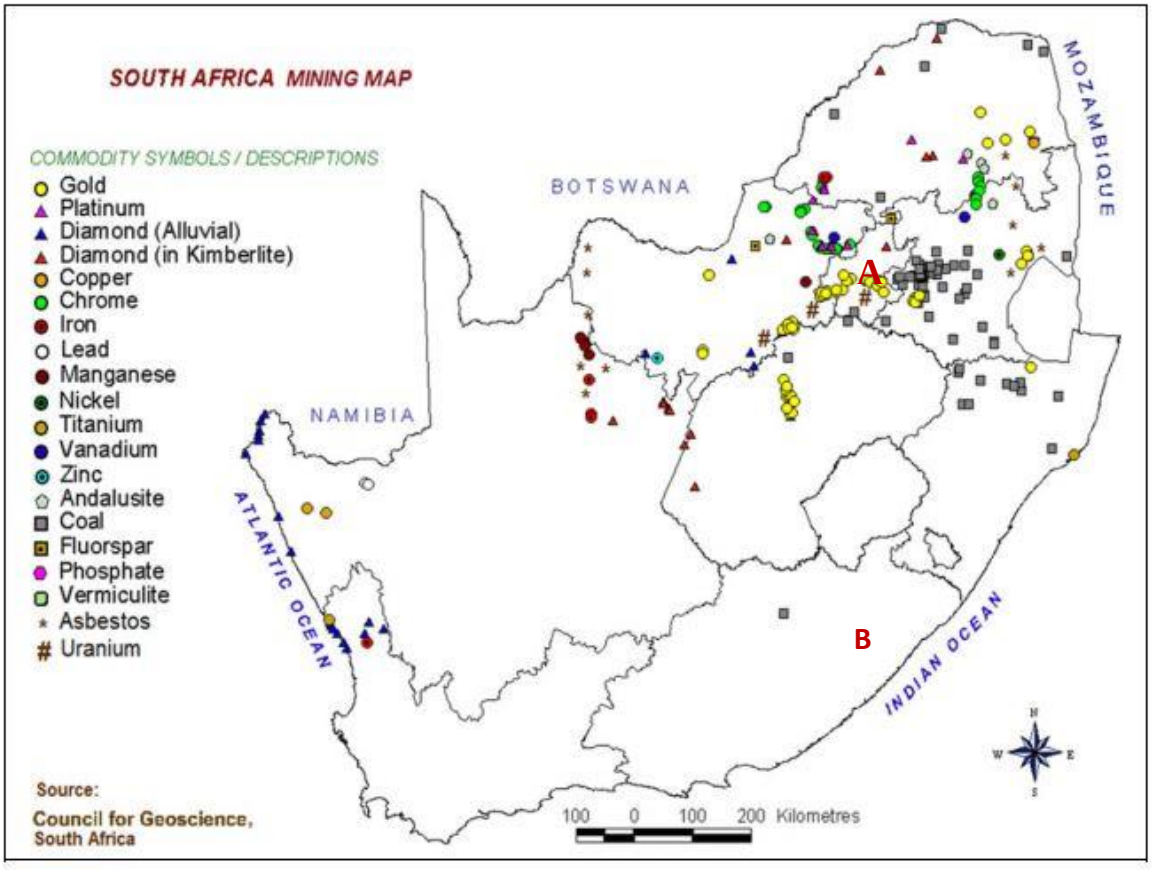


Figure 22: Distribution of mining in South Africa. Point A is the target population and point B is the reference population (From: Council for Geoscience).

Table 10: Detailed classification for both the target and reference population

Category	Description	Location	Population (Data source :StatsSA)
Target population	Exposed population in an area dominated by mining activities and abandoned tailings	Mogale City Local Municipality, Gauteng	362 421
[1]Reference population [2]Reference population	Unexposed population in non-mining area	Joe Gqabi Municipality, Eastern Cape OR Tambo Municipality, Eastern Cape	349 768 (Comparable to the target population) 1 364 943 (Higher than the target population)

6 RESULTS AND DISCUSSION

6.1 Rock and tailings geochemistry

6.1.1 Overall trace element concentration

Figure 23 summarises the concentration of trace elements found in mine tailings and rocks collected in different locations within the study area. The data show overall elevated concentrations in tailings than rocks (Figure 23). This is due to elevated levels of toxic metals concentrated in the ore crushed placed in tailings than it is in the outcropping quartzite and shale found in the study area. Exceptionally high levels in tailings are represented by Cr, Ba, Ni, Zn and Pb (Figure 23). In general, tailings show a wide variability in metal concentration which is dependent upon variable parameters including the amount of elements initially contained in the ore, the content of the matrix, the separation processes used for recovery of gold and oxidation processes (Rosner, 1999). Therefore, in order to get an insight into the elemental abundance, the geometric mean values were used in order to account for the highest values found in specific samples. The trend reveals elemental abundance in a decreasing order of: Cr > Ba > Ni > Zn > Pb > Zr > Cu > Sr >V > Co > Y > U > Ga > Sc > Rb > Nb > Th > Mo. Correspondingly, rocks indicate relative abundance of Cr > Zr > V > Ba > Ni > Cu > Sr > Pb > Y > Rb > Ga > Zn >Co > Nb > Sc > Th > Mo > U in accordance to decreasing order of geometric mean values (Figure 23). In this study, uranium and thorium are of main interest due to their importance in the formation of radon. Also, to the lesser extent the study focuses on Cr, Ni and Pb owing to their carcinogenic nature (IARC, 1990; 1991) and high levels in the studied tailings samples.

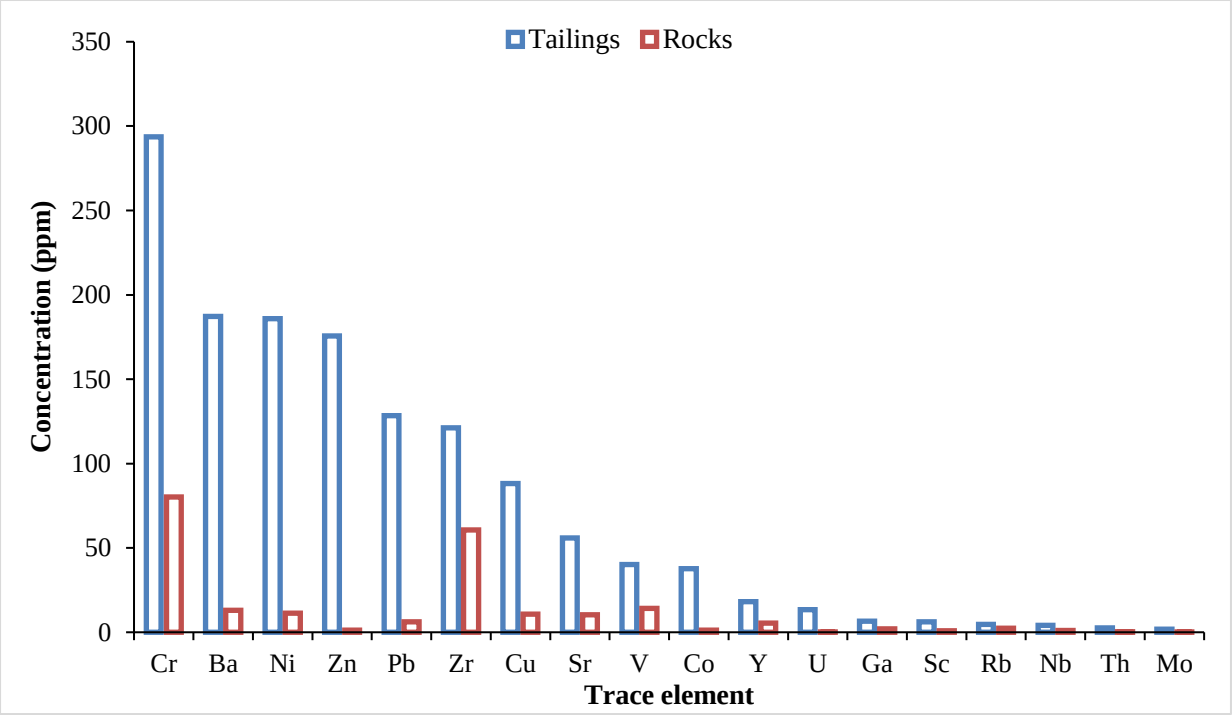


Figure 23: Comparative plot of trace element concentrations in tailings and rocks using geometric mean in order to account for highest concentrations of trace elements for specific samples.

6.1.2 Uranium and thorium concentration in rocks and tailings

The uranium and thorium concentration found in rocks and tailings are presented in Table 11. With respect to uranium, concentration ranged between a detection limit (0.01 ppm) and maximum of 149.76 ppm with a mean value of 48.87 ppm in the tailings (Figure 24). The rocks indicate an extremely low non-detectable content of uranium with a maximum of 1.14 ppm (Table 11), but could not be taken as a representative of the whole area as sampling was limited to outcropping rocks. Nevertheless, the large-scale detailed studies conducted by Wronkiewicz and Condie (1987; 1990), showed that the lithological units distributed within the study area generally contain uranium that ranges between 0.007 ppm to 4.5 ppm**.** To the greatest extent, uranium content in tailings exceeds the concentrations found in rocks; indicating higher concentrations of uranium when compared to typical natural background concentration of about 2 to 4 ppm (NRC, 1999a; Rosner, 1999). This is due to the fact that the geochemical composition of tailings reflects that of the primitive ore which is highly mineralised with uranium bearing minerals such as uraninite (Rosner, 1999) than the outcropping rocks collected.

Similarly, thorium in tailings varied from a minimum of below detection limit to 90.61 ppm with the average 16.69 ppm. In rocks, thorium showed a maximum of 4.47 ppm with an average of 1.28 ppm which falls well within the average thorium concentration of about 10 ppm found naturally in the earth's crust (NRC, 1999a).

Table 11: Statistical summary of uranium and thorium found in tailings and rock samples collected in the study area in ppm (d.i stands for values below detection limit of 0.01 ppm)

Element	Source	Total count	Minimum	Median	Arithmetic Mean	Geometric Mean	Maximum	Standard Deviation
U	Tailings	12	d.i	35.34	48.87	13.42	149.76	48.09
	Rocks	10	d.i	0.00	0.14	0.02	1.4	0.44
Th	Tailings	12	d.i	11.68	16.69	2.49	90.61	24.68
	Rocks	10	d.i	0.52	1.28	0.20	4.47	1.63

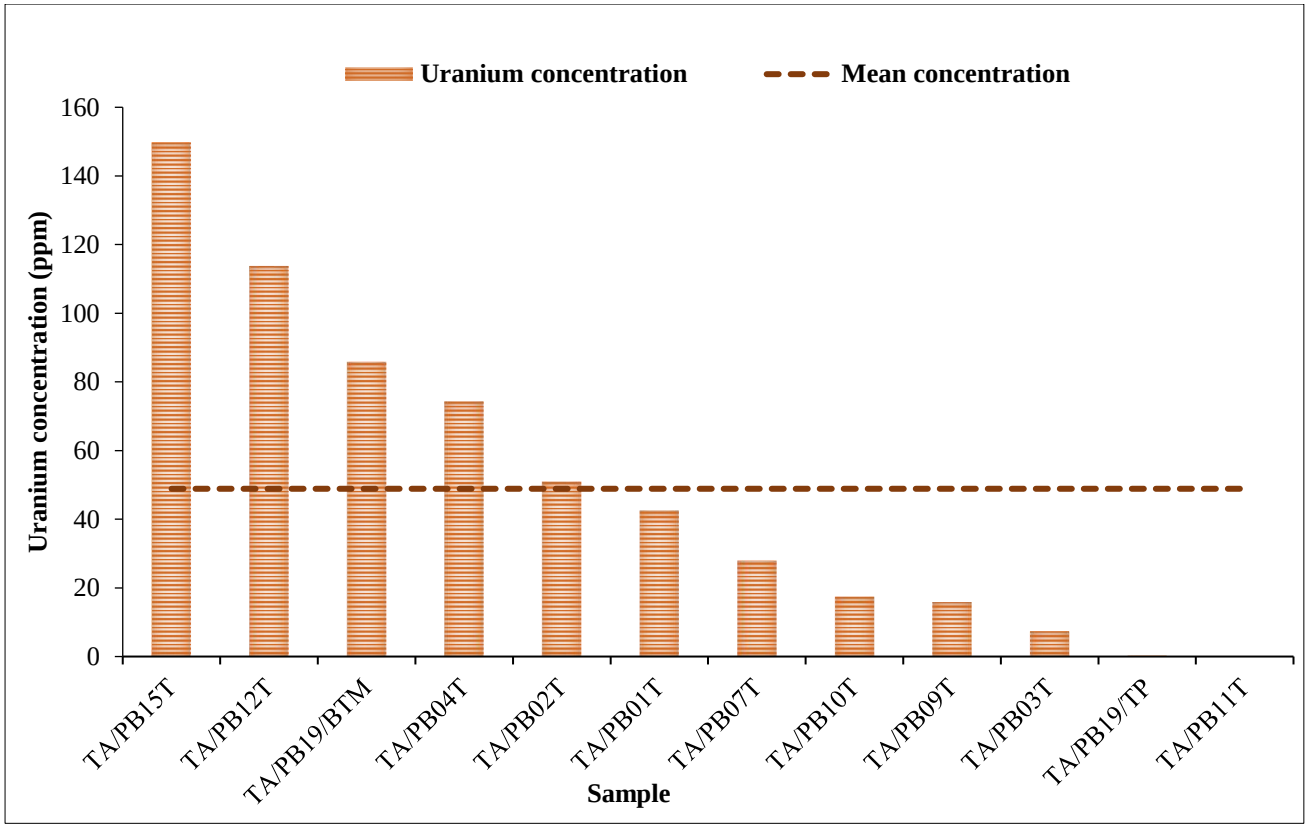


Figure 24: Uranium concentration in tailings samples in the study area with mean value of 48.8 ppm.

6.2 Hydrochemistry

6.2.1 Physiochemical parameters

The physiochemical properties of water samples collected are presented in Table 12. The pH of surface waters found in the study area was highly variable, with mine waters portraying highly acidic pH condition of 2.63. Slightly high pH conditions ranging between 5.09 and 6.33 were measured in the surface water from ponds in the vicinity of the mining area. The levels fall outside the WHO (2008) guideline range of 6.5-9.2 and DWAF (1996) range of 6.0-9.0. Exceptions occur in municipal tap water with pH of 6.52 and sample pbw6 with pH of 6.33.

The mine waters also show very high Total Dissolved Solids (TDS) that fall within a range of 4524 mg/l and 5012 mg/ l with very high electrical conductivity (EC) values that range between 6917 µS/cm and 7594 µS/cm. The pond waters show variable TDS (249-2031 mg/l) and EC (384-3117 µS/cm) with highest levels in pbw5 (Table. 12) which is a result of the dissolved organic matter from the plants at the margin of the pond (Figure 25). Both water from mine effluents and ponds showed TDS values above the permissible range of 100-500 mg/l and 0-450 mg/l recommended by WHO (2008) and DWAF (1996), respectively. The only exception was in tap water with TDS of 137 mg/l. With regards to the Oxidation-Reduction Potential (ORP), mine waters showed values with a range between +410.4 mV and +586.6 mV indicating oxic conditions. In general, the characteristics observed in mine waters portray the natural features of acid mine drainage (Rosner, 1999; Abiye, 2014).

Table 12: Field measured physio-chemical parameters

Parameter	Sample pbw2	Sample pbw3	Sample pbw4	Sample pbw5	Sample pbw6
Location	**Latitude: S26^{0}07.7994 Longitude: E27^{0}46.5621 Tailing dam**	**Latitude: S26^{0}08.2536 Longitude: E27^{0}46.4207 Runoff from tailings (leachates)**	**Latitude: S26 ^{0}06.9978 Longitude: E27^{0}45.6755 Tap water (municipal water)**	**Latitude: S26^{0}08.7300 Longitude: E27^{0}45.4252 Pond**	**Latitude: S26^{0}08.5029 Longitude: E27^{0}45.1326 Pond**
pH	**2.63**	**2.63**	**6.52**	**5.09**	**6.33**
TDS (mg/l)	**4524**	**5012**	**137**	**2031**	**249**
EC (µS/cm)	**6917**	**7594**	**211**	**3117**	**384**
ORP (mV)	**+585.6**	**+410.4**	**-18.5**	**+242.7**	**+1431.2**



Figure 25: Dissolved organic matter in water in ponds found in the study area.

6.2.2 Uranium observations

The results in Figure 26 indicate that uranium concentration varied between 4.0 to 4.7 mg/l in mine waters. Highly acidic and oxidizing condition in waters allow for greater solubility of uranium (Bjorkuland et al., 2017). In mine waters high pH and positive ORP were documented, therefore, explaining the reason for high uranium levels found in mine effluents. In surface water from ponds in the vicinity of the mining area, uranium concentration ranged between l.93 mg/l and 2.59 mg/l, of which when compared to mine waters indicate approximately 2 times decrease in concentration. The wetlands at the inlet of surface water within the Witwatersrand Basin have been characterized as a potential sink for metal removal (Tutu et al., 2008; Abiye et al., 2018), therefore, it could be assumed as one of the phenomenal feature to result in general decrease of uranium in surface water from ponds as they are surrounded by wetlands. In particular with reference to their natural behavior of retaining metals through different processes (Dunbabin and Bowmer, 1992; Shoeran and Shoeran, 2006; Gandy et al., 2016), wetlands in the vicinity of mine tailings could potentially adsorb uranium and associated ^{222}Ra leached from

tailings, thereby, forming a possible hotspot for elevated radon levels. Relative to other water sources, municipal water collected in the area showed extremely low uranium level that is below the level of detection (Figure 26).

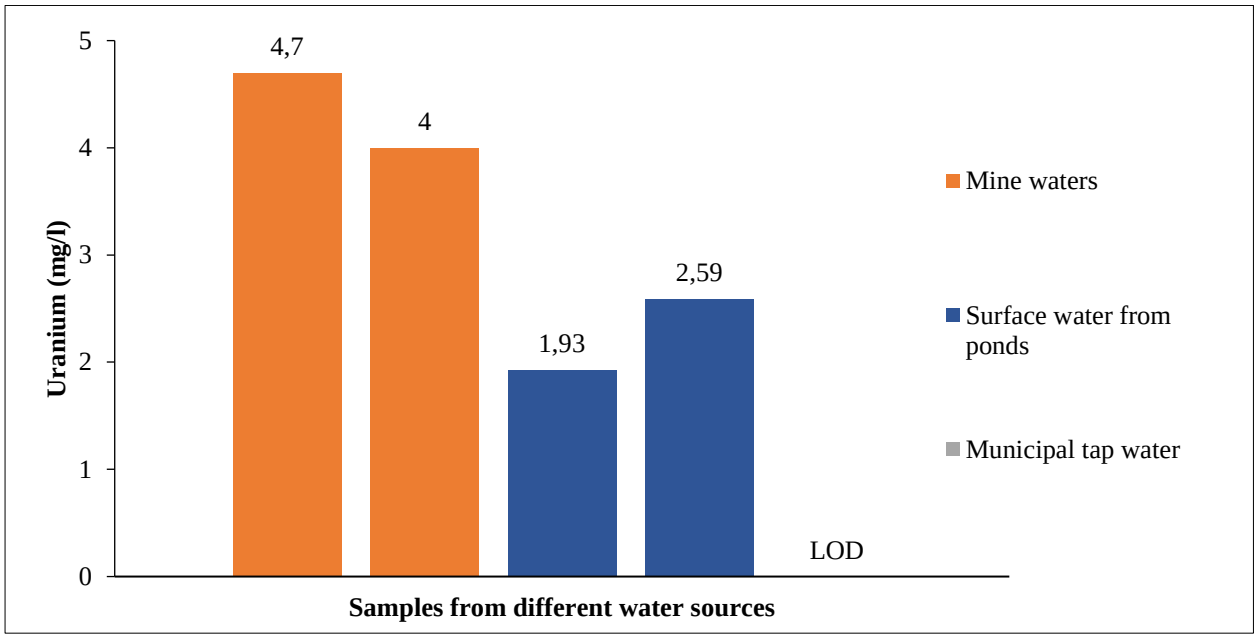


Figure 26: Uranium concentration (mg/l) in water samples collected in the study area. LOD represent Limit of Detection.

All the studied water points showed uranium levels above the guideline value of 0.015 mg/l recommended by WHO (2008) except municipal tap water. The high uranium content found in the pond samples resulted from leaching of tailings as they reflect high concentration of uranium. Thereby, indicating that the relatively high concentrations of uranium directly derived from the mine residues over which water flows**.** This is also evident from field observations (Figure 27). The leached water could subsequently percolate into aquifers that are in greatest proximity to tailings as documented in the studies of Naicker et al. (2003), Winde and Sandham (2004) and Abiye (2014), although it will depend on the flow regimes and direction of flow. The substantial contents of metals and radionuclides leached may concentrate in the soils nearby tailings (Rosner and Van Schalkwyk, 2000; Aucamp and Van Schalkwyk, 2003; Naicker et al., 2003) and result in levels higher than the background values documented from the study of Herselman et al. (2005). However, the contamination will highly be dependent on the availability, mobility and attenuation of such contaminants as well as the relative distance from the highly concentrated source (Rosner and Van Schalkwyk, 2000; Winde and Sandham, 2004).



Figure 27: Observed impact of abandoned gold mine tailings on surface water samples whereby during a rainy season leachate are generated from the gold mine tailings and be transported to nearby water points whereby they become deposited.

To further identify any relation between water leached from tailings and surface waters in the region, stable isotope plot was used where the data were plotted with the global meteoric line (Craig, 1961) and the Pretoria meteoric line (IAEA-GNIP) (Figure 28). The results indicate that mine waters plots adjacent to surface waters, suggesting that there is a likely possibility that these water points could be impacted by leachate from tailings. This also confirms that uranium found in ponds could be derived from the nearby tailings. However concentrations are lower than the amount found in mine waters due to precipitation and metal removal by wetland sediments and plants. This is also supported by physiochemical parameters measured which show low TDS and EC. Mine samples also show enrichment as a result of evaporation since the samples were collected from stagnant ponds. In summary, the hydrogeochemical results obtained indicate that mine dumps concentrate high quantities of uranium in water sources found in the area.

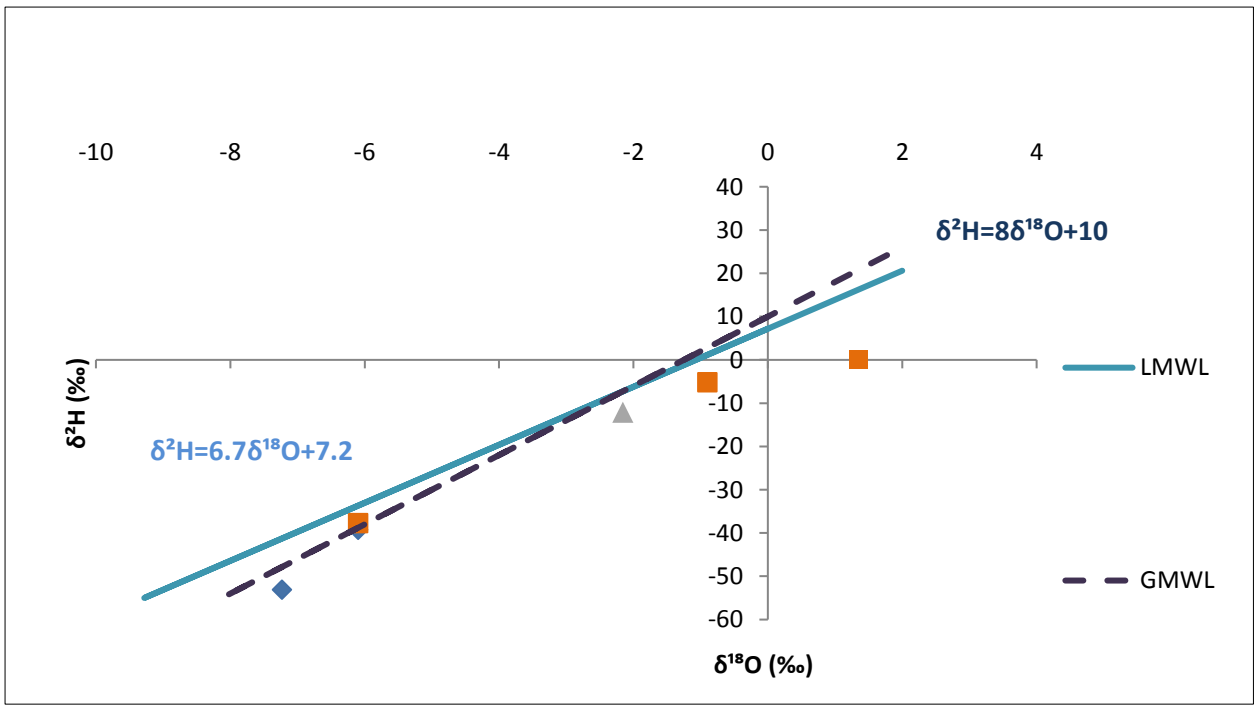


Figure 28: Isotopic signature of water samples collected in the area with orange squares representing mine waters, blue (surface water from ponds) and grey (municipal tap water).

6.2.3 Uranium toxicity and health impact

With regards to uranium, the most prominent health effects arise from chemical toxicity than susceptibility to radiation (WHO, 1998**)**. As such, the elevated concentration of U found in water points which exceeds the standards set by WHO, may be a greater concern to the health of the population residing in the area. However, since 99% of the population have access to municipal water which falls well within the standards set by WHO (2008), the health effects associated with uranium toxicity due to drinking water is less expected in the area. However, the major consequence could be through inhalation of uranium rich dust particles in the air linked with radon and associated radon progeny.

6.3 Radon concentration

6.3.1 Outdoor radon concentration

Table 13 contains the statistical data for outdoor radon levels in the study area. The levels found were highly variable and ranged between 31.7 Bq/m^3 to 1068.8 Bq/m^3, with an average of 146.5 Bq/m^3. Significantly high values with an average of 187.4 Bq/m^3 and geometric mean of 93.3 Bq/m^3 were obtained directly from the tailings. In areas proximal to tailings, radon concentrations showed an average of 86.1 Bq/m^3 and geometric mean of 65.4 Bq/m^3 whereas background concentration averaged 57.7 Bq/m^3 with geometric mean of 53.3 Bq/m^3. The lowest radon levels were found in areas outside the vicinity of mining operations and residues, averaging at 34.0 Bq/m^3. In general, most of the values fall between intervals of 41 to 50 Bq/m^3 (Figure 29). The expected typical outdoor average radon concentration is 10 Bq/m^3 (UNSCEAR, 2000). The overall values for the whole dataset indicated radon levels above the world mean radon concentration in outdoor environments, also higher when compared to levels found in other studies (Man and Yeung, 1998; Zhuo et al., 2005; Murty et al., 2010). The radon levels obtained that are higher than average could be enhanced by elevated uranium and associated radionuclides contained in tailings residues whereas the wide variability observed could be explained by the diversity of mineralization in different sources.

Table 13: Statistical results for outdoor radon levels measured in Krugersdorp and surrounding areas, all reported in Bq/m³

Measurement location	No of measurements	Range	Arithmetic mean	Geometric mean	Median	SD
Directly from Tailings residues	19	37.1-1068.8	187.4	93.3	57.9	298.3
Proximity to tailings	13	31.7-332.9	86.1	65.4	49.8	84.8
Background	7	40.3-688.4	147.7	76.6	42.1	239.8
Background in exclusion to outlier	6	40.3-111.4	57.7	53.3	42.45	28.3
Control	3	30.2-36.8	34.0	33.9	35.4	3.4
All measurements (except controls)	39	31.7-1068.8	146.5	80	54.8	235.8

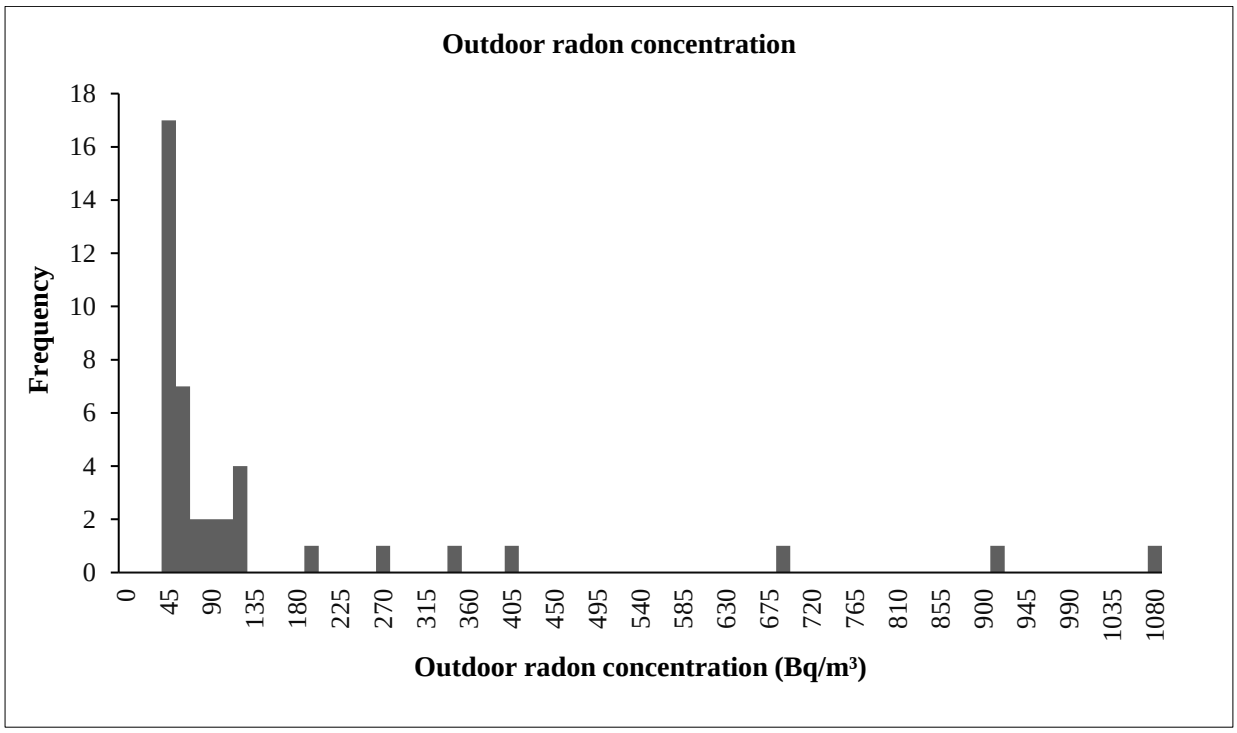


Figure 29: A histogram plot presenting outdoor radon concentration.

6.3.2 Characterisation of prominent radon sources and distribution in outdoor environment

The amount of radon present in the environment is controlled by multiple attributes such as the concentration of the parent radionuclide in sources, nature and permeability of the source, moisture content of the medium and meteorological processes (Ball et al., 1991; Porstendorfer, 1994; Mudd, 2008). The overall findings showed that tailings resulted in exceptionally higher radon levels than the underlying rocks and were found to be highly enriched with uranium and thorium which are the primitive parent radionuclide of radon. In general, there is a gradual decline in radon concentration with increasing distance from the tailings dominated region (Figure 30). In addition, spatial analysis indicated that there are no elevated radon levels confined to any rock type (Figure 31), but rather to tailings (Figure 32). These findings indicate that tailings could be the major source with the greatest strength and have a direct input towards increasing radon levels in surrounding areas.

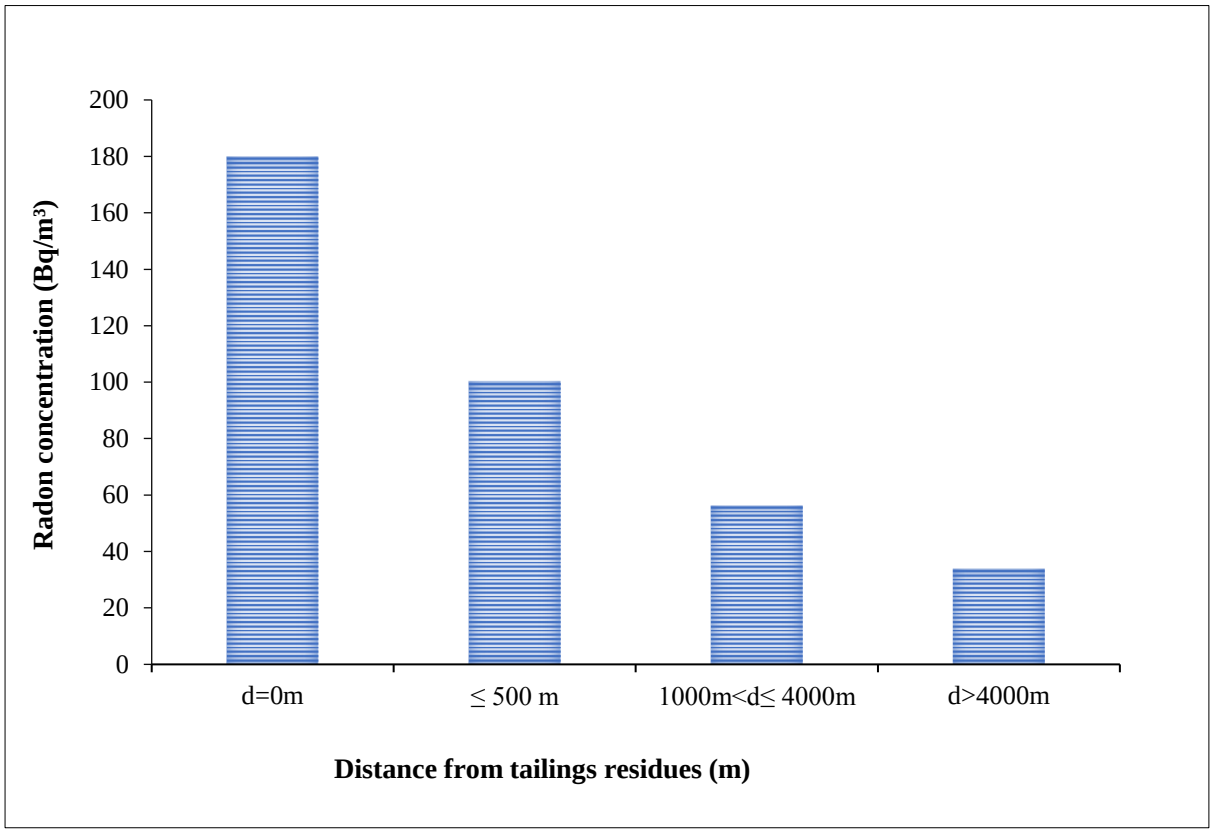


Figure 30: Average radon concentration as a function of distance from the closest tailings residues.

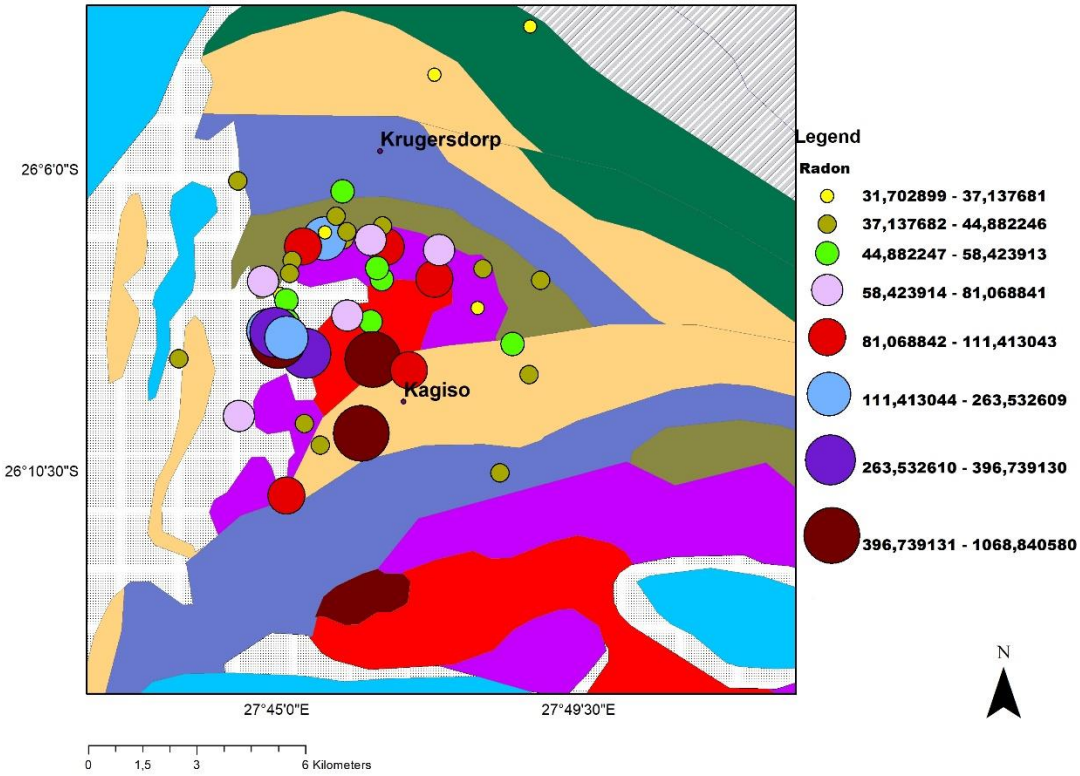


Figure 31: Radon (Bq/m^3) distribution in relation to the underlying geology.

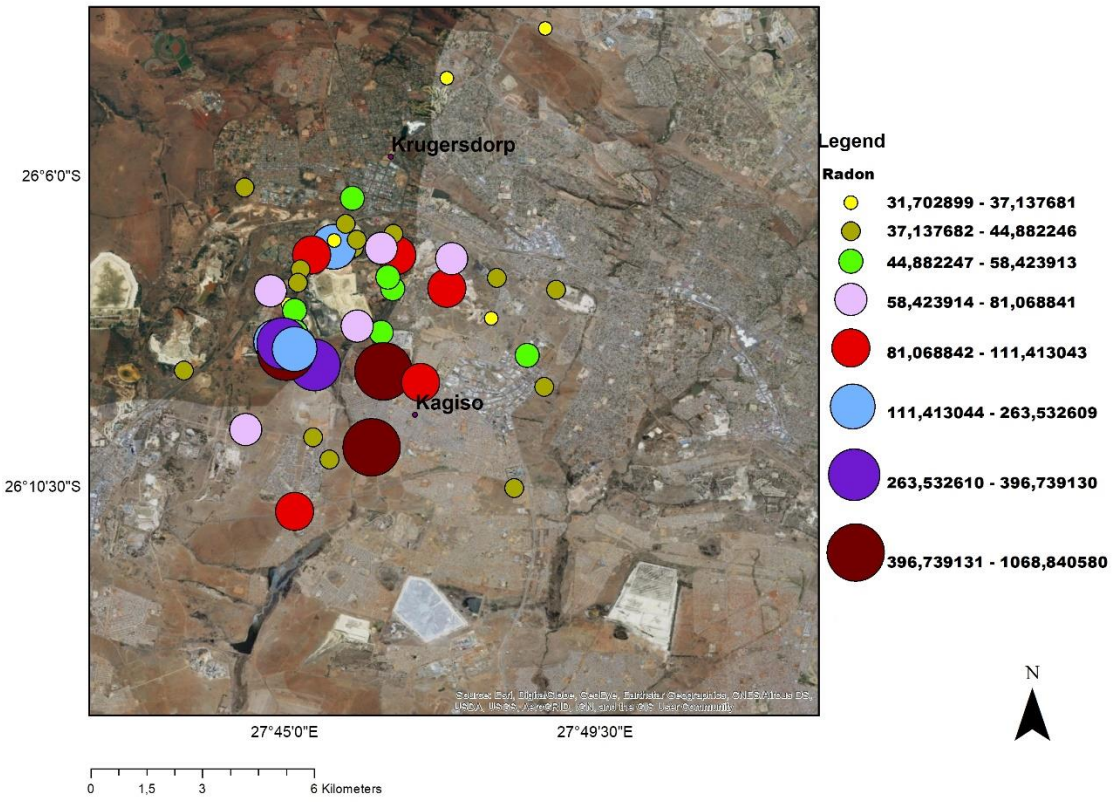


Figure 32: Radon (Bq/m^3) distribution in relation to tailings.

The large slime dam (pond) found in the area (Figure 33) also serves as a constant source of radon in the area since Ra-226 (parent element of radon-222), during leaching processes does not get dissolved and about 97% of the original concentration remains in tailings (Thomas, 1981). It is therefore likely that indefinite radon levels will almost be released. This is supported by outdoor radon concentration of 50 Bq/m^3 found nearby the dam which is 5 times greater than the typical outdoor radon concentration of 10 Bq/m^3.



Figure 33: Large slime dam in the study area which could results in higher radon releases in ambient air.

The geological formations could also serve as a primitive source of prominent radon levels found in the area, although when compared to tailings the contributions of underlying rocks are less than tailings. This is supported by the average level of 34 Bq/m^3 obtained in control points in areas of similar geological setting outside the vicinity of mining activities. The value deviates strongly from the typical outdoor mean radon concentration of about 10 Bq/m^3 (UNSCEAR, 2000). This relation reveals that the high fraction of radon released possibly corresponds to the transuranic elements found in the rocks of the Witwatersrand Supergroup. Although the collected rock samples showed low values of uranium; it is not a representative of the whole area as the levels vary spatially. Detailed geochemistry studies demonstrated levels of up to 4.5 ppm for certain geological formations within the Witwatersrand Supergroup (Wronkiewicz and Condie 1987; 1990). Some studies revealed that rocks with uranium content of about 2 ppm holds a great potential to results in significant radon contributions (Gundersen et al. 1992; Drolet et al. 2013). These observations ascertain that the rocks of the Witwatersrand Supergroup solely make significant radon contributions in outdoor environments. As such the obtained average value of 34.0 Bq/m^3 released from these geological formations can, therefore, be characterized as the baseline value for areas with similar geological makeup were tailings are not dominant.

The examination of comparisons in radon levels observed in areas characterized as controls and background measurements within the selected study area revealed noteworthy differences. It was found that radon levels in background localities (57.7 Bq/m^3) in the study area are approximately 2 times greater than the average levels found in control measurements (34.0 Bq/m^3). Comparable values were expected to occur since both areas comprise similar rock types. This could imply that through air circulation, the radon-rich air released from tailings probably gets dispersed to greater distances depending on wind speed and wind direction and dilute with radon-poor air in background localities. The ability of radon to escape readily from its potential source without any chemical interference and be widely dispersed in the air (Ball et al., 1991; Otton et al., 1992; Levin and Verhagen, 2013), gives a possible explanation to the mixing behavior observed. These findings were supported by results presented in Figure 34 whereby It was found that in distal regions from the mine residues dominated region, particularly, in the direction opposite to the prevailing dominant wind direction (N-NNW), highest radon levels were found in relation to other directions (Figure 34). This reveals the strong impact of wind parameters on radon distribution.

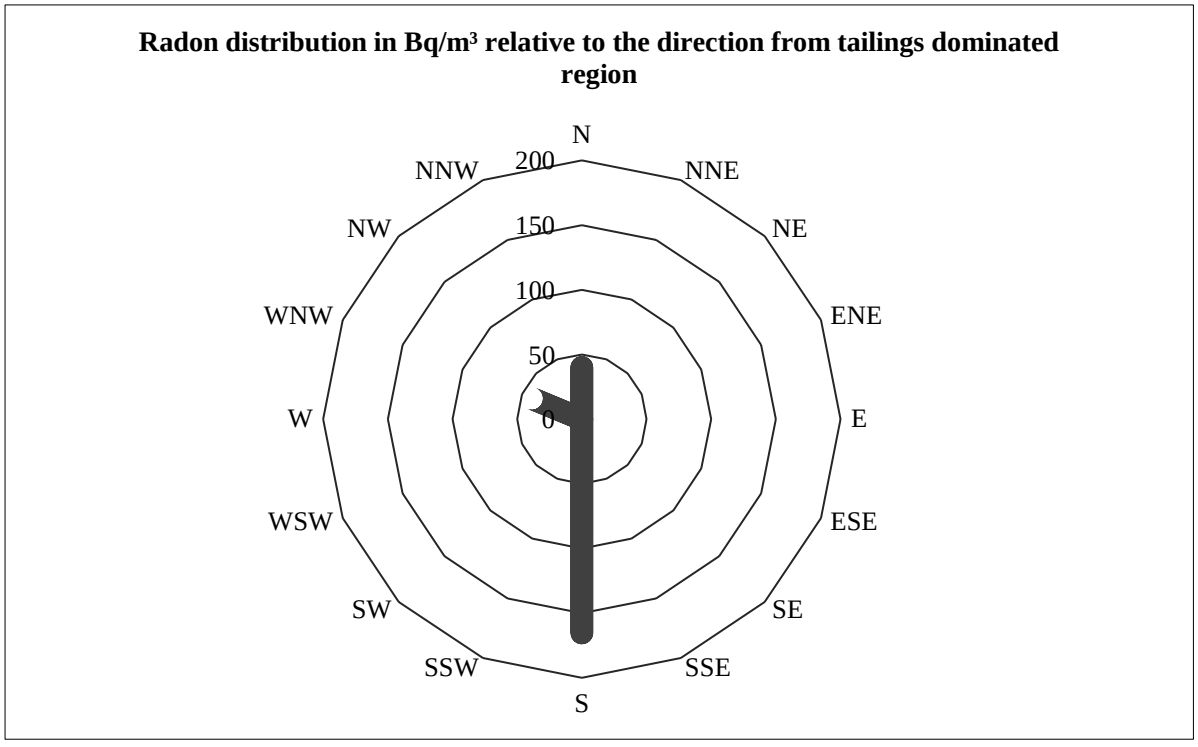


Figure 34: Distribution of radon (Bq/m^3) in different directions from the tailings dominated region which is denoted as zero (0) on the plot.

6.3.3 Uranium and radon correlation

To determine the relationship between uranium and radon, linear regression analysis was used (Figure 35). The results showed a weak positive correlation (R^2 = 0.1483) which also coincides with the results obtained from Spearman correlation analysis (r_s = 0.09440). The weak correlation observed could indicate that although radon is primarily formed from uranium decay chain, its concentration in the environment is not solely controlled by the amount of uranium present but the interplay of multiple parameters which in this case was found to be more related to wind effects. In addition, the relationship observed could also show that the radon concentration may

be proportional to the concentration of the immediate parent radium-226 radionuclide than the primitive uranium-238 radionuclide. As such, detailed analysis on radium-226 would be more relevant in finding the relation between radon concentration and parent radionuclide, hence, this aspect should be explored in future studies.

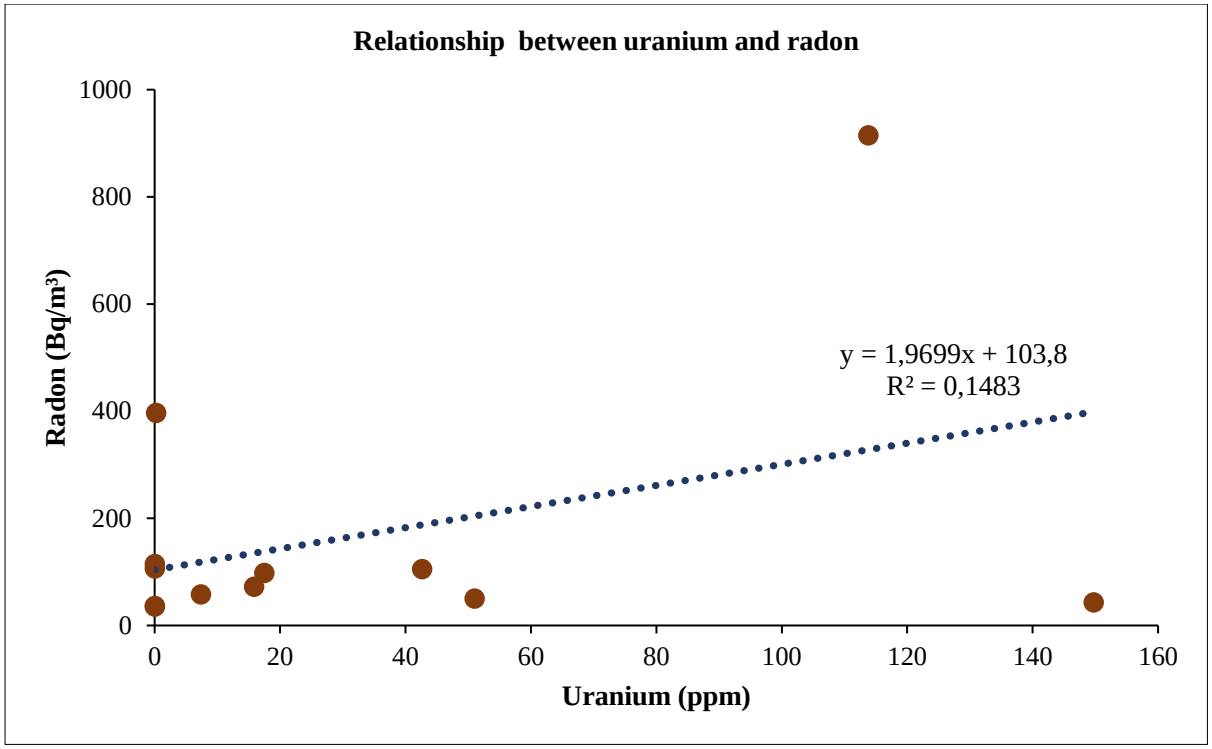


Figure 35: Regression analysis results showing a correlation between uranium and radon.

6.3.4 The radon spatial distribution

In order to delineate radon-prone areas, spatial analysis was conducted. The results from this analysis indicated that radon concentration depicts a wide spatial variability even within relatively small areas (Figure 36). The highest radon zones are located at the central and southern part of the study area. These are regions largely dominated by gold mine tailings. These high radon zone areas cover the densely populated region, Kagiso with population of approximately 115,802. The levels spatially decrease with increasing distance from high concentration zones which agrees with the findings presented in Figure 30. The low radon zones are in the northern part of the study area where the area is largely covered by rocks. Therefore, radon prone areas are concentrated in tailings dominated regions and the distribution pattern is characterized by the combination of wind direction and relative distance from tailings. The results from spatial analysis also agrees with the findings presented in Figure 34. Owing to the fact that dwellings in the area are in close proximity to tailings that release elevated radon, considerably higher levels may be expected indoor.

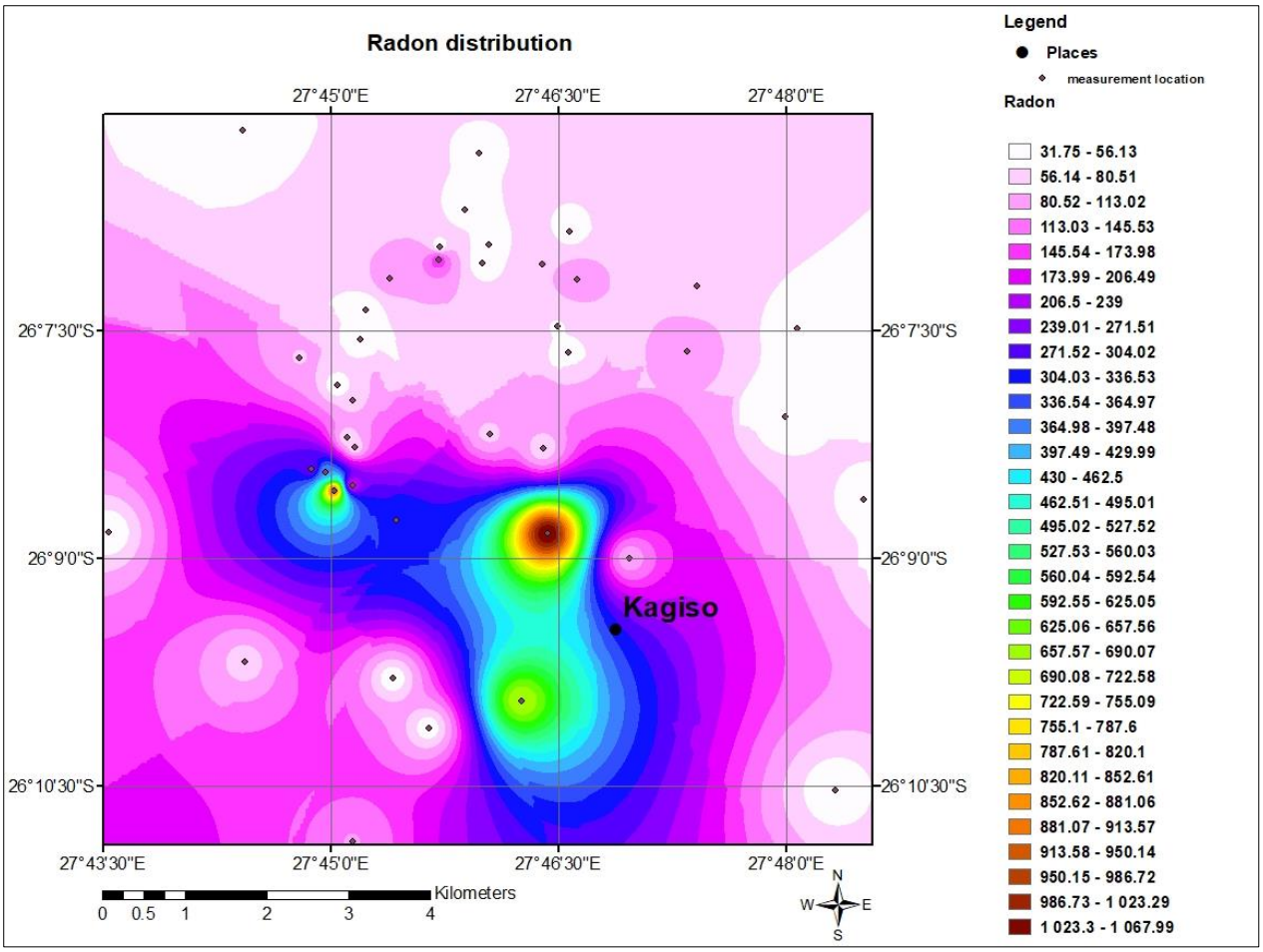


Figure 36: Radon spatial distribution in the study area represented in Bq/m^3.

6.3.5 Indoor radon concentration

The range of measured indoor radon concentration in selected dwellings within the mining and non-mining region are presented in Table 14. The results showed that residential areas nearby tailings are exposed to elevated levels of radon (66.52 Bq/m^3) as compared to those outside the vicinity of mine tailings (41.16 Bq/m^3). The small-scale sampling in the residential areas showed radon levels of up to 173 Bq/m^3, which is above the value of 100 Bq/m^3 recommended by WHO (2009). Also indicated the overall average that is 1.7 times greater than the mean world indoor level of 39 Bq/ m^3 (UNSCEAR, 2000). Again, the study of Leuschener et al. (1992) documented radon levels of up to 273 Bq/m^3 in the Krugersdorp area, which also falls above the recommended values. Therefore, this could indicate that on large-scale elevated levels may occur in the area.

To a great extent it is known that the subsurface lithological units and soil properties are the primary attributes to predispose dwellings to elevated radon concentration (Lueshner et al., 1988; Nazaroff, 1992; Watson et al., 2017), nonetheless, there are multifactorial controlling parameters involved. In this study elevated radon levels in outdoor environments were found in areas dominated by tailings, therefore this could serve as the primary source to predispose dwellings to elevated radon levels since the houses are in proximity to tailings (Figure 37). Among the five main indoor radon entry mechanisms documented by Sextro (1987), the major contributions that results in

high radon accumulation in indoor environments in the study area may be through the entry of radon-rich air released from tailings provided that favorable conditions for air exchange exist, also through the underlying soils which may probably be enriched with radium-226 leached from tailings residues nearby. Nonetheless, the amount that infiltrates into dwellings is dependent upon the construction characteristics of the house and living style of inhabitants.

Table 14: Indoor radon levels obtained in dwellings at various locations

Exposed	**Range**	**Mean**
^{222}Rn (Bq/m^3)	33.5-173.5	66.52
Unexposed		
^{222}Rn (Bq/m^3)	30.2-50.7	41.16

Exposed: Houses located nearby tailings (±1 km)

Unexposed: Houses located far away from tailings (±30 km)



Figure 37: Extensive unprotected tailings which cover a large area nearby residential areas and therefore could affect health status of individuals residing nearby through the dust blown from these sites.

The building materials used for construction of houses contain reasonable uranium content of up to 10.14 ppm (Table 15). The plot in Figure 38 shows a tendency of bricks reflecting the concentrations in tailings. The high mutual reliance could suggest the use of tailings residues as a resource for building bricks, therefore, explaining very high levels of radionuclides found in bricks. Under normal circumstances building materials contribute negligible amounts of radon in indoor air (Samet, 1989). However, in this context they could account for substantial contributions due to their considerable content of uranium and associated radium radionuclides that could be contained. Hence, could place a great number of occupants at risk depending on the number of dwellings made of building materials with similar composition.

Table 15: Uranium, thorium and lead composition of the bricks used for construction in the area

Buildings materials	U (ppm)	Th (ppm)	Pb (ppm)
TA/PB19/B1(Brick)	10.14	49.86	60.98
TA/PB/19/B2 (Brick)	1.45	7.26	82.83

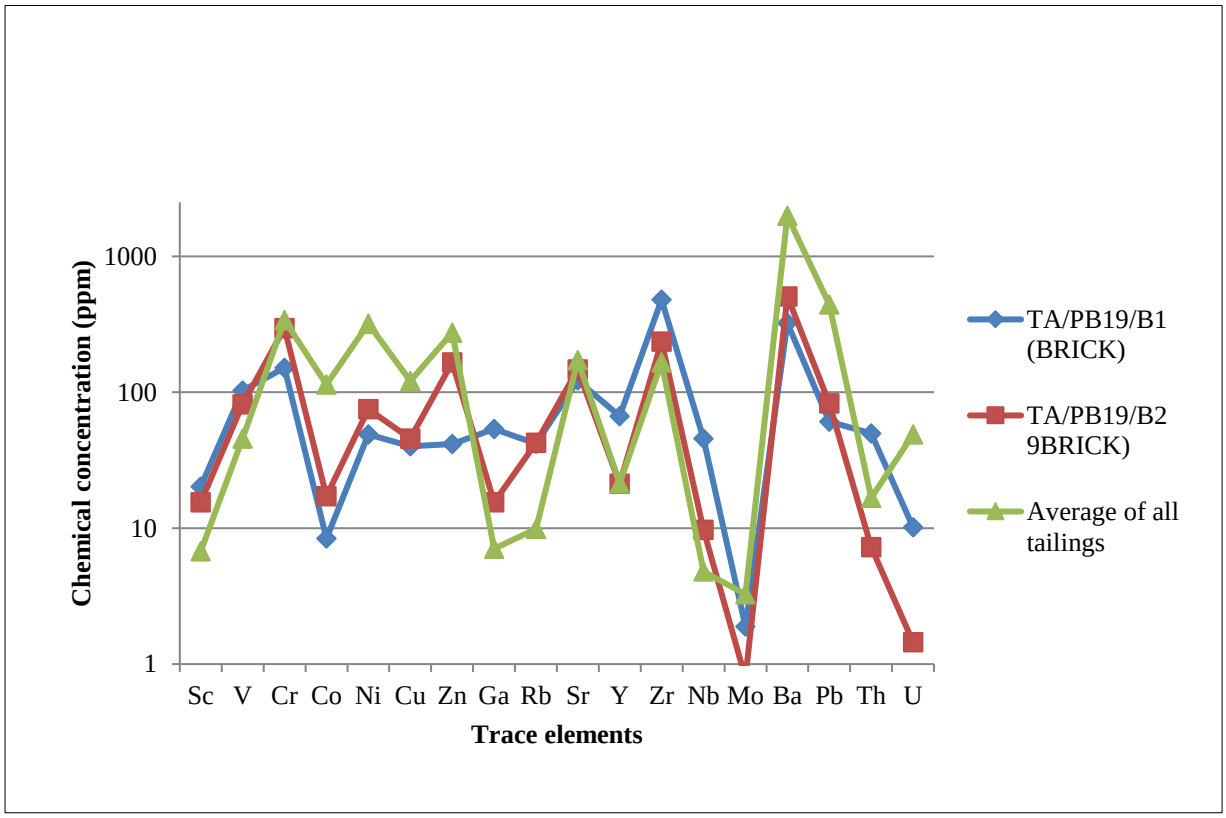


Figure 38: Comparison between trace element concentration found in tailings and bricks collected within the area of study.

Radon derived from water may enter indoor air through de-emanation when the water is used. In this case potable water could not result in any significant indoor accumulations as the population depends on municipal water supplied by Rand Water with non-detectable uranium concentration, which is the primitive source of radon.

6.4 Effective dose

From the measured radon concentration, the annual effective dose received by the population residing in the area was estimated using the equation (2) from the UNSCEAR (2000). It was found that the effective dose estimated to be received by the public from outdoor exposure in different regions ranges between 0.29 mSv/y to 10.11 mSv/y (Figure 39 and 40). In all regions, the levels fall above the typical outdoor expected doses of 0.095 mSv/y (UNSCEAR, 2000). However, some areas depict levels that fall within the recommended limit of 1 mSv/y (NNR, 1999; ICRP, 2013) whereas some regions show high effective doses exceeding the dose constraints. Figure 40

indicate that exceptionally high doses coincide with areas of high radon concentration in the southern part of the study area where most densely populated residential areas are located. Therefore, could indicate a greater probability of health problems associated with substantial exposure to high radiological doses.

In indoor environments, the mean effective dose received is 2.7 mSv/y, however, this could not be a representative of the large area as it was estimated from two measurements obtained from occupied dwellings. The level exceeds the typical dose of 1.0 mSv/y (UNSCEAR, 2000) for indoor environments, however, fall within the action level of 3 mSv/y to 10 mSv/y recommended by ICRP (1993).

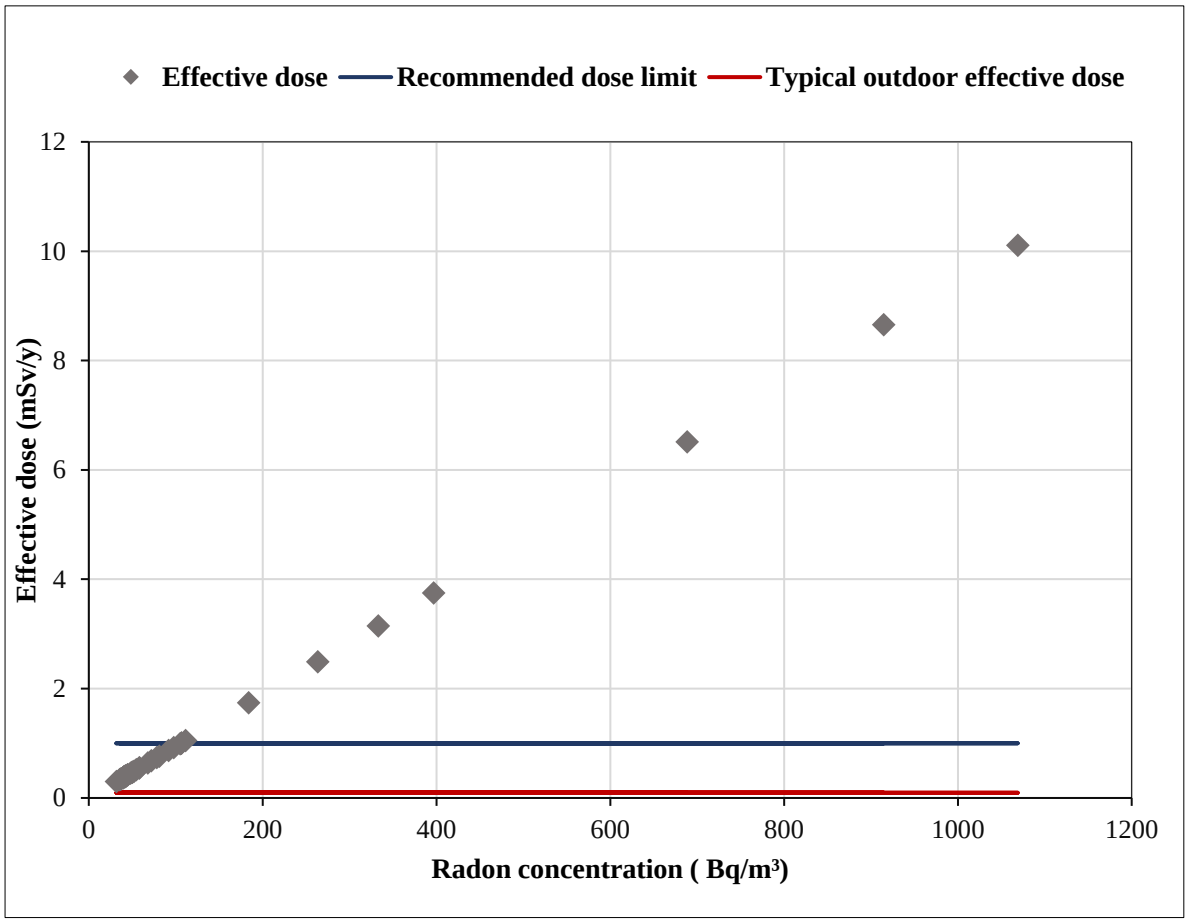


Figure 39: Calculated effective dose estimated from the outdoor radon levels obtained.

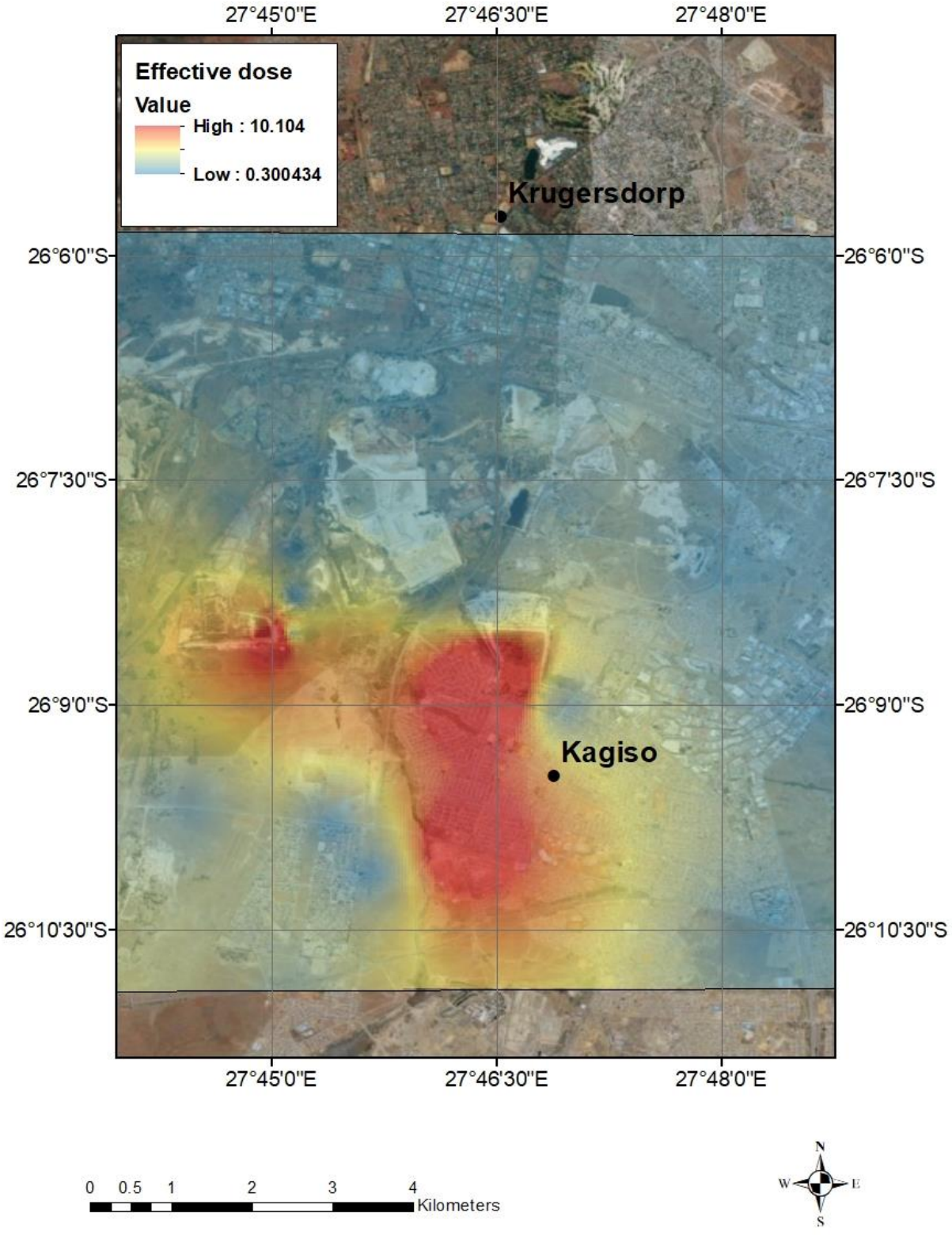


Figure 40: Spatial distribution map of effective doses (mSv/y) received by the population in the area from outdoor exposure.

6.5 Health effects related to radon exposure

To assess the human health effects attributable to radon in the area, the study relied primarily on the statistical data on lung cancer incidences and mortality. Based on latest national cancer statistics, a total of 74577 cancer incidences were diagnosed in South Africa in 2014. Of all the cancers identified, 2727 (3.65%) of them were lung cancer, of which 1791 were males and 936 were females (National Cancer Registry, 2014). The frequency of lung cancer increases with age and its prevalence is greatest from the age 55 to 75 and, thereafter, declines (Figure 41).

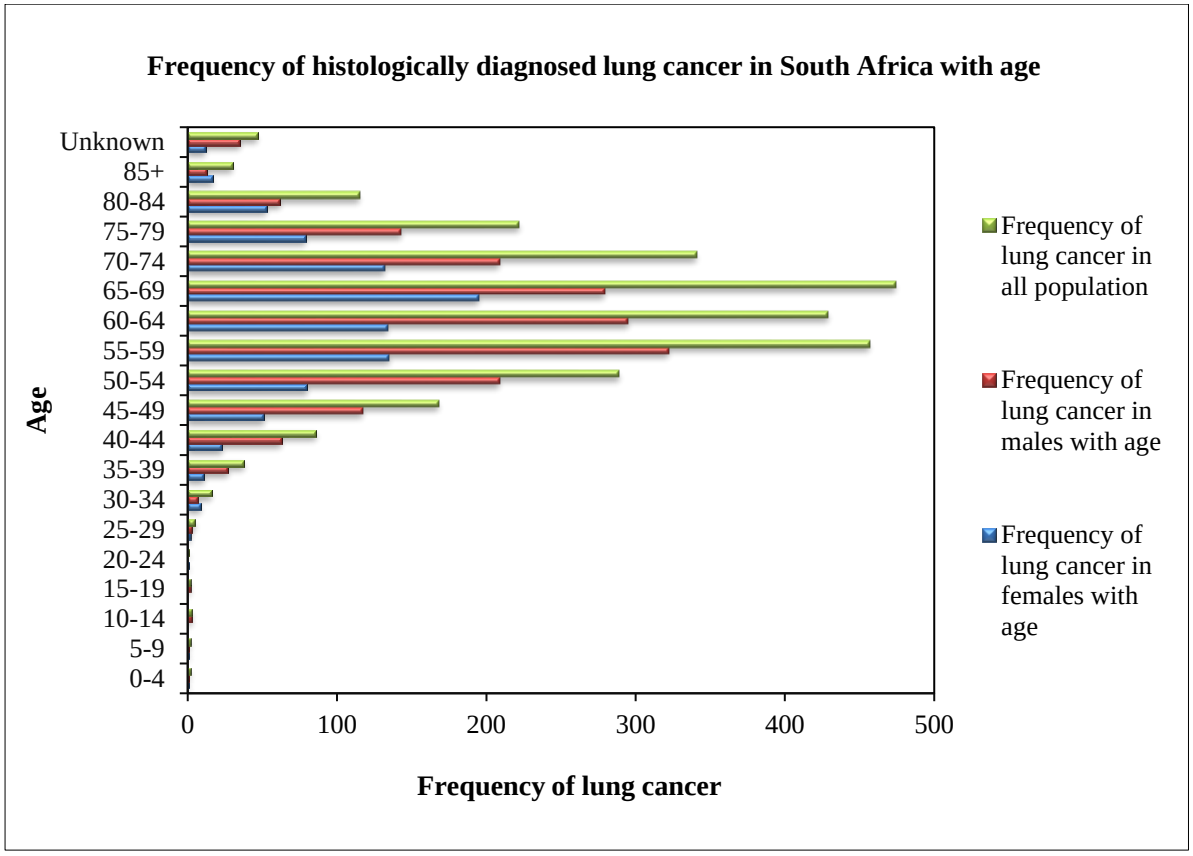


Figure 41: Frequency of histologically diagnosed lung cancer in South Africa with age (Data source: National Cancer Registry).

From 2727 nationwide lung cancer cases identified in 2014, a total of 79 deaths attributable to lung cancer were recorded in the West Rand Municipality for the same year, of which 70 deaths occurred in Mogale City Local Municipality where the study area is located (StatsSA, 2018). In the Mogale City Local Municipality elevated death rates relative to neighboring municipalities are observed (Figure 42). The figures are comparable to the total lung cancer deaths within the West Rand Municipality as a whole. There are fluctuations throughout all years from 1997 to 2016 with increased rates from 2010 and highest in 2015 (Figure 42). This also suggests that higher lung cancer incidences are expected in the area since the discovery of lung cancer is most common when it is advanced (Thomas, 2016). To further compare lung cancer rates and maintain the quality of the findings, municipalities in mining (target) and non-mining regions (reference sites) were compared. The comparative plots indicate that the highest lung cancer deaths are in the target population of the Mogale City Local Municipality as compared to the reference population with comparable demographics. The overall lung cancer deaths are also high even when compared to the reference zone population with higher population (Figure 43).

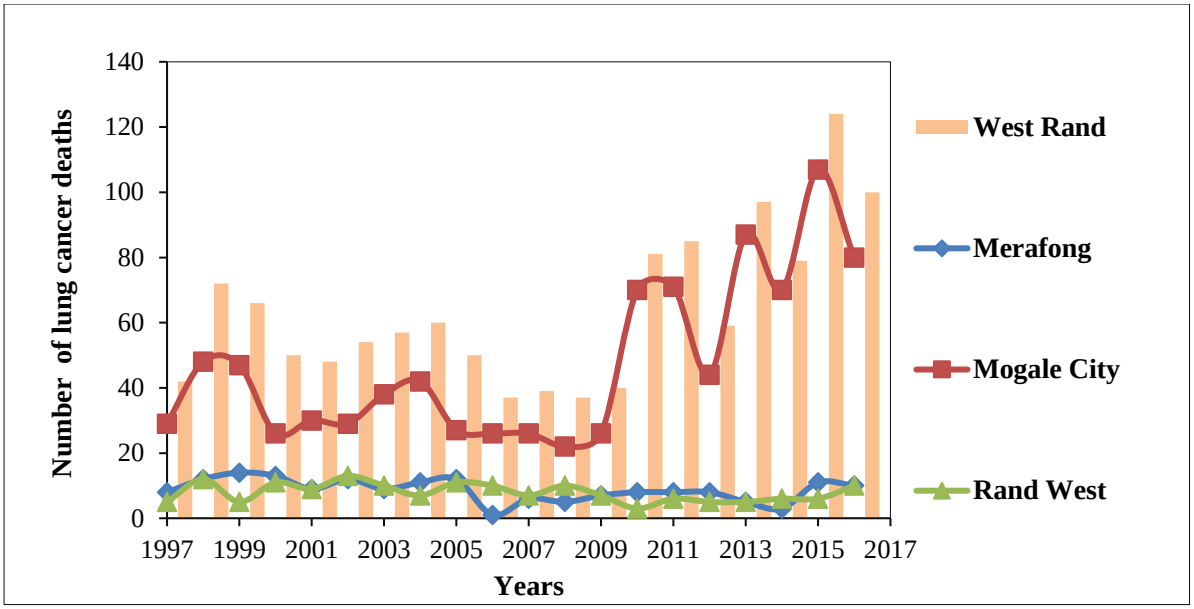


Figure 42: Lung cancer deaths in various municipalities of the West Rand whereby the Mogale City Local Municipality show higher rates than Merafong and Rand West Local Municipality (Data source: StatsSA).

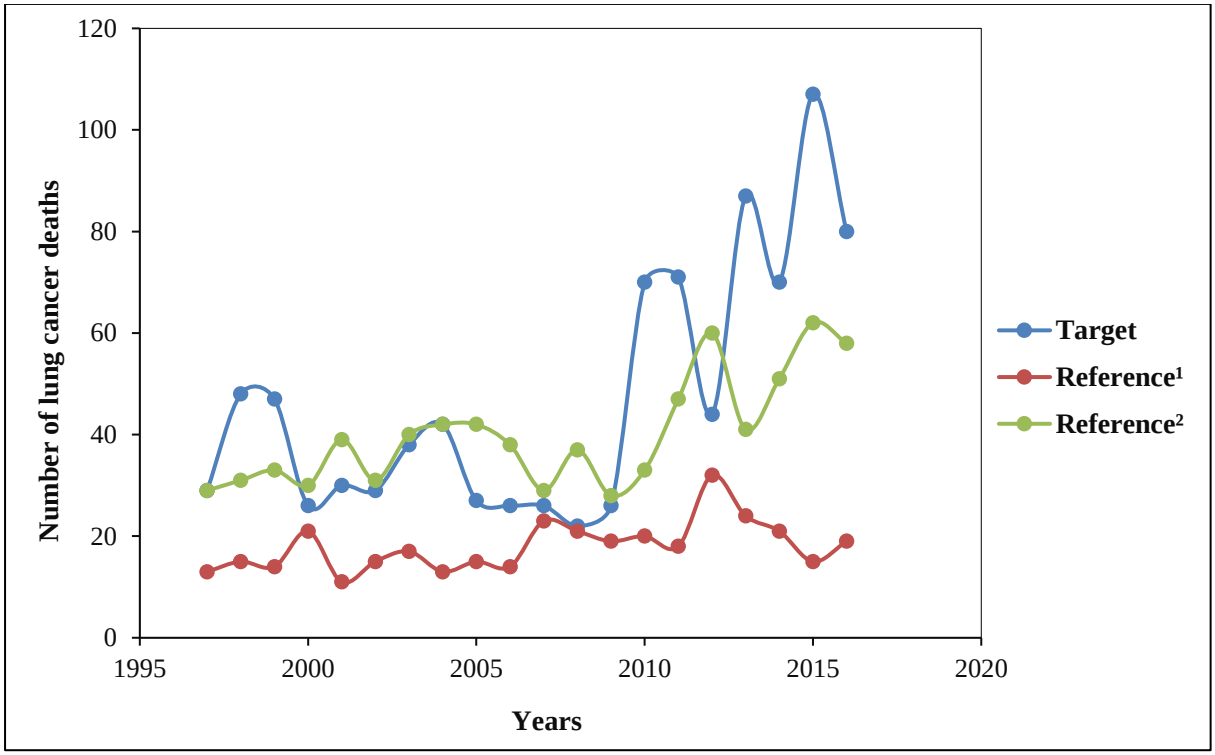


Figure 43: Plot showing a comparison between lung cancer deaths in both radon exposed and non-exposed areas. Target- Mogale City with population of about (362 421) in the West Rand where the study area is located.

***Reference site[1]**- Joe Gqabi district municipality away from mining activities with comparable population number to the exposed region (349 768) (Data source: StatsSA).*

***Referenc site e[2]**- and two municipalities in the Eastern Cape (the highly populated OR Tambo district municipality away from mining activities with population number (1 364 943) (Data source: StatsSA).*

Studies indicated that population exposed to elevated levels are at greatest risk of developing lung cancer (NRC, 1988; Samet, 1989; Lubin et al., 1995; Darby et al 2005, 2006; Krewski et al., 2006). In this study, levels of radon and radiological doses received by the public were found to be above the recommended values. Such levels could result in a potential health risk to the susceptible individuals since radon is considered a carcinogen at all exposures and shows a greater risk at high exposures (Darby et al, 2001). It could, therefore, be assumed that the increased lung cancer mortality in the population group of Mogale City Local Municipality relative to other municipalities may be strongly associated with elevated radon concentrations released from abandoned mine tailings found in the area.

In addition, high levels of trace elements; Ni, Cr, and Pb were found in tailings distributed in the study area (Table 16). The compounds of these traces have long been classified as carcinogens by the International Agency for Research on Cancer (IARC, 1990; 1991) and their exposure results in absolute risk that alters the effects of radon decay products (NRC, 1988; Lubin et al., 1995). As such, the combined effect of radon and these trace elements could be a driving factor to increased lung cancer mortality in the area. It is also taken into account that there are various modification factors in association to the way individuals respond to the dose received from radon exposure (Samet, 1989; NRC, 1991).

Table 16: Statistical summary of trace elements found in tailings samples collected in the study area (reported in ppm) and background and average values found in South African soils (Herselman et al., 2005) and the target standard value from Dutch list (Netherlands Ministry of housing, physical planning and Environment, 1997)

Trace element	Source	Total count	Range	Average	Background	Average	Target value
Cr	Tailings	12	156.22- 1130.39	340.21	5.83-353	71.9	100
Ni	Tailings	12	50.68-1323.72	319.34	3.43-159	38.7	35
Pb	Tailings	12	9.68-3263.48	442.94	2.99-68.8	21.7	85

According to NRC (1999b) the estimated period of lung cancer development due to radon exposure is between 5 to 25 years. It was also found in the study of Lubin et al. (1995) and Kruezer et al. (2015) that long-term exposures give rise to greater lung cancer risks. Thus, the increasing lung cancer deaths with increasing years (Figure 42) could be a resultant of long residence time of inhabitants in the area. Also, the increased lung cancer mortality rate in the MCLM may be that a large number of the population within the MCLM reside in the Kagiso area, which is in closest to the mine residues thus, results in greatest exposures as compared to other municipalities.

The main limitation is that the study assumed the prevalence of lung cancer in the area relative to other regions could potentially be exacerbated due to elevated radon levels found in the area and also the exposure to greater concentrations of toxic metals contained in mine tailings residues. Other risk factors for developing lung cancer include smoking showing a direct relationship with radon exposure (Samet, 1989; Lubin et al, 1995; NRC, 1999b; Darby et al, 2001), and other occupational and environmental substances such as asbestos, arsenic family, genetic risk and age (NRC, 1991) were not considered. The other factor that was not considered is that residents could be

exposed to lung cancer causing agents in other regions outside the study area at their place of work, which could therefore potentially increase the risk of lung cancer. To further ascertain the lung cancer risk associated with radon exposure, detailed epidemiological investigations using levels of individual exposure and health effects on a large scale should be conducted in order to increase statistical power and reliability of results. Nevertheless, the overall findings provide a provision that the radon levels obtained in the study area could be a probable factor to result in elevated lung cancer occurrences in the area.

7 CONCLUSIONS

The geochemical results obtained in this study revealed that the abandoned gold mine tailings in and around the Krugersdorp area contain elevated uranium levels which are above the natural concentration of approximately 4.7 ppm. In addition, the tailings were found to have concentrated and elevated toxic metals. It was found that the tailings residues impact on the surface water resources found in the area and concentrate uranium levels above the recommended limit of 0.015 mg/l. The elevated uranium levels could not result in significant health impacts as 99% of the population depends on municipal water for consumption, with uranium levels below the detection limit of 0.01 ppm.

The highest radon levels were found in areas dominated by tailings residues than in the natural background. This is also in agreement with the chemical composition results where tailings portray a high concentration of uranium than the bedrock. The results from statistical analysis, however, indicate a weak correlation between uranium and radon which, instead, implies that the occurrence of radon in the area is predominately dependent upon the radium-226 concentrations than the primitive uranium radionuclide.

The radon levels exhaled from tailings were found to contribute to unusually high outdoor radon levels at greater distances from tailings depending on the wind direction and speed. In summary, the abandoned gold mine tailings are the predominant source for elevated uranium and radon concentrations as compared to the bedrock in the area. This was accounted for by the fact that tailings dams contain crushed rocks extracted from a depth of several hundred meters, while the surface geology may not have a similar composition.

The high frequency of lung cancer deaths was documented in the study area and was linked to elevated radon levels measured in the area. In addition, high levels of trace elements found in tailings; Ni, Cr, and Pb could also increase the magnitude of lung cancer deaths and other respiratory diseases as they are also known to be carcinogenic. This could attest to the theory of why there are high cases of respiratory diseases in the area.

8 RECOMMENDATIONS

- Following the radon levels obtained, relevant authorities should be made aware of the high potential zones of radioactive materials, uranium and radon and the risk associated with long-term exposure to the radioactive materials released from the abandoned tailings residues. Future studies should focus on indoor radon monitoring on a large scale and detailed epidemiological studies as most residential areas are located in radon prone areas.

- Awareness programs and public education should be established to inform the general population on radon and associated health impacts and what can be done to mitigate the exposure thereof.

- Continuous regular radon monitoring should be implemented and where appropriate application for radon reduction in dwellings should be practiced, such as, improving the house ventilation, underfloor ventilation, sealing cracks on floors and walls and installation of radon sump system.

9 REFERENCES

Abegunde, O. A. (2015). Geologic and geological assessment of Acid Mine Drainage and heavy metals contamination in the West Rand, Witwatersrand Basin, South Africa.

Abdelouas, A. (2006). Uranium mill tailings: geochemistry, mineralogy, and environmental impact. *Elements*, *2*(6), 335-341.

Abiye, T. A. (2011). Provenance of groundwater in the crystalline aquifer of Johannesburg area, South Africa. *International Journal of Physical Sciences*, *6*(1), 98-111.

Abiye, T. A., Mengistu, H., Demlie, M. B. (2011). Groundwater resource in the crystalline rocks of the Johannesburg area, South Africa. *Journal of Water Resources and Protection*, *3*(4), 199-212.

Abiye, T. (2014). Hydrogeochemical footprint as a result of mining activities in the Johannesburg area. In *Technical Report*. University of the Witwatersrand School of Geosciences.

Abiye, T., Masindi, K., Mengistu, H., Demlie, M. (2018). Understanding the groundwater-level fluctuations for better management of groundwater resource: A case in the Johannesburg region. *Groundwater for Sustainable Development*, *7*, 1-7.

Abiye, T., Mkansi, S., Masindi, K., Leshomo, J. (2018). Effectiveness of wetlands in retaining metals from mine water, South Africa. *Water and Environment Journal*, *32*(2), 259-266.

AngloGold Ashanti. (2004). Case studies. Woodlands Project – good progress being made with phytoremediation project. *Environment – AngloGold Ashanti Report to Society.*

Appleton, J. D. (2007). Radon: sources, health risks, and hazard mapping. *AMBIO: A Journal of the Human Environment*, *36*(1), 85-89.

Appleton, J. D. (2013). Radon in air and water. In *Essentials of medical geology* (pp. 239-277). *Springer, Dordrecht.*

Au, W. W., Lane, R. G., Legator, M. S., Whorton, E. B., Wilkinson, G. S., Gabehart, G. J. (1995). Biomarker monitoring of a population residing near uranium mining activities. *Environmental Health Perspectives*, *103*(5), 466.

Aucamp, P., Van Schalkwyk, A. (2003). Trace element pollution of soils by abandoned gold mine tailings, near Potchefstroom, South Africa. *Bulletin of Engineering Geology and the Environment*, *62*(2), 123-134.

Auvinen, A., Salonen, L., Pekkanen, J., Pukkala, E., Ilus, T., Kurttio, P. (2005). Radon and other natural radionuclides in drinking water and risk of stomach cancer: A case-cohort study in Finland. *International Journal of Cancer*, *114*(1), 109-113.

Baias, P. F., Hofmann, W., Winkler-Heil, R., Cosma, C., Duliu, O. G. (2009). Lung dosimetry for inhaled radon progeny in smokers. *Radiation protection dosimetry*, *138*(2), 111-118.

Ball, T. K., Cameron, D. G., Colman, T. B., Roberts, P. D. (1991). Behaviour of radon in the geological environment: a review. *Quarterly Journal of Engineering Geology and Hydrogeology*, *24*(2), 169-182.

Banning, A., Demmel, T., Rüde, T. R., Wrobel, M. (2013). Groundwater uranium origin and fate control in a river valley aquifer. *Environmental science & technology*, *47*(24), 13941-13948.

Barnard, H. C. (2000). *An explanation of the 1: 500 000 general Hydrogeological map: Johannesburg 2526.* Department of Water Affairs and Forestry.

Baskaran, M. (2016). Radon: A tracer for geological, geophysical and geochemical studies. Cham: Springer Geochemistry, 1-257.

Bekteshi, S., Kabashi, S., Ahmetaj, S., Xhafa, B., Hodolli, G., Kadiri, S., Alijaj, F., Abdullahu, B. (2017). Radon concentrations and exposure levels in the Trepça underground mine: A comparative study. *Journal of cleaner production*, *155*, 198-203.

Bench Marks Foundation. (2017). "Waiting to inhale it". A survey of household health in four mine affected communities. Soweto report, Policy Gap 12.

Berkowitz, B., Dror, I., Yaron, B. (2007). Contaminant geochemistry. Springer, (p 51-559).

Bjørklund, G., Christophersen, O. A., Chirumbolo, S., Selinus, O., Aaseth, J. (2017). Recent aspects of uranium toxicology in medical geology. *Environmental research*, *156*, 526-533.

Cecil, L. D., Green, J. R. (2000). Radon-222. In *Environmental tracers in subsurface hydrology* (pp. 175-194). Springer, Boston, MA.

Chen, J. (2005). A review of radon doses. *Radiation Protection Management*, *22*(4), 27.

Churchill, R. (1991). Geologic controls on the distribution of radon in California. *The Department of Health Services, USA*.

Coetzee, H., Chirenje, E., Hobbs, P., Cole, J. (2009). Ground and airborne geophysical surveys identify potential subsurface acid mine drainage pathways in the Krugersdorp Game Reserve, Gauteng Province, South Africa. In *11th SAGA Biennial Technical Meeting and Exhibition*.

Cosma, C., Moldovan, M., Dicu, T., Kovacs, T. (2008). Radon in water from Transylvania (Romania). *Radiation Measurements*, *43*(8), 1423-1428.

Coward, M. P., Spencer, R. M., Spencer, C. E. (1995). Development of the Witwatersrand Basin, South Africa. *Geological Society, London, Special Publications*, *95*(1), 243-269.

Craig, H. (1961). Isotopic variations in meteoric waters. *Science*, *133*(3465), 1702-1703.

Cross, F. T. (1987). Health effects. In *Environmental radon* (pp. 215-248). Springer, Boston, MA.

Dankert, B. T., Hein. K. A. A. (2010). Evaluating the structural character and tectonic history of the Witwatersrand Basin. *Precambrian Research, 177*(1-2), 1–22.

Darby, S.C., Whitely, E., Howe, G.R., Hutchings, S.J., Kusiak, R.A., Lubin, J.H., Morrison, H.I., Tirmarche, M., Tomásek, L., Radford, E.P. and Roscoe, R.J. (1995). Radon and cancers other than lung cancer in underground miners: a collaborative analysis of 11 studies. *JNCI: Journal of the National Cancer Institute*, *87*(5), 378-384.

Darby, S., Hill, D., Doll, R. (2001). Radon: a likely carcinogen at all exposures. *Annals of Oncology*, *12*(10), 1341-1351.

Darby, S., Hill, D., Auvinen, A., Barros-Dios, J.M., Baysson, H., Bochicchio, F., Deo, H., Falk, R., Forastiere, F., Hakama, M. and Heid, I. (2005). Radon in homes and risk of lung cancer: collaborative analysis of individual data from 13 European case-control studies. *Bmj*, *330*(7485), 223.

Darby, S., Hill, D., Deo, H., Auvinen, A., Barros-Dios, J.M., Baysson, H., Bochicchio, F., Falk, R., Farchi, S., Figueiras, A., Hakama, M. (2006). Residential radon and lung cancer—detailed results of a collaborative analysis of individual data on 7148 persons with lung cancer and 14 208 persons without lung cancer from 13 epidemiologic studies in Europe. *Scandinavian journal of work, environment & health*, 1-84.

Department of Water Affairs and Forestry. (1996). South African Water Quality Guidelines. Volume 1: Domestic Use.

Drolet, J. P., Martel, R., Poulin, P., Dessau, J. C., Lavoie, D., Parent, M., Lévesque, B. (2013). An approach to define potential radon emission level maps using indoor radon concentration measurements and radiogeochemical data positive proportion relationships. *Journal of environmental radioactivity*, *124*, 57-67.

Dunbabin, J. S., Bowmer, K. H. (1992). Potential use of constructed wetlands for treatment of industrial wastewaters containing metals. *Science of the Total environment*, *111*(2-3), 151-168.

Durand, J. F. (2012). The impact of gold mining on the Witwatersrand on the rivers and karst system of Gauteng and North West Province, South Africa. *Journal of African Earth Sciences*, *68*, 24-43.

Els, B. G., Van den Berg, W. A., Mayer, J. J. (1995). The Black Reef Quartzite Formation in the western Transvaal: sedimentological and economic aspects, and significance for basin evolution. *Mineralium Deposita*, *30*(2), 112-123.

Eriksson, P. G., Clendenin, C. W. (1990). "A Review of the Transvaal Sequence, South Africa," *Journal of African Earth Sciences, 10*(1-2), 101-116.

Eriksson, P. G., Altermann, W., Hartzer, F. J. (2006). The Transvaal Supergroup and its precursors. In: *M. R. Johnson, C. R. Anhaeusser and R. J. Thoms, Eds.,The Geology of South Africa* (pp. 237-260).

Fitts, C. R. (2002). *Groundwater science*. Elsevier, (p 1-397).

Folger, P. F., Nyberg, P., Wanty, R.B., Poete, E. (1994). Relationship between 222Rn dissolved in groundwater supplies and indoor 222Rn concentrations in some Colorado Front Range houses. *Health Physics*, *67*(3), 245-253.

Fox, P. M., Davis, J. A., Hay, M. B., Conrad, M. E., Campbell, K. M., Williams, K. H., Long, P. E. (2012). Rate-limited U (VI) desorption during a small-scale tracer test in a heterogeneous uranium-contaminated aquifer. *Water Resources Research*, *48*(5).

Frimmel, H. (1997). Detrital origin of hydrothermal Witwatersrand gold—a review. *Terra Nova*, *9*(4), 192-197.

Gandy, C. J., Davis, J. E., Orme, P. H., Potter, H. A., Jarvis, A. P. (2016). Metal removal mechanisms in a short hydraulic residence time subsurface flow compost wetland for mine drainage treatment. *Ecological Engineering*, *97*, 179-185.

Gundersen, L. C., Schumann, R. R., Otton, J. K., Dubiel, R. F., Owen, D. E., Dickinson, K. A. (1992). Geology of radon in the United States. *Geol Soc Am Spec Pap*, *271*, 1-16.

Gundersen, L. C., Schumann, R. R. (1996). Mapping the radon potential of the United States: examples from the Appalachians. *Environment International*, *22*, 829-837.

Hall, F. R., Boudette, E. L., Olszewski Jr, W. J. (1987). Geologic controls and radon occurrence in New England.

Harley, J. H. (1980). Sampling and Measurement of Airborne Daughter Products of Radon. *Health Physics*, *38*(6), 1068-1074.

Herselman, J. E., Steyn, C. E., Fey, M. V. (2005). Baseline concentration of Cd, Co, Cr, Cu, Pb, Ni and Zn in surface soils of South Africa: research in action. *South African journal of science*, *101*(11-12), 509-512.

Hiscock, K. M. (2005). Hydrogeology: Principles and Practices. Blackwell Science, UK. 388.

Hobbs, P. J., Lindsay, R., Maherry, A., Matshaya, M., Newman, R. T., Talha, S. A. (2010). The use of radon 222Rn as a hydrological tracer in natural and polluted environments. *WRC Report*, (1685/1/10).

Hopke, P. K., Borak, T. B., Doull, J., Cleaver, J. E., Eckerman, K. F., Gundersen, L. C. S., Harley, N. H., Hess, C. T., Kinner, N. E., Kopecky, K.J. McKone, T. E. (2000). Health risks due to radon in drinking water.

IARC (International Agency for Research on Cancer). (1988). Man-Made Mineral Fibres and Radon. Monographs on the Evaluation of Carcinogenic Risks to Humans. IARC Scientific Publications, 43, 173-259.

IARC (International Agency for Research on Cancer). (1990). Chromium, nickel and welding. IARC monographs on the evaluation of the carcinogenic risk of chemicals to humans, 49,1–648

IARC (International Agency for Research on Cancer). (1991). Monographs on the evaluation of carcinogenic risks to humans, 43, 53.

IARC. (2012) A review of human carcinogens: radiation. IARC monographs on the evaluation of carcinogenic risks to humans.

ICRP (1993). Protection Against Radon-222 at Home and at Work. ICRP Publication 65. *Annals of the ICRP*, *23*(2).

ICRP. (2007). The 2007 Recommendations of the International Commission on Radiological Protection. ICRP publication 103. *Annals of the ICRP*, *37*(2-4).

ICRP. (2013). Radiological protection in geological disposal of long-lived solid radioactive waste. ICRP publication 122. *Annals of the ICRP*, *42*(3), 1-57.

Ielsch, G., Thieblemont, D., Labed, V., Richon, P., Tymen, G., Ferry, C., Robe, M.C., Baubron, J.C., Bechennec, F. (2001). Radon (222Rn) level variations on a regional scale: influence of the basement trace element (U, Th) geochemistry on radon exhalation rates. *Journal of Environmental Radioactivity*, *53*(1), 75-90.

Ikebe, Y. (1970). Variation of radon and thoron concentrations in relation to the wind speed. *Journal of the Meteorological Society of Japan. Ser. II*, *48*(5), 461-468.

Ishimori, Y., Lange, K., Martin, P., Mayya, Y. S., Phaneuf, M. (2013). Measurement and calculation of radon releases from NORM residues.

Kendall, G. M., Smith, T. J. (2002). Doses to organs and tissues from radon and its decay products. *Journal of Radiological Protection*, *22*(4), 389.

Khan, F., Ali, N., Khan, E.U., Khattak, N.U., Khan, K. (2009). Radon monitoring in water sources of Balakot and Mansehra cities lying on a geological fault line. *Radiation Protection Dosimetry*, *138*(2), 174-179.

Kreuzer, M., Fenske, N., Schnelzer, M., Walsh, L. (2015). Lung cancer risk at low radon exposure rates in German uranium miners. *British journal of cancer*, *113*(9), 1367.

Krewski, D., Lubin, J.H., Zielinski, J.M., Alavanja, M., Catalan, V.S., William Field, R., Klotz, J.B., Létourneau, E.G., Lynch, C.F., Lyon, J.L. and Sandler, D.P. (2006). A combined analysis of North American case-control studies of residential radon and lung cancer. *Journal of Toxicology and Environmental Health, Part A*, *69*(7-8), 533-597.

Kumar, A., Chauhan, R. P., Joshi, M., & Sahoo, B. K. (2014). Modeling of indoor radon concentration from radon exhalation rates of building materials and validation through measurements. *Journal of environmental radioactivity*, *127*, 50-55.

Kurttio, P., Auvinen, A., Salonen, L., Saha, H., Pekkanen, J., Mäkeläinen, I., Väisänen, S.B., Penttilä, I.M. and Komulainen, H. (2002). Renal effects of uranium in drinking water. *Environmental health perspectives*, *110*(4), 337.

LeGrand, H. E. (1987). Radon and radium emanations from fractured crystalline rocks–a conceptual hydrogeological model. *Ground Water*, *25*(1), 59-69.

Lestaevel, P., Houpert, P., Bussy, C., Dhieux, B., Gourmelon, P., Paquet, F. (2005). The brain is a target organ after acute exposure to depleted uranium. *Toxicology*, *212*(2-3), 219-226.

Leuschner, A. H., Van As, D., Grundling, A., Steyn, A. (1988). A survey of indoor exposure to radon in South Africa. In *Proceedings of the international conference on residential air pollution*.

Leuschner, A. H., Steyn, A., Strydom, R., De Beer, G. P. (1992). Indoor radon concentrations in South African homes. In *8. International congress of the International Radiation Protection Association (IRPA8)*.

Levin, M., Verhagen, B. (2013). Application of isotope techniques to trace location of leakage from dams and reservoirs. In " The use of isotope hydrology to characterize and assess water resources in South (ern) Africa". Tamiru Abiye (Editor), (p 9-23)

Lindsay, R., de Meijer, R. J., Maleka, P. P., Newman, R. T., Motlhabane, T. G. K., de Villiers, D. (2004a). Monitoring the radon flux from gold-mine dumps by γ-ray mapping. *Nuclear Instruments and Methods in Physics Research Section B: Beam Interactions with Materials and Atoms*, *213*, 775-778.

Lindsay, R., De Meijer, R. J., Joseph, A. D., Motlhabane, T. G. K., Newman, R. T., Tsela, S. A., Speelman, W. J. (2004b). Measurement of radon exhalation from a gold-mine tailings dam by gamma-ray mapping. *Radiation Physics and Chemistry*, *71*, 797-798.

Lindsay, R., Newman, R. T., Speelman, W. J. (2008). A study of airborne radon levels in Paarl houses (South Africa) and associated source terms, using electret ion chambers and gamma-ray spectrometry. *Applied radiation and isotopes*, *66*(11), 1611-1614.

Liu, C., Shi, Z., Zachara, J. M. (2009). Kinetics of uranium (VI) desorption from contaminated sediments: Effect of geochemical conditions and model evaluation. *Environmental science & technology*, *43*(17), 6560-6566.

Liu, B., Peng, T., Sun, H., Yue, H. (2017). Release behavior of uranium in uranium mill tailings under environmental conditions. *Journal of environmental radioactivity*, *171*, 160-168.

Lubin, J.H., Boice Jr, J.D., Edling, C., Hornung, R.W., Howe, G.R., Kunz, E., Kusiak, R.A., Morrison, H.I., Radford, E.P., Samet, J.M. and Tirmarche, M. (1995). Lung cancer in radon-exposed miners and estimation of risk from indoor exposure. *JNCI: Journal of the National Cancer Institute*, *87*(11), 817-827.

Man, C. K., & Yeung, H. S. (1998). Radioactivity contents in building materials used in Hong Kong. *Journal of radioanalytical and Nuclear Chemistry*, *232*(1-2), 219-222.

Matooane, M., Phala, N., Wright, C. Y., Oosthuizen, M. A. (2014). Risk perceptions of dust and its impacts among communities living in a mining area of the Witwatersrand, South Africa. *Clean Air Journal*, *24*(1), 22-27.

Miles, J., Ball, K. (1996). Mapping radon-prone areas using house radon data and geological boundaries. *Environment International*, *22*, 779-782.

Minter, W. E. L. (1977). A sedimentological synthesis of placer gold, uranium and pyrite concentrations in Proterozoic Witwatersrand sediments.

Mittal, S., Rani, A. and Mehra, R. (2016). Estimation of radon concentration in soil and groundwater samples of Northern Rajasthan, India. *Journal of Radiation Research and Applied Sciences*, *9*(2), 125-130.

Mogale City Local Municipality (MCLM). (2013). Baseline Assessment Report. Zanokuhle Environmental services.

Mogale City Local Municipality (MCLM). (2016). Integrated Development plan. 4th Annual Review of the 5 year IDP 2011-16.

Mudd, G. M. (2008). Radon releases from Australian uranium mining and milling projects: assessing the UNSCEAR approach. *Journal of environmental radioactivity*, *99*(2), 288-315.

Mudd, G. M. (2008). Radon sources and impacts: a review of mining and non-mining issues. *Reviews in Environmental Science and Bio/Technology*, *7*(4), 325-353.

Murty, V. R. K., King, J. G., Karunakara, N., Raju, V. C. C. (2010). Indoor and outdoor radon levels and its diurnal variations in Botswana. *Nuclear Instruments and Methods in Physics Research Section A: Accelerators, Spectrometers, Detectors and Associated Equipment*, *619*(1-3), 446-448.

Naicker, K., Cukrowska, E., McCarthy, T. S. (2003). Acid mine drainage arising from gold mining activity in Johannesburg, South Africa and environs. *Environmental pollution*, *122*(1), 29-40.

National Nuclear Regulator (1999). Act 47 of 1999, and Regulations.

National Research Council. (1988). Health risks of radon and other internally deposited alpha-emitters. *National Research Council: Committee on the Biological Effects of Ionizing Radiation (BEIR)*.

National Research Council. (1991). Comparative dosimetry of radon in mines and homes. National Academies Press.

National Research Council. (1999a). Evaluation of guidelines for exposures to technologically enhanced naturally occurring radioactive materials. National Academies Press.

National Research Council. (1999b). Health effects of exposure to radon: BEIR VI (Vol. 6). National Academies Press.

National Research Council. (1999c). Committee on risk assessment of exposure to radon in drinking water. *Risk assessment of radon in drinking water*.

Nazaroff, W. W., Nero, A. V. (1988). Radon and its decay products in indoor air

Nazaroff, W. W. (1992). Radon transport from soil to air. *Reviews of geophysics*, *30*(2), 137-160.

Nengovhela, A. C., Yibas, B., Ogola, J. S. (2006). Characterisation of gold tailings dams of the Witwatersrand Basin with reference to their acid mine drainage potential, Johannesburg, South Africa. *Water SA*, *32*(4).

Nero, A. V., Gadgil, A. J., Nazaroff, W. W., Revzan, K. L. (1990). Indoor radon and decay products: concentrations, causes, and control strategies.

Netherlands Ministry of Housing, Physical Planning and Environment (1997). Environmental quality standards for soil and water - The Dutch List. Leidschendam

Ongori, J. N., Lindsay, R., Newman, R. T., Maleka, P. P. (2015). Determining the radon exhalation rate from a gold mine tailing dump by measuring the gamma radiation. *Journal of environmental radioactivity*, *140*, 16-24.

Orloff, K.G., Mistry, K., Charp, P., Metcalf, S., Marino, R., Shelly, T., Melaro, E., Donohoe, A.M., Jones, R.L. (2004). Human exposure to uranium in groundwater. *Environmental research*, *94*(3), 319-326.

Othmane, G., Allard, T., Morin, G., Sélo, M., Brest, J., Llorens, I., Chen, N., Bargar, J.R., Fayek, M. and Calas, G. (2013). Uranium association with iron-bearing phases in mill tailings from Gunnar, Canada. *Environmental science & technology*, *47*(22), 12695-12702.

Otton, J. K., Gundersen, L. C. S., Schumann, R. (1992). The Geology of Radon. US Department of the Interior. *US Geological Survey*, *Open Report*, *30*.

Pretorius, D. A. (1976). The nature of the Witwatersrand gold-uranium deposits. *Handbook of stratabound and stratiform ore deposits*, 29-88.

Porstendörfer, J. (1994). Properties and behaviour of radon and thoron and their decay products in the air. *Journal of Aerosol Science*, *25*(2), 219-263.

Ravikumar, P., Somashekar, R. K. (2013). Estimates of the dose of radon and its progeny inhaled inside buildings. *European Journal of Environmental Sciences*, *3*(2).

Reddy, P., Zuma, K., Shisana, O., Jonas, K., Sewpaul, R. (2015). Prevalence of tobacco use among adults in South Africa: Results from the first South African National Health and Nutrition examination survey. *South African Medical Journal*, *105*(8), 648-655.

Robb, L. J., Meyer, F. M. (1995). The Witwatersrand Basin, South Africa: geological framework and mineralization processes. *Ore Geology Reviews*, *10*(2), 67-94.

Robb, L. J., Charlesworth, E. G., Drennan, G. R., Gibson, R. L., Tongu, E. L. (1997). Tectono-metamorphic setting and paragenetic sequence of Au-U mineralisation in the Archaean Witwatersrand Basin, South Africa. *Australian Journal of Earth Sciences*, *44*(3), 353-371.

Rosner, T. (1999). The environmental impact of seepage from gold mine tailings dams near Johannesburg, South Africa (Doctoral dissertation, University of Pretoria).

Rösner, T., Van Schalkwyk, A. (2000). The environmental impact of gold mine tailings footprints in the Johannesburg region, South Africa. *Bulletin of Engineering Geology and the Environment*, *59*(2), 137-148.

Sahoo, B. K., Sapra, B. K., Gaware, J. J., Kanse, S. D., Mayya, Y. S. (2011). A model to predict radon exhalation from walls to indoor air based on the exhalation from building material samples. *Science of the Total Environment*, *409*(13), 2635-2641.

Samet, J. M. (1989). Radon and lung cancer. *JNCI: Journal of the National Cancer Institute*, *81*(10), 745-758.

Scheib, C., Appleton, D., Jones, D., Hodgkinson, E. (2006). Airborne uranium data in support of radon potential mapping in Derbyshire, Central England.

Scheib, C., Appleton, J. D., Miles, J. C. H., Green, B. M. R., Barlow, T. S., Jones, D. G. (2009). Geological controls on radon potential in Scotland. *Scottish Journal of Geology*, *45*(2), 147-160.

Schmidt, A., Stringer, C. E., Haferkorn, U., Schubert, M. (2009). Quantification of groundwater discharge into lakes using radon-222 as naturally occurring tracer. *Environmental Geology*, *56*(5), 855-863.

Schubert, M., Knoeller, K., Treutler, H. C., Weiss, H., Dehnert, J. (2006). 222 Rn as a tracer for the estimation of infiltration of surface waters into aquifers. *Radioactivity in the Environment*, *8*, 326-334.

Seldén, A.I., Lundholm, C., Edlund, B., Högdahl, C., Ek, B.M., Bergström, B.E., Ohlson, C. G. (2009). Nephrotoxicity of uranium in drinking water from private drilled wells.*Environ. Research*, *109*, 486–494.

Sethi, T. K., El-Ghamry, M. N., Kloecker, G. H. (2012). Radon and lung cancer. *Clin Adv Hematol Oncol*, *10*(3), 157-164.

Sextro, R. G. (1987). Understanding the origin of radon indoors—Building a predictive capability. *Atmospheric Environment (1967)*, *21*(2), 431-438.

Sheppard, M. I. (1980). The environmental behaviour of uranium and thorium. *Atomic Energy of Canada Ltd.*

Sheoran, A. S., Sheoran, V. (2006). Heavy metal removal mechanism of acid mine drainage in wetlands: a critical review. *Minerals engineering*, *19*(2), 105-116.

Siegel, M. D., Bryan, C. R. (2004). Environmental geochemistry of radioactive contamination. *Environmental Geochemistry*, *9*, 205-262.

South African Council for Stratigraphy. (1980). Stratigraphy of South Africa. Part 1. Lithostratigraphy of the Republic of South Africa, South West Africa/Namibia, and the Republics of Bophuthatswana, Transkei and Venda. Handbook 8. Kent L.E. (compiler). Pretoria, Geological Survey of South Africa.

Speelman, W. J. (2004). Modelling and measurement of radon diffusion through soil for application on mine tailings dam (Doctoral dissertation, University of the Western Cape).

Strong, K. P., & Levins, D. M. (1982). Effect of moisture content on radon emanation from uranium ore and tailings. *Health Physics*, *42*(1), 27-32.

Tankard, A. J., Jackson, M. P. A., Eriksson, K. A., Hobday, D. K., Hunter, D. R., Minter, W. E. L. (1982). The Golden Proterozoic. In *Crustal evolution of southern Africa* (pp. 115-150). Springer, New York, NY.

Tanner, A. B. (1980). Radon migration in the ground: a supplementary review. *Natural radiation environment III*, *1*, 5-56.

Thomas, K. T. (1981). Management of wastes from uranium mines and mills. *Int. At. Energy Agency Bull*, *23*(2), 33-35.

Thomas, K. W., Gould, M. K. (2016). Overview of the initial evaluation, diagnosis, and staging of patients with suspected lung cancer. *UpToDate*.

Tomášek, L., Kunz, E., Darby, S. C., Swerdlow, A. J., Placek, V. (1993). Radon exposure and cancers other than lung cancer among uranium miners in West Bohemia. *The Lancet*, *341*(8850), 919-923.

Tommasino, L. (1990). Radon monitoring by alpha track detection. *International Journal of Radiation Applications and Instrumentation. Part D. Nuclear Tracks and Radiation Measurements*, *17*(1), 43-48.

Tricca, A., Porcelli, D., Wasserburg, G. J. (2000). Factors controlling the groundwater transport of U, Th, Ra, and Rn. *Journal of Earth System Science*, *109*(1), 95-108.

Turekian, K. K., Nozaki, Y., & Benninger, L. K. (1977). Geochemistry of atmospheric radon and radon products. *Annual Review of Earth and Planetary Sciences*, *5*(1), 227-255.

Tucker, R. F., Viljoen, R. P., Viljoen, M. J. (2016). A review of the Witwatersrand Basin—the world's greatest goldfield. *Episodes*, *39*(2), 105-133.

Tutu, H., McCarthy, T. S., Cukrowska, E. (2008). The chemical characteristics of acid mine drainage with particular reference to sources, distribution and remediation: The Witwatersrand Basin, South Africa as a case study. *Applied Geochemistry*, *23*(12), 3666-3684.

United Nations Scientific Committee on the Effects of Atomic Radiation. (2000). Sources and effects of ionizing radiation. UNSCEAR 2000 report to the General Assembly, with scientific annexes. Volume I: Sources.

Watson, R. J., Smethurst, M. A., Ganerød, G. V., Finne, I., Rudjord, A. L. (2017). The use of mapped geology as a predictor of radon potential in Norway. *Journal of environmental radioactivity*, *166*, 341-354.

Wendle, G. (1998). Radioactivity in mines and mine water-sources and mechanisms. *Journal of the Southern African Institute of Mining and Metallurgy*, *98*(2), 87-92.

Winde, F., Sandham, L. A. (2004). Uranium pollution of South African streams–An overview of the situation in gold mining areas of the Witwatersrand. *GeoJournal*, *61*(2), 131-149.

Winde, F., Van der Walt, I. J. (2004). The significance of groundwater–stream interactions and fluctuating stream chemistry on waterborne uranium contamination of streams – a case study from a gold mining site in South Africa. *Journal of Hydrology*, *297*(1-4), 178–196.

Winde, F. and Wade, P.W. (2006). An Assessment of Sources, Pathways, Mechanisms and Risks of Current and Potential Future Pollution of Water and Sediments in Gold-mining Areas of the Wonderfonteinspruit Catchment: Report to the Water Research Commission. Water Research Commission.

Winde, F., de Villiers, A. B. (2002). The nature and extent of uranium contamination from tailings dams in the Witwatersrand gold mining area (South Africa). In *Uranium in the aquatic environment* (pp. 889-898). Springer, Berlin, Heidelberg.

World Health Organisation (1998). Guidelines for Drinking-Water Quality. Health Criteria and Other Supporting Information, Addendum toVol. 2 WHO/EOS/98.1.Geneva: World Health Organization.

World Health Organization. (2008). Guidelines for Drinking-water Quality [electronic resource]: incorporating 1st and 2nd addenda, Vol. 1, Recommendations.

World Health Organization. (2009). WHO Handbook on Indoor Radon: a Public Health Perspective. WHO, Geneva.

Wronkiewicz, D.J., Condie, K.C. (1987). Geochemistry of Archean shales from the Witwatersrand Supergroup, South Africa: source-area weathering and provenance. *Geochimica et Cosmochimica Acta*, *51*(9), 2401-2416.

Wronkiewicz, D. J., Condie, K. C. (1990). Geochemistry and mineralogy of sediments from the Ventersdorp and Transvaal Supergroups, South Africa: cratonic evolution during the early Proterozoic. *Geochimica et Cosmochimica Acta*, *54*(2), 343-354.

Zeilinski, R. A. (1981). Experimental leaching of volcanic glass. Implications for evaluation of glassy volcanic rocks as sources of uranium.

Zhuo, W., Iida, T., Yang, X. (2001). Occurrence of ^{222}Rn, ^{226}Ra, ^{228}Ra and U in groundwater in Fujian Province, China. *Journal of environmental radioactivity*, *53*(1), 111-120.

Zhuo, W., Furukawa, M., Guo, Q., Kim, Y. S. (2005). Soil radon flux and outdoor radon concentrations in East Asia. In *International Congress Series* (Vol. 1276, pp. 285-286). Elsevier.

10 APPENDICES

Appendix A: Dataset for trace elements found in rock and tailings samples collected in the study area.

	Sc	V	Cr	Co	Ni	Cu	Zn	Ga	Rb	Sr	Y	Zr	Nb	Mo	Ba	Pb	Th	U
	(ppm)	(ppm)	(ppm)	(ppm)	(ppm)	(ppm)	(ppm)	(ppm)	(ppm)	(ppm)	(ppm)	(ppm)	(ppm)	(ppm)	(ppm)	(ppm)	(ppm)	(ppm)
TA/PB 01R	3,21	39,6	104,92	7,83	11,84	13,46	1,19	6,39	2,79	13,54	5,13	57,85	1,56	0,16	18,77	5,98	d.l.	d.l.
TA/PB 01T	8,45	49,92	324,64	51,3	105,57	179,03	138,73	10,95	13,27	37,83	12,97	129,84	4,13	1,43	68,94	92,06	13,41	42,65
TA/PB 02T	9,06	78,39	364,21	71,37	332,46	224,04	516,43	13,92	25,92	65,77	26,18	130,11	5,09	2,66	121,24	94,1	12,53	51,02
TA/PB 03T	2,77	33,89	156,22	40,53	115,47	28,8	47,33	5,65	11,29	27,79	10,17	98,25	2,89	0,94	52,17	9,68	d.l.	7,38
TA/PB 04R	6,47	33,81	135,96	8,06	12,53	6,63	12,05	12,37	1,83	17,35	9,55	69,31	2,55	d.l.	7,5	12,12	2,9	d.l.
TA/PB 04T	3,9	44,1	307,91	69,99	152,11	67,98	249,02	11,22	20,65	63,14	17,97	149,07	4,54	0,57	93,75	32,64	12,06	74,3
TA/PB 07R	3,96	34,92	128,73	7	21,21	10,75	d.l.	7,93	7,5	18,19	7,04	71,62	1,69	0,48	34,45	4,35	0,39	d.l.
TA/PB 07T	3,47	26,04	213,77	33,08	50,68	23,97	87,28	4,86	9,84	31,54	7,78	206,03	5,08	0,5	120,59	445,6	11,3	28,03

Appendix A: Dataset for trace elements found in rock and tailings samples collected in the study area.

	Sc	V	Cr	Co	Ni	Cu	Zn	Ga	Rb	Sr	Y	Zr	Nb	Mo	Ba	Pb	Th	U
	(ppm)	(ppm)	(ppm)	(ppm)	(ppm)	(ppm)	(ppm)	(ppm)	(ppm)	(ppm)	(ppm)	(ppm)	(ppm)	(ppm)	(ppm)	(ppm)	(ppm)	(ppm)
TA/PB 08R	0.36	3.85	46.08	3.62	3.72	6.80	1.19	0.44	4.90	20.54	5.19	43.31	0.52	d.l.	58.21	10.36	0.65	d.l.
TA/PB 10R	0.58	5.60	35.49	0.26	6.16	7.17	2.70	d.l.	1.94	2.31	2.75	38.90	0.71	0.14	2.12	4.12	d.l.	d.l.
TA/PB 12R	2.97	17.72	151.47	18.11	51.14	44.94	13.07	5.70	7.62	26.68	10.18	139.58	3.59	1.04	47.65	12.43	4.47	1.40
TA/PB 14R	16.73	118.95	559.21	d.l.	295.90	37.01	23.14	17.82	d.l.	3.96	21.65	93.92	5.29	0.58	3.20	4.83	d.l.	d.l.
TA/PB 16R	0.37	4.98	27.10	2.54	3.54	5.73	2.47	2.67	7.32	6.18	1.84	40.48	d.l.	d.l.	3.59	4.21	d.l.	d.l.
TA/PB 17R	d.l.	3.56	31.48	2.89	3.59	7.37	d.l.	0.46	4.72	5.35	3.50	39.69	1.18	0.22	13.60	2.19	1.26	d.l.
TA/PB 18R	0.16	9.09	50.76	d.l.	2.57	6.66	2.30	2.03	8.55	18.32	3.70	65.38	2.70	0.37	29.58	12.36	3.11	d.l.
TA/PB 09T	4.86	32.70	217.39	28.68	65.49	52.53	39.37	5.55	8.69	24.51	8.98	114.77	3.96	1.16	51.80	58.78	8.00	15.88
TA/PB 10T	5.92	40.45	232.26	25.61	60.78	24.15	35.89	7.93	14.70	43.27	11.76	157.16	5.22	0.93	83.02	39.79	7.86	17.47
TA/PB 11T	10.79	105.17	1130.39	d.l.	107.33	186.23	252.47	5.68	1.30	1172.57	27.00	30.87	4.91	9.56	15111.88	3263.48	d.l.	d.l.
TA/PB 12T	6.41	18.93	254.09	129.71	238.16	69.41	432.54	4.54	5.50	21.40	20.30	195.19	5.06	1.87	99.01	353.95	90.61	113.79
TA/PB 15T	6.97	20.29	243.49	205.64	700.40	248.83	275.85	4.22	5.73	22.72	31.84	136.48	4.44	1.98	61.43	30.79	15.00	149.76
TA/PB 19/B BOTTOM	6.43	66.40	397.18	440.17	579.96	138.97	291.57	6.24	2.20	21.21	24.55	618.69	11.85	13.73	120.70	396.29	29.46	85.94
TA/PB 19/B1	20.21	102.78	151.69	8.38	49.05	40.11	41.56	53.73	41.86	122.16	66.64	479.93	45.72	1.89	322.61	60.98	49.86	10.14
TA/PB 19/B2	15.47	81.59	297.19	17.22	75.20	45.57	165.92	15.52	42.61	147.24	21.29	235.94	9.70	0.79	508.20	82.83	7.26	1.45
TA/PB 13T/TOP	12.32	31.99	240.96	273.96	1323.72	207.95	937.27	3.94	d.l.	535.74	57.14	21.29	0.59	3.82	7842.37	498.11	d.l.	0.25

Appendix B: Dataset for stable isotope analysis for water samples

Sample Name	δ2H (‰)	± 2H StDev (‰)	δ18O (‰)	± 2H StDev (‰)
PBW2	0,0	1,1	1,35	0,1
PBW3	-5,1	0,3	-0,90	0,1
PBW4	-12,1	0,5	-2,16	0,0
PBW5	-39,3	4,0	-6,10	0,3
PBW6	-53,1	0,6	-7,23	0,1
PBW7	-37,7	1,0	-6,10	0,1

Appendix C: Radon monitoring points (First installation)

Site no	Location	Monitor number	Measurement localities category	Underlying geological units	Picture
1	S26.11933 E27.77701 Outdoor	H63547	Directly on tailings residues	Quartzite (Turffontein)	
2	S26.12739 E27.77606 Outdoor	H63552	Tailings dam	Quartzite (Turffontein)	
3	S26.13794 E27.77329 Outdoor	H63559	Directly on tailings residues.	Andesite (Kliprivierberg)	
4	S26.11754 E27.76666 Indoor	H63554	Placed in the abandoned house, in the bathroom. (less than 1km from tailings)	Quartzite (Turffontein)	

5	S26.11721 E27.76183 Indoor	H63550	Placed in a house made of bricks, very close to the tailings dumps. (less than 1km from tailings)	Quartzite (Turffontein)	
6	S26.11721 E27.76183 Indoor	H 63560	Placed in a shack (less than 1km from tailings)	Quartzite (Turffontein)	
7	S26.14016 E27.74788 Outdoor	H63568	Directly on tailings residues	Quartzite (Black Reef)	
8	S26.14575 E27.75719 Outdoor	H63564	Proximity to tailings (± 750 m), Next to the pond on wetland.	Quartzite (Black Reef)	
9	S26.13676 E27.75182 Indoor	H63551	Placed in an abandoned uranium facility proximity to tailings.	Quartzite (Black Reef)	

10	S26.13102 E27.75075 Indoor	H63549	Installed inside the abandoned house without roofing (less than 1km from tailings)	Quartzite (Black Reef)	
11	S26.14712 E27.72557 Outdoor	H63562	Placed on the tree next to tailings, not far from the operating mine.	Quartzite (Black Reef)	
12	S26.11574 E27.76194 Outdoor	H63561	Directly on tailings residues	Quartzite (Johannesburg and Booysens)	
13	S26.10833 E27.75066 Outdoor	H63543 Lost	Proximity to reworked mine dump site.	Shale (Jeppestown)	
14	S26.10552 E27.76625 Outdoor	H63554	Tied on the trees not far from tailings	Shale (Jeppestown)	

15	S26.12762 E27.81552 Outdoor	H63542	Directly on tailings residues	Quartzite (Johannesburg and Booysens)	
16	S26.14349 E27.80853	H63545	Directly on reworked tailings	Quartzite (Government)	
17	S26.15109 E27.81267 Outdoor	H63557	Proximity to tailings (±800m)	Quartzite (Government)	
18	S26.17548 E27.80537 Outdoor	H63548	Background	Shale (Jeppestown)	

19	S26.17022 E27.78484 Outdoor	H63548 Lost	Background	Shale (Jeppestown)	
20	S26.16610 E27.77412	Lost	Background	Quartzite (Government)	
21	S26.13448 E27.79988	H63558	Proximity to reworked tailings	Quartzite (Turffontein)	
22	S26.12477 E27.80117	H63541	Proximity to tailings	Quartzite (Turffontein)	
23	S26.11533 E27.78215	H63570 Lost	Background	Quartzite (Johannesburg)	

Appendix C: First radon monitoring control localities.

24	S25.79046E28.32255 Indoor	H63567	Control
25	S26.16707E27.93475 Indoor	H63553	Control
26	S26.16707S27.93475 Indoor	H63565	Control
27	S26.19144E28.02950 Outdoor	H63566	Control
28	S26.16048 E27.98284 Indoor	H63546	control
29	S26.1937 E28.03676 Indoor	H63546	Control
30	S26.19100E28.02955 Indoor basement	H63569	Control

Appendix C: Radon monitoring points (Second monitoring)

Site no	Location	Monitor number	Measurement locality category	Underlying geological units	Picture
31	S26.06459 E27.81288 Outdoor	H91306	Control	Quartzite	
32	S26.13637 E27.76744 Outdoor	H91305	Directly on tailings residue.	Andesite (Kliprivierberg)	
33	S26.14730 E27.77381 Outdoor	H91301	Directly on tailings behind residential houses.	Andesite (Kliprivierberg)	
34	S26.12455 E27.77487 Outdoor	H91311	Directly on tailings residues	Quartzite (Turffontein)	

35	S26.11926 E27.75647 Outdoor	H91298	Directly on tailings residues	Quartzite (Turffontein/ Johannesburg and Booysens)	
36	S26.12270 E27.75380 Outdoor	H91307	Proximity to tailings (± 250 m) and ± 50m from residential area	Quartzite (Turffontein/ Johannesburg and Booysens)	
37	S26.13260 E27.75234 Outdoor	H91316	Proximity to industrial plant within vicinity of tailings	Quartzite (Black Reef)	
38	S26.13780 E27.75264 Outdoor	H91313	Proximity to tailings (±150m)	Quartzite (Black Reef)	

39	S26.13929 E27.75527 Outdoor	H91299 Lost	Proximity to tailings (±150m)		
40	S26.14253 E27.75032 Outdoor	H91302	Directly on tailings residues	Quartzite (Black Reef)	
41	S26.14059 E27.74944 Outdoor	H91319	Directly on tailings residues	Quartzite (Black Reef)	
42	S26.14194 E27.75237 Outdoor.	H91310	Proximity to tailings (± 200m)	Quartzite (Black Reef)	

43	S26.12597 E27.75317 Outdoor	H91320	Proximity to tailings (±250)	Quartzite (Black Reef)	
44	S26.11408 E27.77624 Outdoor	H91324	Directly on tailings residues	Quartzite (Johannesburg and Booyssen/Turffontein)	
45	S26.10295 E27.74025 Outdoor	H91318	Background	Quartzite (Black Reef)	
46	S26.10296 E27.74035 Outdoor	H91317	Directly on reworked tailings residues surrounded by vegetation	Quartzite (Turffontein)	

47	S26.16565 E27.77094 Outdoor	H91323	Background	Quartzite (Government)	
48	S26.16320 E27.75682 Outdoor	H91297	Background	Quartzite (Turffontein)	
49	S26.16134 E27.74055 Outdoor	H91326	Background.	Quartzite (Black Reef)	
50	S26.16862 E27.76073 Outdoor	H91300	Background	Quartzite (Government)	

51	S26.18111 E27.75236 Outdoor	H91321	Background	Shale (Jeppestown)	
52	S26.11764 E27.77324 Outdoor	H91322	Proximity to Tailings (±250 m)	Quartzite (Turffontein)	
53	S26.12794 E27.74649 Outdoor	H91315	Tailings residues	Quartzite (Johannesburg and Booysens)	
54	S26.11552 E27.76734 Outdoor	H91304	Tailings residues	Quartzite (Turffontein/ Johannesburg and Booysens)	

55	S26.11594 E27.76764 Outdoor	H91312	Tailings	Quartzite (Johannesburg and Booysens)	
56	S26.12723 E27.78909 Outdoor	H91325	Proximity To tailings	Quartzite (Turffontein)	
57	S26.12010 E27.79023 Outdoor	H91309	Proximity	Quartzite (Turffontein)	
58	S26.07656 E27.78908 Outdoor	H91303	Control	Quartzite (Government)	

59	S26.19539 E28.03777: Indoor	H91314	Control
69	S26.16048 E27.98284 Outdoor	H91308	Control

Appendix D: Radon dataset for first monitoring

Monitor	**Bq h m-3**	**St Dev**								
63541	9.90E+04	1.10E+04								
63542	9.20E+04	1.10E+04								
63544	1.15E+05	1.99E+04								
63545	1.06E+05	1.15E+04								
63546	9.20E+04	1.00E+04								
63547	2.32E+05	3.80E+04								
63548	9.20E+04	1.30E+04								
63549	7.40E+04	1.20E+04								
63550	8.20E+04	1.00E+04								
63551	1.05E+05	1.93E+04								
63552	1.11E+05	1.23E+04								
63553	6.66E+04	1.04E+04								
63554	9.10E+04	1.20E+04								
63555	7.00E+04	1.00E+04								
63556	1.08E+05	1.84E+04								
63557	8.90E+04	1.00E+04								
63559	1.28E+05	1.20E+04								
63560	3.83E+05	5.30E+04								
63561	8.20E+04	1.10E+04								
63562	8.70E+04	1.10E+04								
63564	7.35E+05	3.18E+04								
63565	7.60E+04	1.10E+04								
63566	2.02E+05	1.43E+04								
63567	4.39E+05	4.02E+04								
63568	5.82E+05	4.57E+04								
63569	6.66E+04	1.14E+04								
Note:										
RGM 63563 was damaged by fire, the CR39 plastic thereof broke during work-up and could not be analysed										

Appendix D: Radon dataset for second monitoring

Monitor	**Bq h m^{-3}**	**St Dev**
91297	8,90E+04	1,92E+04
91298	2,16E+05	3,14E+04
91300	9,30E+04	1,95E+04
91301	2,36E+06	2,45E+05
91302	2,02E+06	2,11E+05
91303	7,81E+04	1,90E+04
91304	9,45E+04	1,97E+04
91305	1,59E+05	2,58E+04
91306	8,07E+04	1,84E+04
91307	8,75E+04	1,90E+04
91308	2,85E+05	3,82E+04
91309	1,52E+05	2,52E+04
91310	4,06E+05	5,01E+04
91311	1,21E+05	2,22E+04
91312	9,50E+04	1,97E+04
91313	1,10E+05	2,12E+04
91314	1,12E+05	2,13E+04
91315	1,73E+05	2,72E+04
91316	1,29E+05	2,29E+04
91317	2,03E+05	3,02E+04
91318	9,28E+04	1,95E+04
91319	8,76E+05	9,70E+04
91320	9,37E+04	1,96E+04
91321	2,46E+05	3,44E+04
91322	1,79E+05	2,78E+04
91323	1,52E+06	1,62E+05
91324	9,91E+04	2,01E+04
91325	2,35E+05	3,33E+04
91326	1,50E+05	2,50E+04

Appendix E: Conversion of radon results from Bq. h/m^3 to Bq/m^3

Latitude and longitude	**Monitor**	**Bq h m-3**	**St Dev**	**Duration= 92 days X 24 = 2208 hours**	**Bq/m^3**
S26.12477 E27.80117	63541	99000.00	11000.00	2208	44.83695652
S26.12762 E27.81552	63542	92000.00	11000.00	2208	41.66666667
S26.10552 E27.76625	63544	114660.00	19883.24	2208	51.92934783
S26.14349 E27.80853	63545	106470.00	11475.81	2208	48.2201087
S26.16048 E27.982845	63546	92000.00	10000.00	2208	41.66666667
S26.11933 E27.77701	63547	232000.00	38000.00	2208	105.0724638
S26.17548 E27.80537	63548	92000.00	13000.00	2208	41.66666667
S26.13102 E27.75075	63549	74000.00	12000.00	2208	33.51449275
S26.11721 E27.76183	63550	82000.00	10000.00	2208	37.13768116
S26.13676 E27.75182	63551	104520.00	19329.04	2208	47.33695652
S26.12739 E27.77606	63552	110760.00	12306.67	2208	50.16304348
s26.167074 E27.934750	63553	66600.00	10406.25	2208	30.16304348
S26.11754 E27.76666	63554	91000.00	12000.00	2208	41.21376812
S26.13448 E27.79988	63555	70000.00	10000.00	2208	31.70289855
S26.19370 E28.03676	63556	107640.00	18394.18	2208	48.75
S26.15109 E27.81267	63557	89000.00	10000.00	2208	40.30797101
S26.13794 E27.77329	63559	127920.00	11992.50	2208	57.93478261
S26.11721 E27.76183	63560	383000.00	53000.00	2208	173.4601449
S26.11574 E27.76194	63561	82000.00	11000.00	2208	37.13768116
S26.14712 E27.72557	63562	87000.00	11000.00	2208	39.40217391
S26.14575 E27.75719	63564	735150.00	31847.65	2208	332.9483696
s26.167074 E27.934750	63565	76000.00	11000.00	2208	34.42028986
S26.191005 E28.029559	63566	202020.00	14250.37	2208	91.49456522
S25.790468 E28.322557	63567	439140.00	40226.56	2208	198.8858696
S26.14016 E27.74788	63568	581880.00	45706.59	2208	263.5326087
S26.191440 E28.029504	63569	66600.00	11446.88	2208	30.16304348

Appendix F: Dataset used for Spearman correlation analysis

Number	X-Uranium (ppm)	Y- Radon (Bq/m³)	X	Y	X-Y	(X-Y) ²	r_s
1	42,65	105,1	4	5	-1	1	
2	51,02	50,2	3	9	-6	36	
3	7,38	57,9	7	8	-1	1	
4	0,01	36,5	10,5	11	-0,5	0,25	
5	15,88	72	6	7	-1	1	
6	17,47	97,8	5	6	-1	1	
7	113,79	914,9	2	1	1	1	
8	0,25	396,7	8	2	6	36	
9	0,01	114,4	10,5	3	7,5	56,25	
10	149,76	42,8	1	10	-9	81	
11	0,01	106,4	10,5	4	6,5	42,25	
12	0,01	35,4	10,5	12	-1,5	2,25	
Sum					**0**	**259**	**0.09440**

Appendix G: Lung cancer death's statistics (Data: StatsSA)

Local Munic	Year of death																			
	1997	1998	1999	2000	2001	2002	2003	2004	2005	2006	2007	2008	2009	2010	2011	2012	2013	2014	2015	2016
Merafong City	8	12	14	13	9	12	9	11	12	1	6	5	7	8	8	8	5	3	11	10
Mogale City	29	48	47	26	30	29	38	42	27	26	26	22	26	70	71	44	87	70	107	80
Rand West City	5	12	5	11	9	13	10	7	11	10	7	10	7	3	6	5	5	6	6	10
Unknown	0	0	0	0	0	0	0	0	0	0	0	0	0	0	0	0	0	0	0	1
Unspecified	0	0	0	0	0	0	0	0	0	0	0	0	0	0	0	2	0	0	0	0
Total	42	72	66	50	48	54	57	60	50	37	39	37	40	81	85	59	97	79	124	101